

**ROLE OF AUTOPHAGY IN GM1-MEDIATED NEUROPROTECTION IN
HUNTINGTON'S DISEASE**

by

Sabine Schmelz

A thesis submitted in partial fulfillment of the requirements for the degree of

Master of Science

Centre for Neuroscience
University of Alberta

© Sabine Schmelz, 2015

ABSTRACT

Background: Huntington's disease (HD) is an inherited neurodegenerative disorder caused by an expanded polyglutamine tract in the huntingtin (HTT) protein. Mutant huntingtin (mHTT) accumulates as toxic oligomers and aggregates inside the cell, when it is not removed efficiently by selective autophagy. In HD cells, this degradative pathway is impaired, due to an aberrant interaction of mHTT with p62, an adaptor and cargo recognition protein that guides cargo molecules and organelles to autophagic structures for degradation. Recently, the ganglioside GM1 was shown to protect HD cells from apoptosis, and to restore motor functions in an HD mouse model. These therapeutic effects were accompanied by phosphorylation of mHTT at amino acids Ser13 and Ser16, a post-translational modification that has been proposed to modulate mHTT toxicity and its cellular clearance. The exact mechanism underlying GM1 effects is still unclear. Previous work suggested that gangliosides may stimulate autophagy in brain cells and in other neurodegenerative models.

Hypothesis: The therapeutic effects of GM1 in HD models are due, at least in part, to activation of autophagy and/or restoration of cargo recognition in HD cells, and to enhanced mHTT clearance by autophagy.

Results: Soluble species of mHTT were not significantly decreased in HD cell or mouse models after GM1 treatment. However, mHTT aggregates were reduced in certain brain areas, suggesting that GM1 might affect aggregate formation or clearance. Autophagic markers such as LC3-II and p62 were not affected by GM1 treatment in both HD cell and mouse models. Autophagic flux, measured in a cell model that expressed the reporter protein RFP-EGFP-LC3, was also unaffected by GM1 in our experimental conditions. Immunoprecipitation experiments showed that GM1 treatment decreases the aberrant interaction between mHTT and p62. These data suggest that GM1 might improve cargo recognition and selective autophagy in HD models, potentially leading to increased clearance of mHTT aggregates and decreased mHTT toxicity.

ACKNOWLEDGEMENTS

I am grateful to my supervisor, Dr. Simonetta Sipione, for her guidance, support, encouragement, and constant availability for advice throughout my journey as a graduate student in her lab. Her enthusiasm and energy were inspiring to me and her expertise in the field was very helpful when discussing new ideas. Finally, I want to thank her for giving advice during presentation and poster making, but especially for her suggestions in writing this Master thesis.

I would also like to express my gratitude to my committee members, Dr. David Westaway and Dr. Satya Kar, for their ongoing support and insightful comments. A big thank you also for the opportunity to do a lab rotation course under Dr. Westaways' supervision at the Centre for Prions and Protein Folding Diseases. It was a great learning experience that I think back on with joy.

I would like to thank all current and previous members of the Sipione lab, Melanie Horkey, Melanie Alpaugh, Luis Morales, Danny Galleguillos, and Sebastian Lackey, who were always available for technical support and helpful advice. Mostly, I want to say thanks for their friendship and the good times we shared. I will especially miss our conversations, potlucks, and coffee runs.

I am grateful to the members of the MCBL group, for the opportunity to present my research and to receive their helpful advice on technical questions and feedback on presentation style.

I would like to thank Dr. Sun and Geraldine Barron at the Cross Cancer Institute for their help in confocal imaging and analysis, but also for the welcoming atmosphere and nice conversations.

I would like to thank the Faculty of Graduate Studies and Research and the Faculty of Medicine and Dentistry for their financial support in form of recruitment scholarships.

I am very grateful to Alberta Innovates Health Solutions for their ongoing financial support in form of the AIHS graduate studentship for the majority of my time as a graduate student and throughout my maternity leave.

I am very grateful to my mother and father for their continuous support throughout my life and during my time as a graduate student at the University of Alberta. The comfort of knowing that no matter what happens, they will be there for me, has always empowered me to go after my dreams.

Finally, I would like to thank Casey for his support and encouragement during this journey. Mainly I want to thank him for his love and being the best father to our son that I could imagine.

TABLE OF CONTENTS

1	Background	1
1.1	Huntington's Disease.....	1
1.1.1	General introduction.....	1
1.1.2	Neuropathology	1
1.1.3	Cellular and tissue distribution of huntingtin.....	3
1.1.4	The loss of function of HTT in HD.....	4
1.1.5	The gain-of-function of HTT in HD.....	6
1.1.6	Treatment strategies.....	11
1.2	Proteostatic mechanisms in HD.....	12
1.2.1	Cellular degradation of mHTT	12
1.2.2	UPS	12
1.2.3	CMA.....	13
1.2.4	Macroautophagy.....	13
1.3	Role of autophagy in HD	14
1.3.1	Molecular steps in autophagy.....	14
1.3.2	Nutrient-dependent and selective autophagy	17
1.3.3	Impaired autophagy in HD	19
1.4	Gangliosides in the brain.....	20
1.4.1	Gangliosides: complex glycosphingolipids with pleiotropic functions	20
1.4.2	GM1 and its functions in the brain	23
1.4.3	Gangliosides in HD	26
1.5	Modeling HD	28
1.5.1	Mouse models.....	28
1.5.2	Cell models.....	30
1.6	General hypothesis and Aims of this Master thesis.....	32
1.7	Figures	33
2	Material and Methods	38
2.1	Chemicals.....	38
2.2	Antibodies.....	38
2.3	Animal models	39
2.4	Cell models.....	40

2.5	Chronic GM1 administration <i>in vivo</i>	41
2.6	Cell treatments.....	41
2.7	Transient transfection	42
2.8	Preparation of Cell and Brain Lysates	43
2.9	Detection of soluble and insoluble p62 fractions.....	44
2.10	Co-Immunoprecipitation of HTT and p62	44
2.11	Immunoblotting	45
2.12	Filter trap assay	46
2.13	Analysis of autophagic flux by Confocal microscopy.....	46
2.14	Statistical analysis.....	47
3	Results	48
3.1	Effects of GM1 treatment on mHTT levels and mHTT aggregates	48
3.2	Effects of GM1 treatment on autophagy and autophagic flux	50
3.3	Effects of GM1 on HTT-p62 interaction	54
3.4	Figures	57
4	Discussion	77
4.1	GM1 does not change monomeric mhtt levels, but decreases mhtt aggregates	77
4.2	GM1 does not induce autophagy or enhance autophagic flux.....	82
4.3	GM1 modulates the interaction of mHTT with the cargo recognition molecule p62	85
5	Conclusions.....	88
6	References	90

LIST OF FIGURES

Figure 1.3.1:	Molecular mechanism of autophagy.....	33
Figure 1.3.2:	Huntingtin is a key player in cargo recognition and induction of selective autophagy.....	35
Figure 1.4.1:	Ganglioside biosynthesis.....	36
Figure 1.4.2:	Ganglioside GM1.....	37
Figure 3.1.1:	GM1 does not change monomeric full-length mHTT levels in the cortex of the Q140 mouse model.....	57
Figure 3.1.2:	GM1 does not affect degradation rate of wt or mHTT N-terminal fragments in immortalized striatal cells in serum-free medium.....	58
Figure 3.1.3:	Treatment with GM1 does not change wt or mHTT N-terminal fragment levels in transiently transfected striatal ST14A cells.....	59
Figure 3.1.4:	GM1 decreases mHTT aggregates in the cortex of R6/2 mice.....	60
Figure 3.1.5:	GM1 decreases mHTT aggregates in the striatum of Q140/Q140 mice	61
Figure 3.2.1:	Levels of LC3-II and p62 in the striatum and cortex of Q140 mice are not modulated by GM1 treatment.....	63
Figure 3.2.2:	Levels of LC3-II and p62 are not significantly affected by treatment with GM1 in the cortex of R6/2 or YAC128 mice.....	64
Figure 3.2.3:	100 nM bafilomycin efficiently block autophagic degradation in striatal 7/7 and 111/111 cells.....	65
Figure 3.2.4:	GM1 does not change LC3-II levels in striatal 7/7 or 111/111 cells.....	66
Figure 3.2.5:	GM1 does not change p62 levels in 7/7 or 111/111 cells.....	68
Figure 3.2.6:	P62 levels decrease in serum-free medium conditions when protein synthesis is inhibited.....	69
Figure 3.2.7:	GM1 does not change levels of autophagy markers in striatal HTT N548-15Q or HTT N548-128Q cells.....	70
Figure 3.2.8:	RFP-EGFP-LC3 in nutrient-rich and EBSS conditions.....	72
Figure 3.2.9:	GM1 does not affect autophagic flux in striatal 111/111 cells transiently transfected with RFP-EGFP-LC3.....	73
Figure 3.3.1:	P62 binding to HTT in striatal cells is enhanced when the polyQ stretch is expanded.....	74
Figure 3.3.2:	Normal p62-body formation in striatal 111/111 cells.....	75
Figure 3.3.3:	GM1 modulates binding of p62 to mHTT.....	76

ABBREVIATIONS

aa	amino acid
A β	amyloid- β
AD	Alzheimer's disease
AKT	protein kinase B
ALS	Amyotrophic lateral sclerosis
AMPK	adenosine monophosphate-activated protein kinase
APS	ammonium persulfate
ASO	antisense oligonucleotide
α -syn	α -synuclein
ATG	autophagy-related gene
B3galT4	Beta-1,3-galactosyltransferase 4
B4galT1	Beta-1,4 N-acetylgalctosaminyltransferase 1
Baf	Bafilomycin A1
BATS	Barkor/ATG14L autophagosome-targeting sequence
BDNF	brain derived neurotrophic factor
BNIP3	bcl2/adenovirus E1B 19 kDa interacting protein 3
BSA	bovine serum albumine
Ca ²⁺	calcium
caspase	cysteine-aspartatic protease
Cer	ceramide
CMA	chaperone-mediated autophagy
CO ₂	carbon dioxide
Co-IP	co-immunoprecipitation
Cp-A	cleavage product A
Cp-B	cleavage product B
CREB	cAMP response element binding protein
CSF	artificial cerebrospinal fluid
CT	computerized tomography
DAT	dopamine transporter
DMEM	Dulbecco's modified Eagle's medium
DMP	dimethyl pimelimidate

DNA	deoxyribonucleic acid
Drp1	dynamain-related protein 1
DTI	diffusion tensor imaging
DTT	dithiothreitol
EBSS	Earl's balanced salt solution
EDTA	ethylene diamine tetraacetic acid
EGTA	ethylene glycol tetraacetic acid
ER	endoplasmic reticulum
ERK	extracellular-signal-regulated kinase
FIP200	focal adhesion kinase-family interacting protein of 200 kDa
g	gram
GABA	γ -aminobutyric acid
GABARAPL1	(GABA) receptor-associated protein like 1
GDNF	glial derived neurotrophic factor
GFP	green fluorescent protein
GFR α 1-Ret	(GDNF)-mediated activity of GDNF family receptor alpha-1-Ret
Glc-Cer	Glucosyl-ceramide
Golgi	Golgi apparatus
h	hour(s)
HAP1	huntingtin-associated protein 1
HCl	hydrogen chloride
HDAC	histone deacetylase
HIP1	huntingtin-interacting protein 1
HIP14	huntingtin-interacting protein 14
HIPPI	HIP1 protein interactor
HD	Huntington's Disease
HSB	huntingtin stress body
Hsc70	heat-shock cognate protein of 70 kDa chaperone
HTT	huntingtin
K	lysine
L	liter
Lac-Cer	Lactosyl-ceramide
LAMP1	lysosome-associated membrane glycoprotein 1
LAMP2A	lysosome-associated membrane glycoprotein 2 A

LC3	microtubule-associated protein 1A/1B-light chain 3
mg	milligram
mHTT	mutant huntingtin
min	minute(s)
miRNA	microRNA
mM	millimolar
MMP10	matrix metalloproteinase 10
MRI	magnetic resonance imaging
mRNA	messenger RNA
mTORC1	mammalian target of rapamycin complex 1
Na ⁺	sodium
NBR1	neighbor of BRCA1 gene 1
NCoR	nuclear receptor co-repressor
NF-κB	nuclear factor κ-light-chain-enhancer of activated B cells
NGF	nerve growth factor
NH ₄ Cl	ammonium chloride
NLB	NP40 lysis buffer
nM	nanomolar
NMDA	N-methyl-D-aspartic acid
NMDAR	N-methyl-D-aspartic acid receptor
NP40	Igepal CA-630
NRSE	neuron-restrictive silencer element
Opti-MEM	Opti-Minimal Essential Medium
PAGE	polyacrylamide gelelectrophoresis
PCM1	pericentriolar material 1 protein
PD	Parkinson's disease
PDGF	platelet-derived growth factor
PGC-1α	peroxisome proliferator activated receptor γ coactivator 1 α
PE	phosphatidylethanolamine
PFA	paraformaldehyde
PI3K	class III phosphoinositide 3-kinase
PI3P	phosphatidylinositol 3-phosphate
polyQ	poly-glutamine
PPMP	D-threo-PPMP

REST	repressor element 1-silencing transcription factor
RFP	red fluorescent protein
RNA	ribonucleic acid
rpm	revolutions per minute
rt	room temperature
S	serine
SCA3	Spinocerebellar ataxia type 3
SDS	sodium dodecyl sulfate
sec	second
SFM	serum-free medium
Sp1	specificity protein 1
St3gal2	Beta-Galactoside alpha-2,3-sialyltransferase 2
St3gal5	Lactosylceramide alpha-2,3-sialyltransferase
St8sia1	Alpha-N-acetylneuraminide alpha-2,8-sialyltransferase 1
St8sia3	Alpha-N-acetylneuraminide alpha-2,8-sialyltransferase 3
TAF4	TATA box binding protein-associated factor 4
TAFII30	TATA box binding protein-associated factor, 30 kDa
TBP	TATA-binding protein
TBS	Tris-buffered saline
TBS-T	(TBS)-Tween-20
TEMED	tetramethylethylenediamine
TIM23	translocase of the inner membrane 23
TLB	Triton lysis buffer
TrkA/B	tropomyosin receptor kinase A/B
TRPC5	T type channels and transient receptor potential channel 5
Ube3a	ubiquitin protein ligase E3A
Ugcg	UDP-glucose ceramide glucosyltransferase
ULK1/2	Unc-51 like autophagy activating kinase 1/2
UPS	ubiquitin-proteasome system
Vac8	vacuolar protein 8
Vps34	vacuolar protein sorting 34
wtHTT	wild-type huntingtin
WT	wild-type
YAC128	yeast artificial chromosome 128

1 BACKGROUND

1.1 HUNTINGTON'S DISEASE

1.1.1 General introduction

Huntington's disease (HD) is a dominantly inherited neurodegenerative disorder that occurs with a prevalence of 3-10 patients per 100 000 individuals in Western Europe and North America (1). The disease was first described by George Huntington in the 19th century. He reported irregular and spasmodic action of certain muscles (chorea), often accompanied by more subtle symptoms such as depression, behavioral disturbance, memory impairment and personality changes (2).

Much later, in 1993, the disease-causing gene was discovered. Located on the short arm of chromosome 4 (4p16.3), the HD (or HTT) gene codes for a ubiquitous protein termed huntingtin (HTT) (3). It is characterized by the presence of a polymorphic stretch of CAG repeats in the first gene exon, which is translated into a poly-glutamine (polyQ) tract at the N-terminus of HTT. Expansion over 36 CAG repeats leads to adult HD with a typical age of onset between 35 and 50 years, while expansion over 56 repeats leads to juvenile HD which usually manifests before age 20 (4). Although HTT is a ubiquitously expressed protein, cell degeneration is mostly found in the brain (5).

1.1.2 Neuropathology

The pathological hallmark of HD is the severe atrophy of the caudate nucleus and the putamen in the striatum. The medium-sized projection spiny neurons are the most affected cells in these brain areas and undergo cell death (5). Loss of neurons is followed by astrogliosis. Medium-sized projection spiny neurons receive dopaminergic input from the substantia nigra and glutaminergic input from cerebral cortex and thalamus. Their output

signal is the inhibitory transmitter γ -aminobutyric acid (GABA), together with dynorphin, enkephalin or substance P as co-transmitters. Interestingly, enkephalin-expressing neurons are more susceptible to degenerate in HD. Overall, loss of the inhibitory input from the striatum causes the typical uncontrolled movements in HD (5). The striatum is not the only affected brain area in HD. Atrophy also occurs in layers III, V, and VI of the cerebral cortex, as well as in the globus pallidus, thalamus, subthalamic nucleus, substantia nigra, white matter, hypothalamus, and the cerebellum (4).

The recent development of imaging studies by magnetic resonance imaging (MRI), computerized tomography (CT) scan, or diffusion tensor imaging (DTI) and their combination with physical and mental performance studies has led to the understanding that neuropathological changes occur well before the onset of evident symptoms in HD patients (6, 7). These early neuropathological changes occur in both grey (7, 8) and white matter (9-11). In fact, it was recently shown that white matter changes in the corpus callosum might even precede gray matter atrophy (9, 10). Degeneration of the corpus callosum progresses from more posterior areas in pre-HD patients to anterior regions in advanced stages of HD (10). Neuropathology in both caudate nucleus and putamen is more prominent caudally in early HD stages and progresses in a dorsomedial to ventrolateral direction (8, 12). Volumetric loss of the caudate and shrinkage of the putamen are observed approximately 10 and 3 years before disease onset, respectively (13). In line with this, regional cortical thinning is already detectable in pre-HD patients (6). These early neuropathological changes progress through the course of the disease and together lead to about 25% reduction in total brain weight in advanced HD (14, 15). The assessment of distinct brain areas in advanced HD yielded the following volumetric reductions: 20% cortex, 30% cerebral white matter, 60% striatum, 55% globus pallidus, 30% thalamus (16-18).

1.1.3 Cellular and tissue distribution of huntingtin

HTT is a ubiquitously expressed protein in eukaryotes, and primitive polyQ sequences are conserved as far back as to the deuterostome branch (19). In humans and rodents, HTT expression is high in neurons of the central nervous system. Especially high levels are found in cortical pyramidal neurons in layers III and V that project to striatal neurons (20). HTT is a cytosolic protein, but it has also been found associated with various membrane systems, such as the endoplasmic reticulum (ER) (21), the Golgi apparatus (Golgi) (22), mitochondria (23, 24), clathrin-coated vesicles (25), and caveolae (26). It was shown that HTT can reversibly bind to vesicles and the ER with its amphipathic α -helix formed by the first 18 N-terminal amino acids (21). In addition, HTT can be palmitoylated at C214 by palmitoyl transferase huntingtin-interacting protein 14 (HIP14) (27). Palmitoylation anchors many different proteins to the plasma membrane or other membrane-delimited structures in the cell (28). Aside from its direct interaction with membranes, HTT can localize to various intracellular structures via protein-protein interaction. One such example is the localization of mutant huntingtin (mHTT) to mitochondria via binding to dynamin-related protein 1 (Drp1) (23), a protein involved in mitochondrial fission (29). To date, only mHTT has been shown to co-localize with mitochondria (23). HTT can also interact with microtubules by binding to tubulin (30) or dynactin together with Huntingtin-associated protein 1 (HAP1) (31). Furthermore, it was shown that HTT contains a nuclear localization signal between amino acids 174 and 207, that is recognized by the import receptors importin beta1 and transportin (32). Interestingly, HTT was found to detach from membranes during ER stress and to relocalize to the nucleus. Cytoplasm-nuclear translocation was reversible for wtHTT (but not mHTT), which underwent nuclear export once stress conditions ceased (21).

1.1.4 The loss of function of HTT in HD

Although the genetic origin of the disease is known, it is unclear which molecular dysfunction(s) triggered by mHTT is/are causative of disease onset and progression. The HD mutation confers toxic properties to mHTT (gain of function), while at the same time disrupts at least some of the functions exerted by the normal protein (loss of function) (33, 34). It is likely that both loss-and-gain-of-function of mHTT lead to neuronal dysfunction and eventually the loss of specific subsets of neurons, mainly in striatum and cortex. The resulting brain atrophy is a steady and to date unstoppable process that eventually leads to the death of the patient.

HTT is a scaffold protein involved in several pathways and functions. Various studies showed that HTT knockout mice die before gastrulation (35-37), because of HTT's crucial role in embryonic development and in the formation of extra-embryonic tissue (38-41). Furthermore, it was shown that reduction in HTT levels causes defects in epiblast formation and leads to structural changes in cortex and striatum (42, 43). The role of HTT during embryogenesis is obviously not affected by expansion of the polyQ stretch, since both patients harboring the HD mutation and HD animal models are normal at birth. Recently, HTT was shown to play a role during the morphogenesis of the mammary epithelium in mice by mediating polarized apical vesicular transport of proteins involved in this process (44). HTT also regulates the formation of primary cilia from centrosomes by interacting with huntingtin-associated protein1 (HAP1) and pericentriolar material 1 protein (PCM1). HTT depletion lead to decreased levels of PCM1 at the centrosome and impaired ciliogenesis. In contrast, polyQ expansion of HTT increased levels of PCM1 thereby enhancing ciliogenesis of cilia with abnormal shape and disorganized layers (45). HTT also plays a role in the cellular response to heat shock induced stress. While wtHTT-expressing cells were able to recover from this stress response, cells expressing polyQ-expanded HTT were not,

indicating loss-of-function of the mutant protein (46). HTT has anti-apoptotic function and promotes survival of adult neurons by blocking the formation of both the apoptosome and the proapoptotic HIP1 protein interactor/huntingtin interacting protein 1 (HIPPI-HIP1) complex thereby interfering with caspase-3/-9 and procaspase-8 activation, respectively (47-49). HTT exerts these effects by binding and sequestering HIP1, thereby preventing HIP1 binding to HIPPI. Expansion of the polyQ stretch, however, prevents this interaction and thus favors the formation of pro-apoptotic HIP1/HIPPI complexes, resulting in activation of caspase 8 and apoptosis (50). A role for HTT in axonal transport emerged, when it was shown to mediate both anterograde and retrograde transport of brain derived neurotrophic factor (BDNF) vesicles (51). Through its binding to HAP1 HTT modulates the interaction between motor proteins and cargo vesicles and their transport (31, 52). When the polyQ stretch is expanded, however, the strength of the interaction between HTT and HAP1 increases, HAP1 is no longer able to stably bind the motor protein dynactin and consequently transport along the microtubules is impaired (53).

Another important and well characterized role of HTT is as a modulator of the transcription of BDNF. HTT stimulates the transcription of BDNF messenger RNA (mRNA) in the cerebral cortex, from which the BDNF protein is then transported to striatal neurons via the cortico-striatal afferents (54, 55). The role of HTT in BDNF transcription is mediated by HTT binding to repressor element 1-silencing transcription factor (REST), preventing this transcriptional repressor from entering the nucleus and silencing BDNF transcription (56). When HTT is mutated, its interaction with REST is weakened. As a result, REST enters the nucleus where it binds the neuron-restrictive silencer element (NRSE) in the promoter of the BDNF gene, leading to inhibition of BDNF transcription (56).

Recently HTT has been shown to play an important role also in selective autophagy, a cellular degradative process that is crucial to maintain cellular homeostasis (57, 58). The role of HTT in autophagy will be illustrated in more detail in sections 1.3.2 and 1.3.3.

1.1.5 The gain-of-function of HTT in HD

An expanded polyQ stretch confers toxic properties not only to huntingtin, but also other polyQ containing proteins, such as ataxin-1, -2, -3, -7, and atrophin amongst others (59). In fact, an expanded polyQ stretch is even toxic by itself when overexpressed in cellular models (60). In HTT, the mutation interferes with the correct folding of the protein and makes it prone to aggregate and to abnormally interact with other proteins. This, in turn, results in the loss of most normal HTT functions (as described above), but also in the gain of new toxic properties that cause mitochondrial dysfunction (24, 61), excitotoxicity (62, 63), transcriptional dysregulation (64), disrupted intracellular transport (53, 65), impaired lipid metabolism (66), and dysfunctional selective autophagy (67).

1.1.5.1 MHTT aggregation and fragmentation

The presence of extra glutamines (> 36) in the polyQ stretch promotes aberrant folding of HTT with the acquisition of β -sheet-rich conformations. These β -sheet-rich structures are prone to oligomerize into fibrils and fibres, which eventually form bigger protein aggregates through a nucleated-growth amyloidogenic process (68) similar to that occurring in Alzheimer disease (AD) for amyloid- β (A β) (69) and in Parkinson disease (PD) for α -synuclein (α -syn) (70). The role of aggregates in HD pathogenesis and progression is still controversial, despite many years of research by many different groups. Aggregates might exert toxicity by sequestering specific proteins such as transcription factors (55, 71) or the UPS components heat shock protein 70 (HSP70), heat shock protein 40 (HSP40), and the 20S proteasome (72). In addition, large mHTT aggregates have been shown to occupy entire cross-sections of axons thereby interfering with axonal transport (65). On the other

hand, mHTT aggregates might be protective, because their formation decreases the concentration of more toxic soluble species of mHTT, and might promote their clearance by selective autophagy (aggrephagy) (73, 74).

The expansion of the polyQ stretch also makes mHTT more susceptible than the normal protein to undergo proteolytic cleavage at specific sites by different proteases, yielding mHTT fragments of various lengths (75). Proteases that cleave HTT are calpains (76, 77), cathepsins D, B, and L (78), matrix metalloproteinase 10 (MMP10) (79), and cysteine-aspartic proteases (caspases) (80-82). Proteolytic cleavage of mHTT can have a major impact on toxicity, aggregation, and subcellular localization, and is therefore more than a mechanism of degradation (83). Amongst the indicated proteases, caspase 6 has gained the most attention, as its N-terminal cleavage product (586 amino acids (aa) fragment) of mHTT has been linked to neurotoxicity. An HD mouse model expressing a caspase 6 - resistant form of mHTT did not develop striatal neurodegeneration nor disease symptoms (84). Moreover, in human HD patients, elevated caspase activity has been demonstrated in neuronal cells and the addition of caspase inhibitors reduced mHTT toxicity (77, 81). Other caspases that generate N-terminal cleavage products of mHTT are caspases 2 and 3 (552 aa fragment – caspase 2; 513 aa and 552 aa fragments – caspase 3) (82). However, expression of caspase 2- or caspase 3-resistant mHTT protein in an HD mouse model did not lead to an improvement of the HD phenotype (84). HD mice lacking caspase 2, on the other hand, were protected from behavioral changes but not from HD-specific pathology, including striatal volume loss and testicular degeneration (80). Calpains cleave HTT at aa 469 and 563 (77). Increased calpain activity has been reported in brains of HD mouse models and human patients (75-77). Inhibiting calpain cleavage at both cleavage sites reduced mHTT toxicity in cell culture (76, 77). The lysosomal aspartyl proteases cathepsins D, B, and L can also cleave HTT (78), generating N-terminal fragments called cleavage

product (cp)-A and -B, that are major components of nuclear and cytoplasmic inclusions, respectively (85). The length of N-terminal fragments produced by cathepsin-cleavage can only be estimated, as the exact cleavage sites have not been identified yet. Cp-A is between 104 and 114 aa long, whereas cp-B has an estimated size of 205 and 214 aa. The role of these HTT fragments in HD pathogenesis is not known yet. MMP10, a calcium-dependent zinc-containing endopeptidase, cleaves HTT at aa 402 (79). MMP10 levels are increased in HD mouse models indicating that this protease might play a role in HD pathology (79). Finally, N-terminal HTT fragments have been shown to be generated by alternative splicing (86). Mutant HTT exon1 has been shown to be highly pathogenic in HD mouse models (87). Even non-polyQ containing C-terminal fragments of HTT were recently found to cause toxicity by dilation of the endoplasmic reticulum (ER) and increased ER stress (88).

1.1.5.2 Mitochondrial dysfunction

Mitochondrial defects in HD have been described by many groups and are present even in pre-symptomatic patients (4, 89). Impaired energy metabolism in the basal ganglia and thalamus of HD patients is suggested by depleted levels of N-acetylaspartate (89), a CNS-specific metabolite the synthesis of which depends on mitochondrial function (90). In line with reduced mitochondrial function, an increase in lactate levels is also observed in affected brain areas in HD patients, suggesting a shift from aerobic energy metabolism to glycolysis (89, 91). Biochemical studies revealed decreased activity of the mitochondrial respiratory complex I (92, 93), as well as II, III, and IV (94, 95), all of which are involved in oxidative phosphorylation. Mitochondria isolated from lymphoblasts from HD patients show decreased resistance to Ca^{2+} challenge compared to normal mitochondria and membrane depolarization occurring at lower Ca^{2+} load (24). Mitochondrial dysfunction in HD is likely to depend on both direct and indirect effects of mHTT. In fact, certain aspects of mitochondrial dysfunction can be reproduced in normal mitochondria by incubation with mHTT fragments

(96). A mechanism linking mHTT and mitochondrial dysfunction was described very recently by which mHTT directly interacts with the TIM23 mitochondrial protein import complex, thereby inhibiting mitochondrial protein import and causing neuronal death (97). In addition to its direct effects on mitochondria, mHTT also represses expression of the peroxisome proliferator activated receptor γ coactivator 1 α (PGC-1 α), a transcriptional coactivator and master regulator of the expression of genes involved in mitochondrial biogenesis and respiration (98). Finally, accumulation of dysfunctional mitochondria might result from impaired selective autophagy of mitochondria (mitophagy) (67). The role of HTT in selective autophagy will be discussed in section 1.3.2.

1.1.5.3 Excitotoxicity

The term excitotoxicity describes the process by which neurons are damaged or destroyed by prolonged or excessive exposure to the neurotransmitter glutamate, leading to overactivation of NMDA receptors followed by increased and sustained Ca^{2+} influx and mitochondrial damage. Early studies found that injection of NMDA receptor agonists such as quinolinic acid can replicate, in mouse models, the selective loss of striatal neurons that occurs in HD (99). In addition, administration of the mitochondrial toxin 3-nitropropionic acid caused striatal lesions resembling HD that were rescued by NMDAR antagonists (100). These early studies suggested that excitotoxicity could play an important role in the pathogenesis of HD. Indeed, increased glutamate release together with reduced reuptake by astrocytes was found in HD (101, 102). In addition, increased concentration and activity of extrasynaptic NMDAR, major players in excitotoxic neuronal death (103), were found in striatal neurons in a transgenic mouse model of HD (104-106). Activation of extrasynaptic NMDAR was also shown to increase levels of soluble and more toxic species of mHTT (105). The exact pathway that leads from expression of mHTT to increased extrasynaptic NMDARs in striatal neurons is still unknown.

1.1.5.4 Transcriptional dysregulation

Transcriptional dysregulation in HD has been reported by many groups and was shown to occur early in the disease, even before the onset of symptoms. The expression of hundreds of genes is affected, including metabotropic and ionotropic receptor subunits (73). It was found that mHTT can bind to deoxyribonucleic acid (DNA) directly to disrupt transcription. In addition, it interacts with several specific proteins involved in transcription, including the nuclear receptor co-repressor (NCoR), the TATA-binding protein (TBP), the TATA box binding protein-associated factor, 30 kDa (TAFII30), p53, specificity protein 1 (Sp1), and REST, thereby altering their activity (55, 73, 107, 108). As described earlier mHTT has also been shown to bind the promoter of PGC-1 α preventing cAMP response element binding protein/ TATA box binding protein-associated factor (CREB/TAF4) activation (98). In addition, mHTT causes a myriad of epigenetic changes in HD cells, including histone acetylation (109, 110), methylation (111, 112), ubiquitylation (113), and phosphorylation (114), as well as DNA methylation (115) at specific loci, leading to transcriptional dysregulation. Histone acetylation, which facilitates transcriptional activity, is reduced in HD models (109) as well as in HD patients (110). Hypoacetylation of histones H3 and H4 was also found in cells transfected with mHTT and administration of histone deacetylase (HDAC) inhibitors reversed this phenotype (116). Changes in histone methylation, which generally inhibits transcriptional activity, were also observed in HD. An increase in di-methylation and tri-methylation of histone H3 lysine 9 was detected in HD mice (111) and patients (117). A reduction in histone H3 lysine 4 trimethylation at transcriptionally repressed promoters in an HD mouse model and in human brain were also found (112). This latter methylation, however, is associated with activation of genes (118). Lastly, microRNA (miRNA) deregulation also contributes to altered gene transcription in HD. Various miRNAs have been shown to be decreased in HD, which in turn leads to de-repression and increased translation of target mRNAs (119-121). Interestingly, mHTT has also been shown to be

directly involved in the processing of miRNAs as it associates with Argonaute proteins that are catalytic components of the RNA-induced silencing complex (122).

1.1.6 Treatment strategies

A wealth of treatment strategies to target the above described pathogenic mechanisms induced by mHTT are under investigation. Treatments that target mitochondrial dysfunction and energy deficits, such as CoenzymeQ₁₀ and creatine have failed to provide any significant benefit in clinical trials (123-125), in spite of initial encouraging results in animal models (126, 127). Strategies to target excitotoxicity (128, 129), to increase BDNF levels with gene therapy (130) or BDNF-releasing cell grafts (131, 132), to target transcriptional dysregulation with histone deacetylation (HDAC) inhibitors (133, 134), or to prevent proteolytic cleavage of mHTT into more toxic N-terminal fragments by inhibiting the responsible proteases (135-137) are still at the preclinical stage or very early clinical evaluation. Because of the vast array of cellular and molecular dysfunctions triggered by mHTT, treatments that target individual dysfunction might lead to only limited, if any, benefits.

The best success in treating the disease might therefore be achieved by inhibiting mHTT expression by RNA interference or by the use of antisense oligonucleotides (ASOs). Strategies to lower HTT levels have been very successful in pre-clinical studies using animal models (138-140) and highly encouraging. In fact, one such strategy using an ASO called 'Isis HTT-Rx' will enter phase I clinical trials this year (Prof. Sarah Tabrizi and Isis Pharmaceuticals, Inc will be lead investigators). A potential problem with this specific treatment is that it also targets normal HTT RNA (HD patients are generally heterozygous for the HD mutation and carry one mutant and one wt allele) and a loss of the normal HTT protein might result in side effects. Targeting only and specifically the mutant allele is desirable and also under investigation (141).

Another approach to diminish overall levels of the toxic mHTT protein in the cell is to enhance its cellular degradation. Indeed, a few studies have shown that upregulation of degradative pathways reduced mHTT levels and resulted in decreased toxic effects in both cell and animal models (142, 143).

1.2 PROTEOSTATIC MECHANISMS IN HD

1.2.1 Cellular degradation of mHTT

Neurons rely heavily on intracellular protein quality control systems and protein degradation pathways as they are post-mitotic cells and cannot simply dilute misfolded or aggregated proteins by cell division. Mutant HTT is one such misfolded and aggregation-prone protein and can be degraded by the ubiquitin-proteasome system (UPS) or by autophagy. The process of autophagy can be further subdivided into macroautophagy, chaperone-mediated autophagy (CMA), and microautophagy. The UPS, macroautophagy and CMA are involved in the degradation of mHTT species, microautophagy is not. While the proteasome and CMA break down only certain species of mHTT, mostly soluble, macroautophagy can degrade all forms of mHTT from fragments and soluble misfolded monomers to protein aggregates. When cells age, both UPS (144) and autophagy (145, 146) become less efficient and HD cells are believed to eventually become overwhelmed with clearing the increased misfolded protein load caused by mHTT expression (147).

1.2.2 UPS

The UPS targets mainly short-lived and misfolded intracellular proteins. These proteins are marked with a poly-ubiquitin chain and targeted to the proteasome, where they are unfolded and proteolytically degraded (147). The proteasome can degrade full-length mHTT or its fragments. Whether the UPS is impaired in HD is controversial, as some groups found dysfunctions while others reported no changes in UPS function in various HD models (148,

149). The mechanism by which mHTT supposedly impairs the proteasome is also not clear. One theory is that polyQ-containing polypeptides might “clog” the proteasome thereby inhibiting its function (150, 151). Enhancing proteasomal degradation by overexpression of the ubiquitin protein ligase E3A (Ube3a), the expression of which is reduced with ageing, has been shown to have beneficial effects in HD cell and animal models (144). This E3 ubiquitin ligase promotes K48-ubiquitination (a modification that targets proteins for proteasomal degradation) of mHTT and when overexpressed reduces K63-ubiquitination (which targets proteins for autophagic degradation) and aggregation of mHTT (144).

1.2.3 CMA

CMA is a degradative process with higher selectivity compared to other forms of autophagy. Only cytosolic proteins containing a specific recognition motif (KFERQ) for the heat-shock cognate protein of 70 kDa chaperone (Hsc70) are translocated into the lysosome via Lysosome-associated membrane glycoprotein 2 A (LAMP2A) for degradation (152). HTT contains two putative recognition motifs, one at amino acids 99-103, and a second one at amino acids 248-252. A third motif at amino acids 14-18 is considered KFERQ-like when it is phosphorylated at serine 16 (153, 154). Experimental evidence shows that a HTT fragment, HTT-552, is indeed transported into the lysosome for degradation (154). CMA selectively targets N-terminal HTT fragments while full-length mHTT is spared (154, 155). CMA activity has been reported to be increased in HD mouse and cell models (155).

1.2.4 Macroautophagy

Macroautophagy (hereafter referred to as autophagy) is important for cell nutrient and energy homeostasis, and it is upregulated during nutrient starvation to break down cell own material to generate energy and new building blocks for protein synthesis (156). In addition, damaged organelles, protein aggregates and intracellular pathogens are also targeted by this process (Figure 1.2.1) (157). Autophagy is the only degradative process in the cell that

can break down all forms of mHTT and therefore it represents an important therapeutic target to reduce overall levels of mHTT in the cell and decrease toxicity. In addition, the removal of dysfunctional mitochondria (mitophagy) is also carried out by autophagy and in HD, as well as in other neurodegenerative conditions, is key to preventing oxidative stress and reactive oxygen species damage (158).

In the next chapter I will describe in detail the process of autophagy and its role in HD.

1.3 ROLE OF AUTOPHAGY IN HD

1.3.1 Molecular steps in autophagy

Most of our knowledge on autophagy comes from studies in yeast (*Saccharomyces cerevisiae*). Many of the autophagy-related genes (ATGs) identified in yeast are conserved in mammals and orchestrate autophagy in a similar manner (156). The process of autophagy can be divided into five stages: i) phagophore formation; ii) ATG5-ATG12 conjugation, interaction with ATG16L and multimerization at the phagophore; iii) Microtubule-associated protein 1A/1B-light chain 3 (LC3) processing and insertion into the phagophore membrane; iv) capture of cargo (selective or unselective) and v) autophagosome-lysosome fusion, followed by degradation of cargo by lysosomal proteases (Figure 1.3.1).

i) Phagophore formation: The phagophore is a double membrane system that, in mammals, is probably derived from the endoplasmic reticulum (ER), the trans-Golgi or endosomes (159, 160). The formation of phagophores requires the assembly of a large macromolecular complex consisting of class III phosphoinositide 3-kinase (PI3K), vacuolar protein sorting 34 (Vps34), Beclin-1, ATG14 and ATG15. This complex generates phosphatidylinositol 3-phosphate (PI3P), which is essential for phagophore elongation and recruitment of other ATG proteins to the phagophore. The activity of the mentioned complex is dependent on

Unc-51 like autophagy activating kinase 1 (ULK1) and Unc-51 like autophagy activating kinase 2 (ULK2), ATG13 as well as on focal adhesion kinase (FAK)-family interacting protein of 200 kDa (FIP200) (161).

ii) ATG5-ATG12 conjugation: ATG7 (acts like an E1 ubiquitin activating enzyme) binds to ATG12 and activates it. Subsequently ATG12 is transferred to ATG10 (an E2-like ubiquitin carrier protein), which mediates conjugation of ATG12 to ATG5. Finally, ATG5-ATG12 forms a multimeric complex with ATG16L which is thought to induce membrane curvature into the phagophore by recruiting LC3-II (156).

iii) LC3 processing: Upon induction of autophagy the mammalian homologue of ATG8, microtubule-associated protein light chain 3 (LC3), is proteolytically cleaved by ATG4 to generate LC3-I, which now presents a glycine residue on its carboxy-terminus. This residue is activated by ATG7 (again acting like an E1 ubiquitin-activating enzyme). Then LC3-I is transferred to ATG3 (an E2-like carrier protein) and a phosphatidylethanolamine (PE) residue is conjugated to the glycine at the carboxy-terminus. As mentioned in ii) the multimeric ATG5-ATG12-ATG16L complex recruits LC3-II to the phagophore where it can integrate into both sides of the double membrane system through its lipophilic PE molecule. LC3-II is necessary for hemi-fusion of phagophore membranes and for binding cargo recognition or adapter molecules. LC3-II is the only autophagy-related protein that remains attached to the autophagic membrane throughout the whole process of autophagy, whereas all other autophagy-related proteins diffuse off the phagophore when the latter closes into an autophagosome (156). The measurement of LC3-II levels in the presence of an inhibitor of autophagic flux (i.e. bafilomycin A1) is commonly used as a marker of induction of autophagy.

iv) Capture of cargo: Phagophores can engulf cargo in a non-selective manner by randomly trapping cytosolic cargo in their lumen, or they can target specific cargo. LC3-II is thought to be involved in selective cargo recognition as it interacts with cargo recognition or adaptor molecules on target structures such as protein aggregates or mitochondria. The best known adaptor molecule is p62, which recognizes and binds K63-polyubiquitinated proteins and protein aggregates. Since p62 is also degraded via autophagy it is commonly used as a marker for autophagic flux (a measure of how much cargo is being degraded in a certain time) (156). Other known adaptor molecules in mammalian cells are bcl2/adenovirus E1B 19 kDa interacting protein 3 (BNIP3, which recognizes mitochondria) (162) or neighbor of BRCA1 gene 1 (NBR1, which - like p62 - recognizes polyubiquitinated protein aggregates) (163). An interdependence between NBR1 and p62 has been described, in which p62 body formation was reduced when NBR1 expression was inhibited (163). Interestingly, NBR1-containing aggregates can form in cells lacking p62. It is not clear, however, if these aggregates can substitute for p62 bodies. Details on selective cargo recognition will be discussed below.

v) Fusion with lysosome: Once the phagophore has engulfed the cargo, the two loose membrane ends fuse together to form an autophagosome. This autophagosome then fuses with lysosomes generating an autolysosome, which has an acidic lumen and contains degradative enzymes such as cathepsins B and D. It has also been suggested that autophagosomes can fuse with early and late endosomes as well (156, 164). As autophagosome formation in neurons occurs mainly in neurites and synaptic terminals in the distal axon, transport of autophagosomes along microtubules back to the cell soma, where the bulk of lysosomes is located (165), is crucial in neurons (166). In fact, drugs that disrupt microtubules also block the generation of autolysosomes (167). A very important protein for the transport of autophagosomes (168) and endosomes (169) along microtubules

is Rab7. This protein is also involved in the biogenesis and maintenance of lysosomes (170), as well as the fusion of autophagosomes with lysosomes (171).

1.3.2 Nutrient-dependent and selective autophagy

There are two different forms of autophagy, namely nutrient-dependent and selective autophagy. Nutrient-dependent autophagy is activated during nutrient (i.e. amino acids, growth factors, or glucose) deficiency and breaks down cytosolic proteins to provide the cell with recycled essential molecules. Due to its lack of specificity and the engulfment of random cargo this process is also called bulk autophagy. In contrast, selective autophagy, which is also active when nutrients are abundant, ensures quality control of proteins and organelles by degradation of specific targets such as protein aggregates, dysfunctional mitochondria or other organelles. As mentioned above, specific selection of cargo is carried out by adapter molecules such as p62, NBR1 (recognize protein aggregates) or BNIP3 (recognizes mitochondria) (172). Both forms of autophagy follow the same mechanism of phagophore, autophagosome, and autolysosome formation followed by degradation of the cargo (described above). So how are the two different forms of autophagy activated and regulated?

For nutrient-dependent autophagy the induction process has been long known and is studied in detail. The main regulator of this autophagy pathway is the mammalian target of rapamycin complex 1 (mTORC1), which, when nutrient levels are high, represses autophagy by phosphorylating ULK1 at serine residue 757 to repress its kinase activity (173) and therefore its ability to induce phagophore formation through phosphorylation of beclin-1 (174), FIP200 (175) and ATG13 (176) (Figure 1.2.1). Vice versa, when nutrient levels are low, mTORC1 is inhibited and releases ULK1 to activate nutrient-dependent autophagy (172). Additional activation of ULK1 occurs by phosphorylation at serine residues 317 and 777 by adenosine monophosphate-activated protein kinase (AMPK) when glucose levels

are low (173). In contrast to the well-studied induction of nutrient-dependent autophagy, the activation of selective autophagy has long been elusive. Researchers are just beginning to shed light on key molecules involved in this process. Interestingly, normal HTT was found to be a crucial protein involved in selective autophagy (58). Genetic screens revealed that HTT contains regions with structural similarity to three yeast proteins that are involved in selective autophagy, namely ATG23, Vacuolar protein 8 (Vac8), and ATG11 (57). The N-terminal part of HTT resembles ATG23 (1-586 amino acids (aa)), whereas the C-terminus is similar to ATG11 (1743-3144 aa). The central part of HTT corresponds to Vac8 (807-1653 aa) (57, 177) (Figure 1.3.2). It was demonstrated that the C-terminal part of HTT co-immunoprecipitated with human orthologs of yeast ATG11-interacting proteins, such as p62, BNIP3, ULK1, FIP200, ATG13, the ATG8 homolog (GABA) receptor-associated protein like 1 (GABARAPL1), as well as with the N-terminal region of HTT. The central part of HTT that resembles Vac8 co-immunoprecipitated with beclin-1 (57). Studies performed by another group showed co-immunoprecipitation of the central part of HTT with ULK1 (58). It was found that the latter interaction with ULK1 is crucial for the induction of selective autophagy. HTT binds ULK1 and thereby releases it from its inhibitory association with mTORC1. ULK1, when bound to HTT initiates autophagosome formation for selective autophagy (58). Another group recently reported that a myristoylated (myr) caspase 3 - and 6- HTT cleavage product, myr-HTT₅₅₃₋₅₈₆, induced autophagosome formation, even in nutrient-rich conditions. Myristoylation of HTT₅₅₃₋₅₈₆ was reduced with polyQ expansion and blocking myristoylation resulted in abrogation of autophagosome induction (178). It was shown that HTT₅₅₃₋₅₈₆ shares sequence homology with the Barkor/ATG14L autophagosome-targeting sequence (BATS) domain of ATG14L (178). This BATS domain is involved in sensing and maintaining membrane curvature of the phagophore and in the recruitment of ATG proteins to the isolation membrane (179). Furthermore, it was shown that alkyl chains of fatty acids (such as those found in myristate) can sense membrane curvature (180). Based on these findings

it was postulated that the myr moiety of HTT₅₅₃₋₅₈₆ may be involved in facilitating membrane curvature, while the HTT₅₅₃₋₅₈₆ fragment may stabilize membrane curvature and/or recruit ATG proteins to the phagophore (178).

Not only does normal HTT facilitate the induction of selective autophagy, but it also functions as a scaffold for p62-mediated cargo recognition. It was proposed that p62 needs to be bound to HTT in order to be able to recognize, bind, and guide K63-polyubiquitinated proteins to autophagosomes. In line with this, knockdown of HTT results in diminished formation of p62 bodies, which are made up mostly of p62 and K63-polyubiquitinated proteins that are meant to undergo autophagic degradation (58). Expansion of the polyQ stretch in HD might be expected to affect HTT interaction with autophagic proteins. As detailed below, autophagy is indeed affected at multiple levels in HD.

1.3.3 Impaired autophagy in HD

Changes in autophagy in HD patients' brains were described already in the 1970s, when an abnormal proliferation of endosomes and lysosomes was reported (181). In line with this finding, striatal neurons from HD patients showed an increase in endosome-lysosome-like organelles and HTT-immunoreactive tubovesicular structures compared to healthy controls (182). In addition, enhanced autophagosome counts have been reported in HD mouse models and human fibroblasts from HD patients (67). What triggers the enhanced formation of autophagy related structures? It was found that mTORC1 is sequestered by mHTT aggregates, leading to inhibition of its activity and to induction of autophagy (142). Given this evidence, one might think that the rate of protein degradation is increased in HD. This is, however, not the case. Although autophagosomes form at normal or even enhanced levels in HD cells, they fail to efficiently trap specific cargo such as mitochondria, protein aggregates, or lipid droplets in their lumen (67). In electron micrographs HD autophagosomes appear empty. It has been proposed that reduced amount of cargo in

autophagosomes might be due to an increased and aberrant interaction between mHTT and p62, which would decrease the efficiency by which p62 performs cargo recognition and recruitment (67).

In addition to its recently recognized role in selective autophagy, HTT is also involved in vesicular transport through its interaction with HAP1 (see section 1.1.4). Retrograde transport of autophagosomes is crucial to fusion with lysosomes and formation of autolysosomes. Recent evidence shows that in neurons, HTT and HAP1 colocalize with autophagosomes and mediate their intracellular transport by regulating dynein and kinesin motors. When mHTT was expressed in the same neurons, autophagosome transport and subsequent degradation of cargo was impaired (166). In another study, expression of mHTT in fibroblasts from HD patients was found to affect lysosomal positioning and to result in perinuclear lysosomal accumulation entailed by increased basal mTORC1 activity (183). The increased basal mTORC1 activity measured in this study stands in contrast to previous work describing decreased mTORC1 activity due to the complex being trapped within mHTT aggregates (142).

1.4 GANGLIOSIDES IN THE BRAIN

1.4.1 Gangliosides: complex glycosphingolipids with pleiotropic functions

Gangliosides are sialic acid containing glycosphingolipids comprising a ceramide backbone and a complex oligosaccharide headgroup. Highest levels of gangliosides can be found at the plasma membrane with the sugar residues facing the extracellular space (184). Gangliosides are also present in smaller quantities inside the cell located to organelles or vesicles (184). *De novo* synthesis of gangliosides (reviewed by (184) and demonstrated in Figure 1.4.1) begins with the formation of ceramide (Cer) at the endoplasmic reticulum from

which it is transported via a yet unknown mechanism to the Cis-Golgi where it is inserted into the membrane facing the cytosolic side (184), glucosylated by the UDP-glucose ceramide glucosyltransferase (*Ugcg*) (185) and flipped to the lumen of the cis-Golgi stack (184). There, lactosyl-ceramide synthase catalyses the galactosylation of glucosyl-ceramide (Glc-Cer) to lactosyl-ceramide (Lac-Cer). Lac-Cer is then sialosylated to GM3 by the Lactosylceramide alpha-2,3-sialyltransferase (*St3gal5*, also known as GM3 synthase). GM3 is sialosylated to GD3 by Alpha-N-acetylneuraminide alpha-2,8-sialyltransferase 1 (*St8sia1*, also known as GD3 synthase), and GD3 is sialosylated to GT3 by Alpha-N-acetylneuraminide alpha-2,8-sialyltransferase 3 (*St8sia3*, also known as GT3 synthase). GM3, GD3, and GT3 give rise to a-series, b-series, and c-series gangliosides, respectively (184). In the adult brain, the most common gangliosides are GM1, GD1a, GD1b and GT1b (186), with the first two belonging to the a-series and the latter two to the b-series gangliosides. Beta-1,4 N-acetylgalctosaminyltransferase 1 (*B4galnt1*, also known as GM2/GD2 synthase) is the first enzyme involved in the synthesis of more complex gangliosides from GM3 and GD3 by attaching N-acetylgalactosamine and giving rise to GM2 and GD2, respectively (184). GM2 and GD2 are galactosylated by Beta-1,3-galactosyltransferase 4 (*B3galt4*, also known as GM1/GD1b synthase) to produce GM1 and GD1b, respectively. Beta-Galactoside alpha-2,3-sialyltransferase 2 (*St3gal2*, also known as GD1a/GT1b synthase) generates GD1a from GM1 and GT1b from GD1b (184). All glycosylations occur in the Golgi, with earlier glycosylations taking place in the cis/medial Golgi and later ones in the trans Golgi (187). Gangliosides leave the Golgi via budding vesicles to reach their final destination (184). They are primarily found at the outer leaflet of the plasma membrane, but are also located to intracellular membrane systems (186). In the plasma membrane, gangliosides together with proteins, sphingomyelin and cholesterol are components of membrane microdomains called 'lipid rafts' (188). There they take part in cell-cell-adhesion through direct interaction with membrane proteins or facilitating interaction

of other binding partners. In addition, gangliosides modulate cell signaling through regulating membrane receptor activities (186). Examples of biological processes activated by such ganglioside actions in the brain include neurite outgrowth and axon-myelin interaction for example (189, 190). While GM1 ensures proper compartmentalization of glial (neurofascin-155) and axonal (contactin-associated protein 1) proteins in paranodal structures (191), both GD1a and GT1b interact with myelin-associated glycoprotein to ensure proper myelination of axons (192). In intracellular membranes gangliosides play a role in modulating biological processes such as clathrin-independent endocytosis (193), apoptosis (194), and autophagy (195). GD3 specifically has been shown to interact with autophagic molecules PI3P, LC3-II and Lysosome-associated membrane glycoprotein 1 (LAMP1), where it takes part in the biogenesis and maturation of autophagic vacuoles (196). Vice versa, reduced GD3 levels by knockdown of *St8sia1* (encodes the enzyme that generates GD3 from GM3) lead to impairments in autophagy (196). Other gangliosides could play a role in the induction of autophagy in astrocytes, as a ganglioside mix containing GM1, GD1a, GD1b, and GT1b activated autophagy via activation of Nuclear factor κ -light-chain-enhancer of activated B cells (NF- κ B) (195). GM1, one of the molecules present in the ganglioside mix, might play a role in autophagy. In fact, brains of mouse models with GM1 gangliosidosis, a genetic condition that leads to impaired degradation and accumulation of ganglioside GM1 within lysosomes (197), show enhanced autophagy (198). Inhibition of ganglioside synthesis (including GM1) in PD models lead to autophagy inhibition due to impaired autophagosome-lysosome fusion, downregulation of beclin-1 and ATG5 and upregulation of mTORC1. Interestingly, GM1 administration reversed both lysosomal pathology and impairment of autophagy in these models (199, 200). Further specific functions of GM1 in the brain are discussed below (Chapter 1.4.2).

Defects in ganglioside synthesis cause severe neurodegeneration and neurological symptoms (201, 202), highlighting the crucial role of gangliosides in the nervous system. In humans, mutation of the gene encoding GM3 synthase results in expression of a dysfunctional enzyme leading to infantile-onset epilepsy syndrome, brain atrophy, and blindness (201). GM2/GD2 knockout mice display motor dysfunction and deficits in strength, coordination, and balance (203). Aberrant ganglioside synthesis has been described in Alzheimer's disease (AD) (204), amyotrophic lateral sclerosis (ALS) (205) and HD (66).

1.4.2 GM1 and its functions in the brain

GM1 (Figure 1.3) is a ganglioside the structure of which is constituted by ceramide attached to a glycan made of glucose, galactose (2x), acetylgalactosamine, and N-Acetylneuraminidate (sialic acid). The ceramide moiety of GM1 can have differing lengths and saturation of its fatty acid chain (206). GM1 is enriched in the brain and is a component of membrane microdomains known as lipid rafts (186). Besides residing in the plasma membrane, GM1 can localize to many different places in the cell, such as early, recycling and late endosomes, lysosomes, as well as to the trans Golgi network, and the endoplasmic reticulum. Depending on the length and saturation of its fatty acid chain, GM1 is trafficked differently in the cell (206). GM1's cellular functions are manifold as it plays a role in ion transport, neuronal differentiation, neurotrophin signaling, cell-cell interactions, and modulating protein aggregation.

Ion transport: GM1 has been shown to be able to modulate ion transport both at the plasma membrane and at intracellular loci. At the plasma membrane GM1 regulates Ca^{2+} influx through T type channels and transient receptor potential channel 5 (TRPC5) (207, 208). Intracellularly, GM1 plays a role in the $\text{Na}^+/\text{Ca}^{2+}$ exchange at the level of nuclear membranes and Ca^{2+} transfer from nucleoplasm to the ER lumen (209, 210).

Neuronal differentiation: In developing neurons, Ca^{2+} signaling is important for neurite outgrowth. As described above, GM1 modulates Ca^{2+} flux and therefore might be involved in neuronal development. In fact, very little GM1 levels are found during neuron migration and mitosis, but levels drastically increase during neurite outgrowth (190). It was shown that endogenous upregulation of GM1 leads to axonal outgrowth via activation of extracellular-signal-regulated kinase (ERK) (211, 212), whereas exogenous application of GM1 triggered the formation of dendrites (213). Dendrite induction needs higher concentrations of GM1 (as is the case for exogenously administered GM1). It has been speculated that exogenously administered GM1 might have additional or even different effects than the endogenously produced ganglioside (214), due to differences in concentrations achieved, intracellular traffic and kinetics of incorporation into various cellular membranes, including the plasma membrane. Whereas endogenous GM1 is integrated into the plasma membrane and other intracellular membranes, most of the exogenously administered GM1 has been shown to be loosely associated with the membrane glycolyx (215), and only part of it is internalized by endocytosis and redistributed to cellular membranes (216).

Neurotrophin signaling: GM1 associates with a number of membrane receptors thereby modulating their activity. It has been shown to enhance nerve growth factor (NGF)-mediated activation of tropomyosin receptor kinase A (TrkA) (217), BDNF-mediated activation of tropomyosin receptor kinase B (TrkB) (218), and glial derived neurotrophic factor (GDNF)-mediated activity of GDNF family receptor alpha-1-Ret ($\text{GFR}\alpha\text{1-Ret}$) (219). In contrast to this, GM1 was shown to block platelet-derived growth factor (PDGF) signaling by forcing the PDGF receptor outside of lipid rafts (220).

Protein aggregation: GM1 has been shown to affect aggregation of β -amyloid ($\text{A}\beta$) and α -synuclein (α -syn), two proteins involved in the pathogenesis of Alzheimer's (AD) and Parkinson's Disease (PD), respectively (221, 222). $\text{A}\beta$ aggregation is a hallmark of AD

pathology and causes neurotoxicity. Intraventricular infusion of GM1 had beneficial effects on early onset AD patients (5 subjects) in an open-label and uncontrolled clinical study, potentially through sequestration of A β by GM1, although a direct effect of GM1 on patient A β levels and neuropathology was not measured (223). In contrast, several studies have demonstrated a direct interaction of GM1 with A β , *in vivo* (224) and *in vitro* (225), and linked this binding to increased seeding and aggregation of A β and increased cytotoxicity (226). Therefore, the role of GM1 in AD remains controversial, especially in light of recent studies showing that genetic disruption of ganglioside biosynthesis (resulting in lack of GM1, but increased levels of the precursor ganglioside GM3) does not improve, but rather worsen, A β -related phenotypes in an animal model of AD (227). GM1 is also able to interact with and inhibit fibrillation of α -syn (222), the aggregation of which is a hallmark of PD pathology (228). In short, depending on the specific protein, GM1 can modulate aggregation potentially through direct interaction with aggregate prone proteins and/or induce conformational changes that lead to enhanced or decreased aggregation.

Due to its neurotrophic and neuroprotective properties, the effect of GM1 on various neurological disorders such as stroke, Parkinson's disease, and spinal cord injury was tested in animal models and in clinical trials. GM1 was suggested to have neuroprotective actions during ischemic lesions in the rat cortex (229), and ameliorated MPTP-induced parkinson-like symptoms in primates while increasing striatal dopamine levels and enhancing dopaminergic innervation of the striatum (230). Moreover, GM1 significantly accelerated the recovery of motor functions in a rat model of spinal cord injury (231). However, the outcomes of early clinical trials using GM1 as a potential treatment for stroke (232, 233), PD (234), or spinal cord injury (235, 236) were not as promising as the experiments in animal models. This might have been due to inadequate dosage of GM1 or its poor blood-brain-barrier permeability (237). However, in both stroke and PD the blood-

brain-barrier is at least partially compromised (238, 239), suggesting that in these conditions, some of the peripherally-administered GM1 could reach the brain. A recent clinical trial in which GM1 was administered to PD patients showed more promising results. PD patients received subcutaneous injections of 200 mg GM1/day for an extended period of 120 weeks (early-start group) (240). A delayed start group received placebo for the first 24 weeks of the trial (delayed-start group). While the early-start group showed a significant improvement in motor scores at week 24, the delayed-start group displayed significant decline on the same tests. The study also showed that use of GM1 for up to 120 weeks resulted in slower disease progression. Positron emission tomography analysis of dopamine transporter (DAT) binding, which correlates inversely with PD progression, revealed increased binding in some striatal regions in patients that had received GM1 (241). A long-term treatment study (5 years) in which PD patients received GM1 by subcutaneous injection supports long-term safety and efficacy of exposure to GM1 (242).

1.4.3 Gangliosides in HD

Recently, Dr. Sipione's research group reported that HD cells produce decreased levels of specific gangliosides (66). While GD1a levels were reduced in YAC128 cortex, GT1b abundance was lower in the YAC128 striatum (the YAC128 mouse model is described in chapter 1.5.1). GM1 levels were decreased in three different cell models of HD (namely STHdh^{111/111} cells, HTT N548-128Q cells, and human fibroblasts from HD patients) and in YAC128 cortical and striatal tissue lysates. In the brain, the decrease in GM1 levels could be cell-type specific as it is recapitulated in primary cultures of HD neurons, but not in primary cultures of astrocytes (66). Whether astrocytes and other brain non-neuronal cells have impaired ganglioside synthesis *in vivo* remains to be investigated. Real-time PCR analysis of enzymes involved in the synthesis of GD1a, GT1b, and GM1 revealed decreased expression of B3galt4 (GM1/GD1b synthase) in the three HD cell lines mentioned above.

Expression of this enzyme was also downregulated in YAC128 cortex, along with St8sia1 (GD3 synthase). In the YAC128 striatum, lower expression levels of Ugcg (UDP-glucose ceramide glucosyltransferase), St3gal5 (GM3 synthase), B4galnt1 (GM2/GD2 synthase), and St8sia3 (GT3 synthase) were detected. Together, these results suggest that mHTT affects the synthesis of specific gangliosides by interfering with expression of enzymes involved in this process. Two studies analyzing GM1 levels in postmortem HD patients showed an increase in the cerebellum, a brain area that is relatively spared in HD, and no statistically significant difference in the caudate, respectively (243, 244). However, due to the low number of human brains analyzed and potential confounding effects related to the stage of neurodegeneration, neuronal loss and astrogliosis in post-mortem tissue, it is still unclear whether GM1 levels are affected in HD patients' brains. Reduced plasma membrane levels of GM1 made STHdh^{111/111} cells more susceptible to stressful stimuli and to undergo apoptosis. Exogenous administration of GM1 restored normal GM1 plasma membrane levels in these cells and protected them from cell death. Interestingly, when GM1 synthesis in normal STHdh^{7/7} cells was inhibited using the pharmacological Ugcg inhibitor D-threo-PPMP (PPMP), the cells became more susceptible to apoptosis and resembled the STHdh^{111/111} cell phenotype, suggesting that reduced GM1 content in HD cells is causative of cell dysfunction. Further studies by our group revealed that chronic intraventricular infusion of GM1 restores motor and non-motor functions in HD mouse models (245-247). The precise mechanism underlying the profound therapeutic effects of GM1 are still unclear. There is evidence, however, that GM1 administration leads to the activation of the pro-survival kinase protein kinase B (AKT) (66). Besides its pro-survival functions, AKT can phosphorylate mHTT at amino acid Ser421, a post-translational modification that was shown to decrease mHTT cleavage and toxicity (248). However, inhibiting the PI3K/AKT pathway led only to a partial loss of GM1 neuroprotection in an HD cell model, indicating that other pro-survival mechanisms must be activated at the same time (66). Another effect of GM1

administration is the phosphorylation of amino acid residues Ser13 and Ser16 in the N-terminal region of mHTT (245). Phosphorylation at these residues has been shown to be of great therapeutic importance, as transgenic mice expressing phosphomimetic (S13D, S16D) mHTT showed reduced motor and psychiatric symptoms, decreased mHTT aggregates and decreased neurodegeneration (249). The mechanism/s by which phosphorylation at these residues decreases mHTT toxicity is/are still under investigation. It has been suggested that this post-translational modification might alter the kinetics of aggregation of mHTT fragments (249). In addition, phosphorylation at Ser13 and Ser16 has been shown to trigger mHTT acetylation at Lys444 and subsequent protein degradation by autophagy (250).

1.5 MODELING HD

1.5.1 Mouse models

Mouse models of HD are meant to provide insight into disease pathology and mechanisms and into the effect of potential therapeutic strategies. HD mice, therefore, need to display typical neuropathology, cellular dysfunction, and symptoms found in human patients. Before the discovery of the *HTT* mutation in 1993, the study of HD in rodents involved the use of toxins such as quinolinic acid (251) or 3-nitropropionic acid (252), which induce excitotoxicity and mitochondrial impairment, respectively, and striatal neurodegeneration. The discovery of the disease-causing gene, however, led to the generation of various transgenic and knock-in mouse models expressing full-length HTT or HTT fragments with polyQ expansions of various lengths. Since these mice carry a similar genetic defect to humans, both HD pathology and progression in these models mirror the human disease more closely than previous chemical animal models. The three mouse models used in my studies are discussed below.

The R6/2 mouse model is a very commonly used transgenic model with a CBAxC57BL/6 background that overexpresses mutant exon 1 of the human *HTT* gene with 144 CAG repeats (87). The large number of repeats corresponds to HD with an early (or juvenile) onset in human patients. R6/2 mice show early behavioural symptoms that include resting tremor, chorea-like movements, and clasping behaviour (87). By 5 weeks of age R6/2 mice show progressive decline in motor ability as revealed by rotarod and beam walking test (253). These mice display progressive and more widespread brain atrophy than in human HD patients with loss of 44% total brain and 41% striatal brain mass at 12 weeks and neuropil aggregates can be found throughout the brain (87). R6/2 mice die young at 10 to 13 weeks of age (87).

The yeast artificial chromosome 128 (YAC128) mouse model is another commonly used transgenic model, originally developed on an FVB/N background, that overexpresses the full-length human *HTT* gene with 128 CAG repeats under control of the human *HTT* promoter (254). Motor symptoms in these mice occur between 8 and 12 weeks of age and are represented by hyperkinesia in an open field test and decreased performance on the rotarod. These behavioral changes correlate with reduced striatal and cortical volume, decreased striatal neuron count and brain weight. Striatal volume is decreased by 15% at 9 months of age, and cortical volume is decreased by 7% at 12 months of age (254). Similar to the human disease, which progresses from chorea to dystonia and rigidity, in these mice an initial hyperkinetic behavior (at 3 months of age) is followed by hypokinesia (at 6 months of age) (255). YAC128 mouse brains show mHTT inclusions in striatal cells at 18 months (254). As these mice display a normal life span, they make a good model to study long-term therapeutic effects of drugs.

The HdhQ140 (Q140) mouse model is a knock-in mouse model with a C57BL/6 background generated by knock-in of the first exon of the human *HTT* gene containing 140 CAG repeats

into the endogenous mouse *HTT* gene (256). Both heterozygous (Q7/Q140) and homozygous (Q140/Q140) mice were developed and characterized. Phenotypically, both HD mouse models are similar as they show the same extent of motor deficits by 10 weeks of age on both fixed and accelerated rotarod (257). In addition, both homo- and heterozygous Q140 mice show a progressive decrease in cortical thickness starting at 6 months of age (257). A study focused on neuropathological changes in homozygous Q140 mice, detected a 38% loss in striatal volume and 40% reduction in the number of striatal neurons compared to WT control mice (258). Nuclear and neuropil inclusion bodies can be found in the striatum, cortex, hippocampus, and cerebellum of Q140 mice (256). Like the YAC128 mouse model, Q140 mice display a normal life-span, which makes them another attractive model for long-term therapeutic studies (4).

1.5.2 Cell models

Cell models of HD represent a useful tool to study molecular mechanisms underlying cell dysfunction in HD in a cell type specific manner. Many neuronal and non-neuronal cell lines have been established to study the effects of full-length HTT or HTT fragments containing various lengths of the polyQ stretch on intracellular processes. Cell lines provide a good and fairly convenient approach to screen therapeutic compounds and to study their effects, before testing in more expensive and complex animal models. The two HD cell models used in my studies are described below.

STHdh^{Q7/Q7} and STHdh^{Q111/Q111} cells are mouse striatal knock-in cells derived from striatal tissue of STHdh knock-in mice at embryonic day 14 and express full-length endogenous mouse HTT with a polyQ sequence containing either 7 or 111 glutamines (259). Both WT and HD cells were immortalized with a temperature-sensitive form of the SV40 Large T antigen (260), which is stable at 33°C and binds p53, thereby keeping cells in a constant state of cell division and preventing apoptosis. When these cells are grown at 39°C the SV40

Large T antigen is slowly degraded, with consequent release of p53 and induction of apoptosis. The striatal origin of STHdh^{Q111/Q111} cells and the fact that they show many of the cellular impairments and enhanced susceptibility to cell death seen in HD makes these cells a good model to study further the molecular mechanisms induced by mHTT and to investigate the effects of therapeutic compounds.

The fact that mHTT fragments occur in HD cells and HD patients brains and are believed to be even more toxic than the full-length protein, have made cell lines expressing mHTT fragments a useful tool to study the cellular effects of fragments of various lengths. In my studies I used immortalized rat striatal cells (ST14A) stably overexpressing the first N-548 amino acids of the human HTT protein with 15Q (HTT N548-15Q) or 128Q (HTT N548-128Q) (48). I also used ST14A cells transiently overexpressing HTT exon 1 with 25Q (WT) or 72Q (HD) and fused to the green fluorescent protein (GFP) for easy detection of transgene expression.

1.6 GENERAL HYPOTHESIS AND AIMS OF THIS MASTER THESIS

Based on the information summarized above, the overall goal of my thesis was to determine whether the therapeutic effects of GM1 in cell and animal models of HD are due, at least in part, to changes in the accumulation of mHTT soluble protein or protein aggregates and to increased aggregate clearance by autophagy. The overarching hypothesis of my thesis is that

the beneficial effects of GM1 in HD models are at least in part mediated by stimulation of autophagy and restoration of cargo recognition in selective autophagy, with consequent enhancement of mHTT clearance.

In chapter 3.1 I will address the question of whether GM1 decreases accumulation of soluble and insoluble forms of mHTT in HD mouse and cell models. I will present immunoblotting data for monomeric full-length HTT and N-terminal HTT fragment levels, and the results of a filter trap assay for mHTT aggregates.

In chapter 3.2 I will address the question of whether GM1 can trigger autophagy induction and/or increase autophagic flux. I will show immunoblotting data for the autophagy markers LC3-II and p62 and the analysis of intracellular localization of the chimeric protein RFP-EGFP-LC3, overexpressed in HD cells in order to measure autophagic flux.

In chapter 3.3 I will test the hypothesis that GM1 restores a normal interaction between mHTT and p62. I will show the results of co-immunoprecipitation studies to assess the interaction of wt and mHTT with p62 before and after treatment with GM1.

1.7 FIGURES

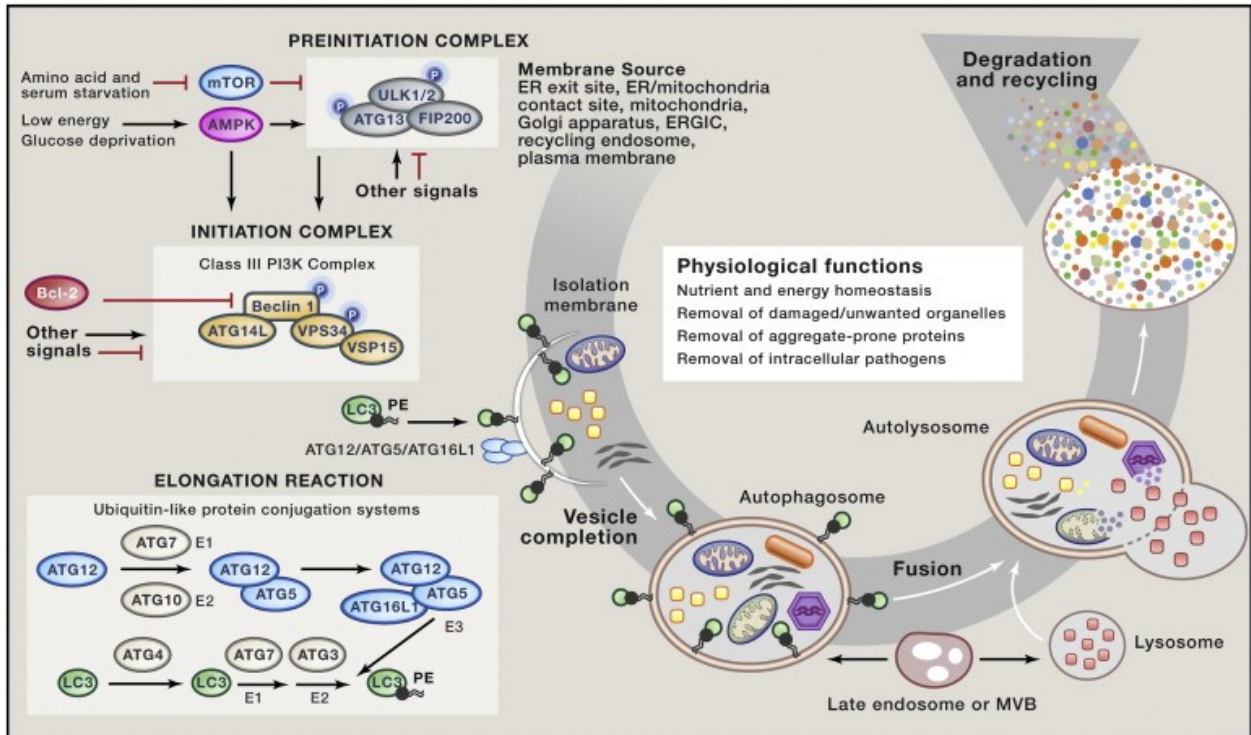


Figure 1.3.1: Molecular mechanism of autophagy. Autophagy can be induced by lack of nutrients such as amino acids and glucose or lack of serum and growth factors, which are sensed by AMPK and mTORC1. MTOR is a negative regulator of autophagy and represses autophagy by phosphorylating ULK1. AMPK can phosphorylate and activate ULK1 when glucose levels are low. Active ULK1 forms a pre-initiation complex with ATG13 and FIP200, which in turn activates the class III PI3K or initiation complex essential for phagophore elongation and recruitment of ATG proteins. LC3 processing and recruitment to the phagophore depend on two ubiquitin-conjugation systems: ATG4 cleaves LC3 to generate LC3-I to which a PE residue is attached with help from ATG7 and ATG3 to yield LC3-II. ATG7 and ATG10 mediate conjugation of ATG12 to ATG5 which, together, form a complex with ATG16L. This complex recruits LC3-II to the phagophore which engulfs cargo and

closes into an autophagosome. Autophagosomes fuse with lysosomes that contain degradative enzymes to form autolysosomes, where the cargo is degraded (157).

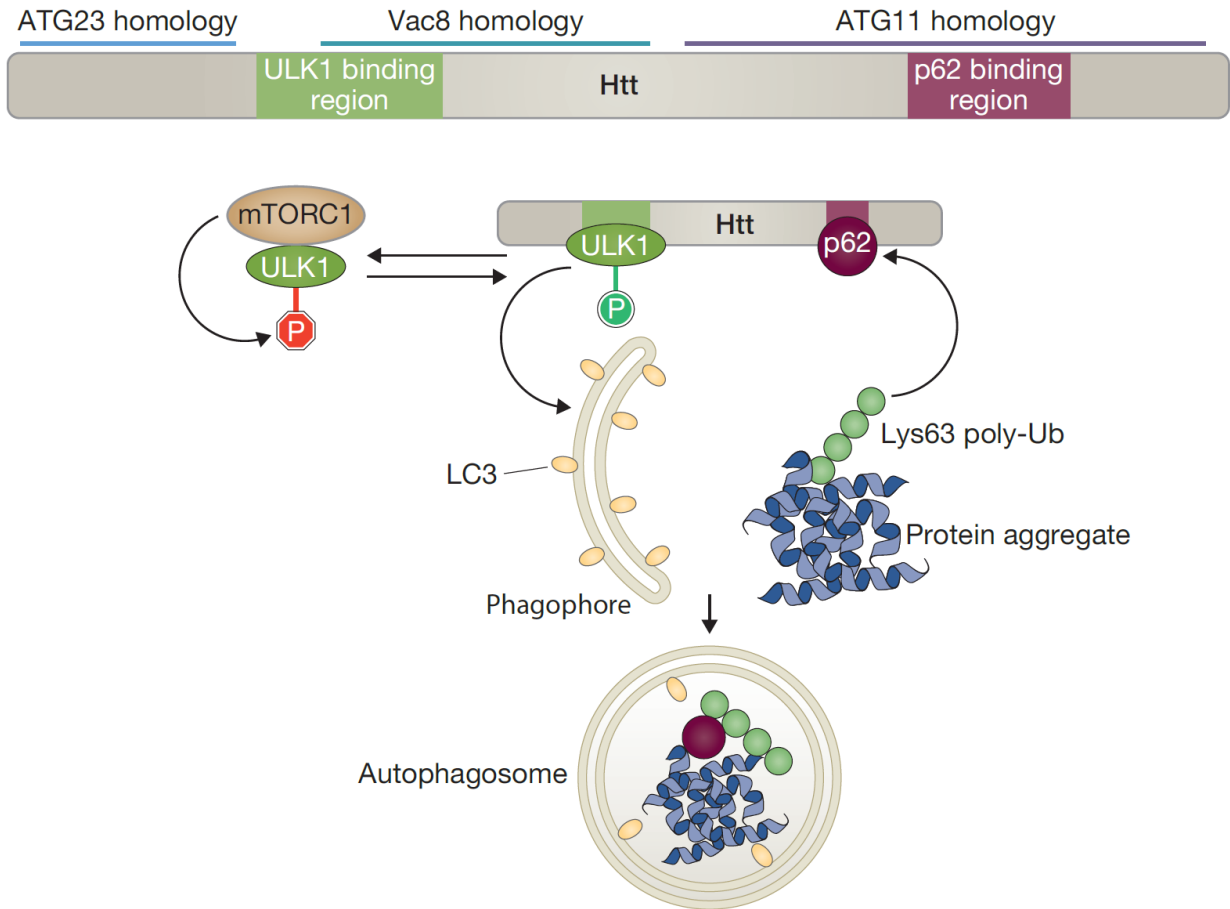


Figure 1.3.2: Huntingtin is a key player in cargo recognition and induction of selective autophagy. The HTT protein contains regions with structural similarity to three yeast proteins that are involved in selective autophagy, namely ATG23, Vac8, and ATG11. HTT has binding sites for ULK1 and p62 (amongst binding sites for other autophagy related proteins that are not shown). HTT binds ULK1 and causes its release from its inhibitory interaction with mTORC1. ULK1 is subsequently activated by phosphorylation and induces autophagosome formation. P62 can only recognize K63-polyubiquitinated cargo and deliver it to the autophagosome, when it is bound to HTT (261).

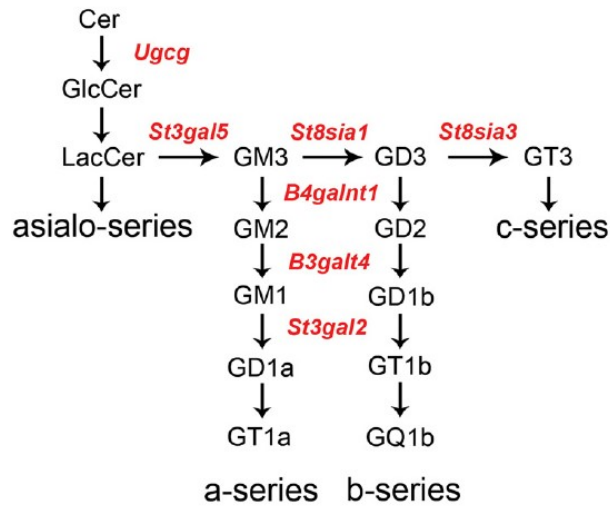


Figure 1.4.1: Ganglioside biosynthesis. *De novo* synthesis of gangliosides begins with glycosylation of ceramide (Cer) to glycosylceramide (GlcCer) by UDP-glucose ceramide glucosyltransferase (Ugcg). Galactosylation of GlcCer leads to the synthesis of lactosylceramide (LacCer), which gives rise to the asialo-series of gangliosides, or which is further sialosylated to GM3 by Lactosylceramide alpha-2,3-sialyltransferase (St3gal5). GM3 is sialosylated to GD3 by Alpha-N-acetylneuraminide alpha-2,8-sialyltransferase 1 (St8sia1), or to GM2 by Beta-1,4 N-acetylgalctosaminyltransferase 1 (B4galnt1), giving rise to the a-series of gangliosides. GD3 is sialosylated by B4galnt1 to give rise to b-series gangliosides, and to GT3 by Alpha-N-acetylneuraminide alpha-2,8-sialyltransferase 3 (St8sia3) to give rise to the c-series of gangliosides (66).

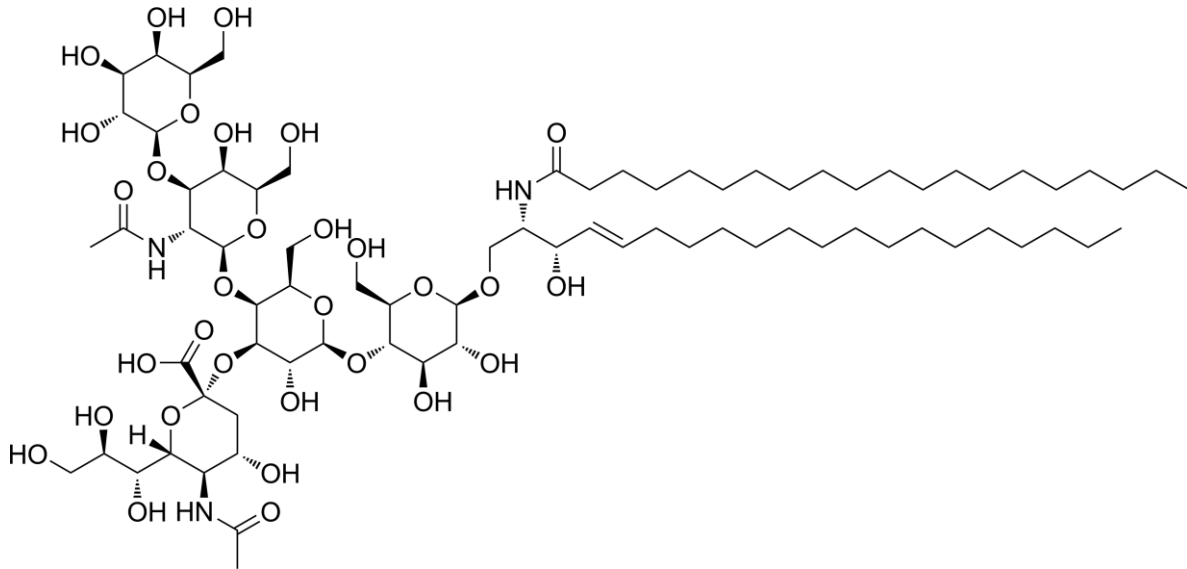


Figure 1.4.2: Ganglioside GM1. GM1 contains a ceramide backbone and attached oligosaccharides, which contains one sialic acid residue. The ceramide backbone can vary in length and saturation of fatty acid chains. The hydrophobic ceramide moiety of GM1 integrates into membranes where GM1 contributes to form microdomains known as lipid rafts (262).

2 MATERIAL AND METHODS

2.1 CHEMICALS

The following chemicals and reagents were used in my studies: GM1 (synthetic, Seneb BioSciences Inc. or bovine, Alexis Biochemical), artificial cerebrospinal fluid (CSF, Harvard Apparatus), Dulbecco's modified Eagle's medium (DMEM) high glucose (HyClone), fetal bovine serum (Sigma), L-glutamine (Gibco), Sodium (Na) pyruvate (Gibco), geneticin (G418, Gibco), Opti-Minimal Essential Medium (Opti-MEM, Gibco), Earl's balanced salt solution (EBSS, Sigma), bafilomycin A1 (baf, Sigma), ammonium chloride (NH₄Cl, Sigma), MG132 (EMD), cycloheximide (Sigma), TRIZMA base (Tris, Sigma), hydrogen chloride (HCl, Fisher), Igepal CA-630 (NP40, Roche), ethylene diamine tetraacetic acid (EDTA, Sigma), ethylene glycol tetraacetic acid (EGTA, Sigma), protease inhibitor cocktail (Roche), PhosStop phosphatase inhibitor cocktail (Roche), acrylamide (Biorad), ammonium persulfate (APS, Sigma), tetramethylethylenediamine (TEMED, Sigma), sodium dodecyl sulfate (SDS, Sigma), glycine (Fisher), methanol (Fisher), Tween-20 (Sigma), dithiothreitol (DTT, Sigma), poly-L-lysine (Sigma), paraformaldehyde (PFA) (Sigma), ProLong gold mounting media (Life Technologies), urea (Sigma), dimethyl pimelimidate (DMP, Sigma), triethanolamine (Sigma)

2.2 ANTIBODIES

Primary antibodies used in this study were: Mouse monoclonal anti-HTT (MAB2166, 1:5000; Millipore) was used to detect monomeric full-length HTT and N548-terminal HTT fragments in HTT N548-15Q or HTT N548-128Q cells. Goat polyclonal anti-GFP (1:2000; gift from Dr. Luc Berthiaume, University of Alberta, Edmonton, AB, Canada) and rabbit polyclonal anti-HTT (PW0595, 1:10,000, Enzo) were used to detect transiently transfected chimeric GFP-HTT fragments in ST14A cells. Rabbit polyclonal anti-HTT (N18, 1:10,000; gift from Dr. R.

Truant, McMaster University, Hamilton, ON, Canada), mouse monoclonal anti-HTT (MW8, 1:2000; Developmental Studies Hybridoma Bank), mouse monoclonal anti-HTT (EM48, 1:1000; Chemicon), and rabbit polyclonal anti-HTT (PW0595, 1:2000; Enzo Life Sciences) were used to detect mHTT aggregates. The antibodies MW8 and EM48 recognize specifically aggregated forms of mHTT, but not the soluble protein. Mouse monoclonal anti-HTT antibodies (MAB2166 and MAB2168, 2 μ L per immunoprecipitation; Millipore) and mouse IgG1 isotype control (ab18448-500, 20 μ L per immunoprecipitation; Abcam) were used for co-immunoprecipitation experiments. Rabbit polyclonal anti-LC3B (2775, 1:1000; Cell Signaling), mouse monoclonal anti-p62 (ab56416, 1:500; Abcam), mouse monoclonal anti- α -tubulin (T5168, 1:10,000; Sigma-Aldrich), mouse monoclonal anti-ubiquitin (3936, 1:1000; Cell Signaling) were used for autophagy studies.

Secondary antibodies: IRDye 800CW and IRDye680RD (1:10,000; LI-COR).

2.3 ANIMAL MODELS

Three different transgenic and knock-in mouse models of HD were used in this study. They differ for genetic background, severity of neuropathology and symptoms as indicated below.

HdhQ140 mice: Knock-in mouse model on a C57BL/6 background (herein referred to as Q140) were generated by knock-in of the first exon of the human *HTT* gene containing 140 CAG repeats into the endogenous mouse *Htt* gene (256). Both homozygous (Q140/Q140) and heterozygous (Q7/Q140) animals, as well as WT (Q7/Q7) littermates were used in this study. R6/2 mice: Transgenic HD mice on a CBAxC57BL/6 background that overexpress exon 1 of the human *HTT* gene with 144 CAG repeats (87). YAC128 mice: Transgenic mice on an FVB/N background that overexpress the full-length human *HTT* gene with 128 CAG repeats (254). YAC128 and Q140 mice were originally obtained from the Jackson

Laboratories and maintained in our animal facility at the University of Alberta. R6/2 mice were purchased from the Jackson Laboratories at 5-7 weeks of age to use for experiments.

All procedures on animals were approved by the University of Alberta's Animal Care and Use Committee and were in accordance with the guidelines of the Canadian Council on Animal Care.

2.4 CELL MODELS

STHdh^{Q7/Q7} and STHdh^{Q111/Q111}: Mouse striatal knock-in cells derived from striatal tissue of STHdh knock-in mice at embryonic day 14 (259) and immortalized with a temperature-sensitive form of the SV40 Large T antigen (260). These cells will be referred to as 7/7 and 111/111 cells in this thesis. They express full-length endogenous mouse HTT with a polyQ sequence containing either 7 or 111 glutamines. The cells were a gift from Dr. M.E. MacDonald (Massachusetts General Hospital, Boston, MA, USA) and were maintained in DMEM containing 4500 mg/L glucose, 10% fetal bovine serum, 2 mM L-glutamine, 0.11 g/L Na pyruvate, and 400 µg/mL G418. ST14A, HTT N548-15Q or HTT N548-128Q: Immortalized rat striatal cells (ST14A), stably transfected with pLXSP vector expressing the first N-548 amino acids of the human HTT protein with 15Q (HTT N548-15Q) or 128Q (HTT N548-128Q) (48). These cells were a gift from Dr. E. Cattaneo (University of Milan, Milan, Italy) and were maintained in DMEM containing glucose, 10% fetal bovine serum, 2 mM L-glutamine, and 0.11 g/L Na-Pyruvate.

All cell lines used in this study were maintained at the permissive temperature of 33°C (to ensure integrity of the immortalizing SV40 Large T Antigen – (260)) in 5% CO₂ and used between passage number 8 and 36. All cells were seeded one day prior to the start of the experiment to reach a confluence between 80 and 90% with the exception of RFP-EGFP-LC3 transfected cells that were seeded to reach a confluence between 55 and 65%.

2.5 CHRONIC GM1 ADMINISTRATION *IN VIVO*

Chronic administration of synthetic GM1 was previously described (245). Briefly, mice were anesthetized either intraperitoneal injection of 100/20 mg/kg ketamine/xylazine (Wyeth/Bayer) for YAC128 or isoflurane (PPC, DIN 02237518) at 4% in oxygen for induction and 1-2% in oxygen for maintenance for Q140 and R6/2 mice. Then, a microcannula connected to an osmotic pump (Alzet, 28 d: flow-rate 0.25 $\mu\text{L/h}$; 42 d: flow-rate 0.15 $\mu\text{L/h}$) was stereotaxically inserted into the right ventricle (1.25 mm right lateral, 0.6 mm posterior to bregma, 3 mm deep). The osmotic pump – implanted subcutaneously in the mouse's back - infused a solution of 3.6 mM (28 d-pump, in R6/2 and YAC128 mice) or 6 mM GM1 (42 d-pump in Q140 mice) for 28 or 42 days, respectively. Synthetic GM1 was used in experiments with R6/2 and YAC28 mice, while bovine GM1 was used in Q140 mice. Treatment started when mice displayed motor symptoms, i.e. between 6 and 8 months of age for Q140, 8 weeks of age for R6/2 and between 5 and 6 months of age for YAC128 mice.

2.6 CELL TREATMENTS

i) Analysis of steady-state HTT levels: ST14A cells were transiently transfected 24 h before treatment (for details on transfection, see section 2.7) and plated for experiments 6 h after transfection. Transiently transfected ST14A cells and HTT N548-15Q/128Q cells were treated with 50 μM synthetic or bovine GM1, respectively, in serum-free medium (SFM) at 33°C for the indicated time.

ii) Analysis of autophagy markers: For bafilomycin titration experiments, 7/7 and 111/111 cells were treated with the indicated bafilomycin A1 concentrations (50 - 200 nM) or 20 mM NH_4Cl in serum-free medium for 4 h. To assess GM1 effects on autophagy, 7/7, 111/111, HTT N548-15Q and HTT N548-128Q cells were treated with 50 μM bovine GM1 (except for the experiment where cells were incubated with GM1 for 4 h, where synthetic GM1 was

used) in SFM for the indicated time. Where indicated, cells were exposed to 100 nM bafilomycin 1A (1 - 4 h) (to block autophagic flux and protein degradation). Incubation with 5 µg/mL cycloheximide for the indicated time at 33°C was used to inhibit protein synthesis and to study autophagic degradation of p62. To measure autophagic flux using the RFP-EGFP-LC3 chimeric protein, 111/111 cells were transiently transfected (for details on transfection see section 2.7) 24 h before starting treatment with 50 µM synthetic GM1 (or vehicle) in SFM for 3 h. Controls with low or high levels of autophagy were generated by growing cells in nutrient-rich growth medium or nutrient-depleted medium (EBSS), respectively, for 3 h.

iii) Co-immunoprecipitation of HTT with p62 and p62 sequestosome studies: Cells were grown in regular growth medium. Where indicated, cells were exposed to 10 µM MG132 for 5 h to enhance proteasome inhibition-induced autophagy prior to incubation with 50 µM GM1 (bovine) for 10 min to study possible GM1 effects on HTT-p62 interaction.

2.7 TRANSIENT TRANSFECTION

For assessment of steady-state HTT fragment levels in response to GM1, ST14A cells were transiently transfected with pEGFP/C1 control vector (Clontech), or with wt (Exon 1-25Q-GFP) or mHTT (Exon 1-72Q-GFP) N-terminal fragments tagged with the green fluorescent protein (GFP) as a fusion protein. These constructs were a gift from Dr. D. Housman (Massachusetts Institute of Technology, Cambridge, MA, USA). Transient transfection was performed using Lipofectamine® 2000 (Invitrogen) according to manufacturer's instructions. Briefly cells were seeded in 100 mm dishes one day prior to transfection to reach a confluence between 80 and 90%. Eight µg of DNA were used together with 10 µL Plus reagent and 48 µL Lipofectamine in 1000 µL Opti-Mem and added to cells. Six h after

transfection cells were trypsinized and plated to reach a confluence of 75-80% the next day for experiments (see section 2.6 i)..

To determine autophagic flux, 111/111 cells were transiently transfected with a vector expressing an RFP-EGFP-LC3 chimeric protein (gift from Dr. I. S. Goping, University of Alberta, Edmonton, AB, Canada). Transfections were performed with the Nucleofector™ 2b Device (Lonza) and the Amaxa Cell Line Nucleofector Kit V (Lonza) according to the manufacturer's instructions. Briefly, 2×10^6 cells were resuspended in 100 μ L SG solution containing 8 μ g DNA and transfected by applying the Amaxa program CM137.

2.8 PREPARATION OF CELL AND BRAIN LYSATES

All steps were performed on ice or at 4°C. Unless otherwise stated, cells were washed once with PBS and lysates were prepared in NP40 lysis buffer (NLB: 20 mM Tris-HCl, pH 7.4, 1% NP40, 1 mM EDTA, 1 mM EGTA, 50 μ M MG132, 1 X protease inhibitor cocktail and 1 X PhosStop phosphatase inhibitor cocktail) by homogenization through a 27-gauge needle (10 times) using an 1 mL syringe followed by sonication (2 x 10 sec, power intensity 1). Lysates were incubated on ice for 30 min and centrifuged at 14000 rpm for 10 min at 4°C.

Mice were euthanized by cervical dislocation, then cortex and striatum were dissected out and snap-frozen in liquid nitrogen. Brain areas were immediately homogenized in NLB using a motor-driven Potter-Elvehjem PTFE pestle and performing 10 (cortex) or 8 (striatum) strokes at approximately 800 rpm. Lysates were incubated on ice for 30 minutes, then sonicated 2 x for 10 sec and finally centrifuged at 14000 rpm for 10 min at 4°C. Supernatants were used as tissue lysates for detection of HTT and autophagic markers. Lysates for Filter Trap Assay were not centrifuged after sonication.

BCA Assay (Pierce) was carried out according to manufactures instructions to determine protein concentrations. Briefly, 25 μ L of 1:10 diluted lysate were used per well (96-well plate). Quantitation was carried out in duplicates for cell lysates and in quadruplicates for tissue lysates.

2.9 DETECTION OF SOLUBLE AND INSOLUBLE P62 FRACTIONS

Cells were homogenized in Triton lysis buffer (TLB: 20 mM Tris-HCl, pH 7.4, 1% Triton X100, 150 mM NaCl, 1 mM EDTA, 1 mM EGTA, 2.5 mM sodium pyrophosphate, 50 μ M MG132, 1 X protease inhibitor cocktail and 1 X PhosStop phosphatase inhibitor cocktail) by homogenization through a 27-gauge needle using an 1 mL syringe, followed by incubation on ice for 30 min. Protein concentrations were measured by BCA-Assay (see section 2.8). Forty μ g of protein lysates were diluted in equal volumes of TLB. After centrifugation at 14,000 rpm for 10 min at 4°C, supernatants (soluble p62 fraction) were resolved by SDS-polyacrylamide gel electrophoresis (PAGE). Pellets (insoluble p62 fraction) were washed once with 50 μ L TLB, centrifuged at 14,000 rpm for 10 min at 4°C, resuspended by incubation in SDS-urea buffer (2% SDS, 6 M urea) for 30 min at rt with vortexing every 10 min and finally resolved by SDS-PAGE using 4-15% gels.

2.10 Co-IMMUNOPRECIPITATION OF HTT AND P62

Cells were lysed in TLB as reported in section 2.9. Co-immunoprecipitation (co-IP) was performed on whole lysates that were not subjected to a clearing centrifugation step, to avoid loss of HTT insoluble aggregates. 0.8 mg protein in 300 μ L TLB and a combination of MAB2166 and MAB2168 antibodies (2 μ L/co-IP) cross-linked to 50 μ L/co-IP Dynabeads® Protein G (Life Technologies) were used for the co-IP overnight at 4°C. Antibody cross-linking was performed as follows: After incubation of beads with the indicated antibodies for 30 min at rt on a rotating shaker, beads were washed twice in 1 mL 0.2 M triethanolamine,

pH 8.2. Then antibodies were cross-linked by resuspending beads in 1 mL 20 mM DMP in 0.2 M triethanolamine and incubating at rt for 30 min. The reaction was terminated by resuspending the beads in 1 mL 50 mM Tris, pH 7.5 and incubation at rt for 15 min. The beads were then washed 3 x with 1 mL 0.01% Tween-20/PBS before use for co-IP. Immunoprecipitated material, supernatants (one tenth of the co-IP volume), and inputs (80 ug) were resolved by SDS-PAGE using 4-15% gels.

2.11 IMMUNOBLOTTING

4-12% SDS-PAGE gradient gels were used for separation of most proteins. Exceptions were LC3-II, which was separated on 14% SDS-PAGE gels, transiently transfected N-terminal wt and mHTT fragments, which were loaded on 10% SDS-PAGE gels, and samples from co-IP and p62 sequestosome studies, which were loaded on 4-15% gels. Protein samples boiled in SDS-Laemmli buffer were separated by SDS-PAGE and transferred to Immobilon-FL PVDF membrane (Millipore). Transfer conditions for all but full-length HTT protein were 100 V for 1 h in 25 mM Tris and 192 mM glycine transfer buffer containing 20% methanol. Full-length HTT and protein aggregates were transferred at 30 V overnight at 4°C in 25 mM Tris and 192 mM glycine buffer containing 0.05% SDS and 16% methanol. After transfer, membranes were blocked with 5% BSA in Tris-buffered saline (TBS) containing 0.1% Tween-20 (TBS-T) (exception: membranes from co-IP and p62 sequestosome studies were blocked in 5% BSA/TBS without Tween-20) for 1 h at rt and incubated with primary (overnight at 4°C) and appropriate IRDye (LICOR) secondary antibodies (1 h at rt) in 5% BSA/TBS-T. Signals were detected by the Odyssey Infrared Imaging System (LICOR) and quantified using Odyssey application software version 3.0 (LICOR).

2.12 FILTER TRAP ASSAY

Thirty μg of protein lysates (which had not been subjected to centrifugation to remove cellular debris) were denatured and reduced in 2% SDS and 100 mM DTT (final sample volume: 100 μL) at 100 $^{\circ}\text{C}$ for 10 min. Samples were then filtered through a cellulose acetate membrane (0.2 μm pore size, Sterlitech) in a Bio-Dot microfiltration unit (Bio-Rad), using a manifold vacuum pump. The membrane was washed 2 x with 200 μL PBS and then left to dry for 30 min prior to further washing 3 x with 2% SDS in PBS to remove all SDS-soluble proteins. The membrane was then blocked with 5% BSA/TBS-T and incubated with the indicated primary (overnight at 4 $^{\circ}\text{C}$) and appropriate IRDye secondary antibodies (1 h at rt) in 5% BSA/TBS-T. Signals were detected by the Odyssey Infrared Imaging System (LICOR) and quantified using the Odyssey application software version 3.0 (LICOR).

2.13 ANALYSIS OF AUTOPHAGIC FLUX BY CONFOCAL MICROSCOPY

111/111 cells transfected with RFP-GFP-LC3 were plated onto poly-L-lysine-coated coverslips. The following day, cells were incubated with nutrient-rich growth medium, EBSS, or with 50 μM synthetic GM1 (or vehicle) in SFM for 3 h and then fixed with 4% PFA in PBS for 15 min at rt. Coverslips were mounted using ProLong gold mounting media and let dry for 1 d at rt. Images were acquired as 0.3 μm z-stacks using a Zeiss LSM 710 confocal microscope and 63X objective, and underwent deconvolution using Huygens Essential X11 software (Scientific Volume Imaging). Whole cell images were reconstructed from z-stacks using Imaris 7.4 software (Bitplane). Yellow (RFP-GFP-LC3 in autophagosomes) and red puncta (RFP-GFP-LC3 in autolysosomes) were counted in each transfected cell. A total number of 23 untreated and 31 GM1 treated cells were examined. An estimate of autophagic flux was obtained by calculating the ratio of red puncta over yellow puncta.

2.14 STATISTICAL ANALYSIS

Two-way ANOVA followed by multiple comparisons Bonferroni test was used to compare genotype and treatment groups in all experiments that involved WT and HD mice treated with GM1 or vehicle. One-way ANOVA analysis followed by Bonferroni post-test was used to compare differences among three groups (WT CSF, HD CSF, and HD GM1). Unpaired two-tailed t-test analysis was performed to compare soluble and aggregated HTT levels in HD mice, and to compare soluble N-terminal fragment levels in HTT-N548-15Q/128Q- and transiently transfected ST14A cells at individual time-points. Unpaired t-test analysis was also performed to assess potential differences in autophagic markers LC3-II and p62 in striatal cells at individual time-points and to compare untreated and GM1-treated RFP-GFP-LC3 transfected 111/111 cells. All comparisons were performed using a statistical significance level of 0.05.

3 RESULTS

3.1 EFFECTS OF GM1 TREATMENT ON MHTT LEVELS AND MHTT

AGGREGATES

Decreasing mHTT levels by activation of autophagy was shown to be beneficial in HD cell and animal models (142, 143). We have demonstrated that ganglioside GM1 confers neuroprotection to HD cells and restores motor deficits in HD mouse models (66, 245). GM1 increased phosphorylation of mHTT at serine residues 13 and 16 (245), a post-translational modification that has been proposed to increase mHTT degradation (250). To investigate, whether treatment with GM1 results in decreased mHTT levels, WT (Q7/Q7), heterozygous (Q7/Q140) and homozygous Q140/Q140 knock-in mice underwent chronic ventricular infusion with GM1 (or vehicle) for 42 days. Motor and non-motor tests were performed before and during the treatment phase and showed a dramatic improvement of motor and non-motor dysfunction in GM1-treated Q7/Q140 and Q140/Q140 mice (246, 247). At the end of treatment, mice were euthanized and cortical tissue was used to measure HTT levels by immunoblotting. No statistically significant differences in mHTT levels could be observed after GM1 treatment in Q7/Q140 or Q140/Q140 mice (Figure 3.1.1 A and B). However, levels of wtHTT were significantly decreased in Q7/Q7 and Q7/Q140 mice treated with GM1 compared to vehicle-treated animals (Figure 3.1.1 A). Wild-type HTT levels were also significantly reduced in Q7/Q140 compared to Q7/Q7 mice. The latter finding is expected since Q7/Q7 mice express two *wtHtt* alleles whereas Q7/Q140 mice only express one.

To more specifically investigate the effects of GM1 on cells of neuronal origin, we used striatal rat cell clones expressing the first N-548 amino acids of the human HTT protein containing a polyQ stretch of 15Q (HTT N548-15Q) or 128Q (HTT N548-128Q). Expression levels of HTT N548-128Q are 1.5-fold higher than HTT N548-15Q in basal conditions (Figure

3.1.2 A). When growing the cells in serum-free medium (SFM), HTT fragment levels decreased most likely due to enhanced autophagic degradation during growth factor and lipoprotein deprivation in SFM. However, there was no difference in the degradation rate between wt and mHTT N-terminal fragments in a 48 h time-course (Figure 3.1.2 A). Treatment with GM1 for 24, 48, or 72 h in SFM did not further enhance degradation of wt or mHTT N-terminal fragments (Figure 3.1.2 B).

To exclude confounding effects related to the clonal origin of HTT N548-15Q and HTT N548-128Q cell lines, rat striatal ST14A cells were transiently transfected with a vector carrying the cDNA for a chimeric HTT fragment encoding exon 1 of the human HTT gene with 25 or 72 CAG repeats, fused to the nucleotide sequence for GFP. These vectors allow for the expression of chimeric HTT N-terminal fragments containing the first 67 amino acids of the protein with either 25 (Exon 1-25Q-GFP) or 72 glutamines (Exon 1-72Q-GFP), fused to GFP. Transfected cells were incubated with GM1 for 1, 4, or 12 h in SFM. GM1 did not change levels of wt or mHTT N-terminal fragments, nor did it affect levels of GFP compared to untreated cells (Figure 3.1.3).

Next, we sought to determine whether GM1 could affect levels of mHTT insoluble aggregates. To this aim, we performed filter trap assay (263) on cortical and striatal tissue lysates from R6/2 mice (overexpressing the first exon of the human HTT gene) and Q7/Q140 and Q140/Q140 mice (expressing full-length mHTT) that had been treated with either vehicle (artificial CSF) or GM1 for 28 or 42 days, respectively. Equal amounts of tissue lysate were filtered through a cellulose acetate membrane and SDS-insoluble aggregates trapped on the membrane (263) were detected by dot-blotting with anti-HTT antibodies. Treatment with GM1 resulted in decreased mHTT aggregates in R6/2 cortex as well as in Q140/Q140 striatum, while there was no effect of GM1 on R6/2 striatum or Q140/Q140 cortex (Figures

3.1.4 and 3.1.5). Q7/Q140 mice had very little amount of mHTT aggregates detectable by filter-trap assay, and GM1 did not affect their levels (Figure 3.1.5).

In summary, GM1 did not significantly decrease levels of full-length mHTT or N-terminal fragments, but reduced mHTT aggregates in some brain areas in HD mouse models.

3.2 EFFECTS OF GM1 TREATMENT ON AUTOPHAGY AND AUTOPHAGIC FLUX

Decreased mHTT aggregates in specific HD mouse brain regions could result from decreased aggregate formation or increased degradation. Since levels of soluble mHTT were not significantly changed by treatment with GM1 (Figures 3.1.1, 3.2.1, and 3.1.3), I sought to determine whether GM1 increases autophagy induction and/or flux as a possible explanation for the reduction of mHTT aggregates after GM1 treatment. It has been shown previously that a ganglioside mix containing GM1 can induce autophagy in astrocytes (195). Cortical and striatal LC3-II and p62 levels were measured by immunoblotting as markers of induction of autophagy (264) and autophagic flux (265), respectively, in the Q140 mouse model of HD.

No statistically significant differences in LC3-II or p62 levels could be detected in striatal or cortical tissue from Q7/Q7 and Q7/Q140 mice after GM1 treatment (Figure 3.2.1). However, due to the high variability in levels of LC3-II within each experimental group (Figure 3.2.1 A), it is likely that a much higher number of animals than used in this study will have to be analyzed to obtain conclusive results. Of note, two-way ANOVA revealed statistically significant differences in cortical LC3-II and p62 levels between Q7/Q7 and Q7/Q140 mice (Figure 3.2.1 A). As argued in more detail in the “Discussion”, decreased LC3-II levels in combination with reduced p62 might indicate enhanced autophagic flux in the Q7/Q140 mice.

As in the Q7/Q140 mice, GM1 did not have an effect on LC3-II levels in the cortex of Q140/Q140 mice (Figure 3.2.1 B). Unfortunately, striatal tissue was not available from these mice and therefore I could not determine whether the observed decrease in mHTT aggregates in the striatum of mice treated with GM1 (Figure 3.1.5) correlated with changes in LC3-II or p62 levels.

I also measured LC3-II levels in the cortex of R6/2 and YAC128 mice, two additional mouse models of HD where GM1 was shown to have therapeutic effects (245-247). LC3-II levels were unchanged in the cortex of R6/2 mice (Figure 3.2.2 A). Due to technical difficulties, p62 levels could not be detected in these mice. In YAC128 mice, no effect of GM1 on LC3-II or p62 levels could be detected (Figure 3.2.2 B). However, p62 levels were slightly but statistically significantly lower in YAC128 cortex compared to WT (Figure 3.2.2 B).

To more directly look at potential GM1 effects on initiation of autophagy and autophagic flux in cells of neuronal origin, cell lines expressing either full length (7/7 and 111/111 cells) or N-terminal (HTT N548-15Q or HTT N548-128Q) HTT fragments were used. Bafilomycin was used in these experiments to block autophagic protein degradation and to get insights into autophagic flux in the cell lines mentioned above (265).

First, the bafilomycin concentration that completely blocks autophagic degradation of proteins in our cell lines was investigated. In 7/7 and 111/111 cells, 100 nM bafilomycin efficiently inhibited autophagy as no further increase in LC3-II levels could be observed with higher bafilomycin concentrations or another autophagy inhibitor, NH_4Cl (265) (Figure 3.2.3 A and B).

Next, 7/7 and 111/111 cells were treated with GM1 for 4 h in the absence or presence of 100 nM bafilomycin to inhibit autophagic flux (Figure 3.2.4 A). LC3-II levels were increased in bafilomycin-treated samples (compared to bafilomycin-untreated) to about the same

amount in both 7/7 and 111/111 cells, regardless of the presence or absence of GM1. This indicates, that in the 4 h-treatment, autophagy was induced and flux occurred at similar rates in all samples.

To determine whether the time-course of autophagy induction and protein degradation might be affected by GM1 at different time-points, cells were incubated in SFM with GM1 or vehicle in the absence or presence of bafilomycin for 1, 4, and 12 h. Autophagy was induced already 1 h after incubation in SFM, as revealed by the increase of LC3-II levels in the presence of bafilomycin (to block autophagic flux and LC3-II degradation) (Figure 3.2.4 B). A further increase of LC3-II levels was detected in bafilomycin-treated cells at 4 and 12 h in SFM, as expected. Accumulation of LC3-II in cells treated with bafilomycin occurred at a similar rate up to the 4 h timepoint. At 12 h, 7/7 cells treated with GM1 displayed higher levels of LC3-II compared to cells that did not receive GM1. On the contrary, in 111/111 cells in SFM for 12 h, levels of LC3-II were slightly higher if the cells had not been treated with GM1.

The protein p62 is a common marker of autophagic flux and levels of p62 often decrease over time when autophagy is induced and as p62 is degraded through the autophagic flux along with its cargo (265). However, in our experiment, levels of p62 did not change upon incubation of the cells in SFM, nor did they change upon treatment with GM1 (Figure 3.2.5). These data suggest that, in spite of published literature (265), levels of p62 might not be a very reliable marker of autophagic flux, especially when one considers that p62 expression can be induced during autophagy at the same time that p62 is degraded (266). This was probably the case in my experiment, as p62 levels did decrease in 111/111 cells in SFM (autophagy activated), when cells were concomitantly treated with cycloheximide (an inhibitor of protein synthesis) (267, 268) (Figure 3.2.6). Overall levels of ubiquitinated proteins (potential cargo) decreased over time along with p62 levels.

To make sure that clonal effects in the 7/7 and 111/111 cell lines would not interfere with our analysis, similar experiments were carried out in HTT N548-15Q or HTT N548-128Q cells. When these cells were grown in SFM for 48 h, LC3-II levels increased steadily and were comparable between HTT N548-15Q or HTT N548-128Q (Figure 3.2.7 A). GM1, however, did not further enhance autophagy or autophagic flux in HTT N548-15Q or HTT N548-128Q cells over a timecourse of 72 h, as LC3-II (Figure 3.2.7 B) and p62 (Figure 3.2.7 C) levels did not change with the treatment. As in previous experiments, p62 levels did not decrease over time in SFM (Figure 3.2.7 C), suggesting once again that p62 is not a good marker of autophagic flux in our cell models.

Because of the limitations of p62 as a marker of autophagic flux, as revealed by my studies, I measured autophagic flux by confocal microscopy after transfecting 111/111 cells with RFP-EGFP-LC3. This chimeric form of LC3 is fused to a pH-sensitive form of the green fluorescent protein (EGFP), as well as with the red fluorescent protein (RFP) (269). Consequently, the chimera gives a yellow signal when present in autophagosomes and a red signal after fusion of the autophagosomes with lysosomes, when EGFP is quenched due to low pH in autolysosomes. The red/yellow ratio, measured by confocal microscopy, provides information on autophagic flux. In nutrient-rich growth conditions, nutrient-dependent autophagy is not active and RFP-EGFP-LC3 is mostly distributed diffusely in the cytosol (Figure 3.2.8). Only few puncta point towards basal levels of active selective autophagy. When cells were grown in EBSS under nutrient-depletion, nutrient-dependent autophagy and autophagic flux were activated as can be seen by the increase in yellow and red puncta (Figure 3.2.8). Incubation of 111/111 cells in SFM for 3 h (UNTR, Figure 3.2.9), also resulted in the appearance of autophagic puncta, suggesting that autophagy was also activated in the absence of growth factors (SFM), as expected. Treatment with GM1 in SFM for 3 h did not result in changes in the total autophagosome (yellow puncta) and

autolysosome (red puncta) count. Also the red/yellow ratio did not yield a significant difference (Figure 3.2.9) indicating no change in autophagic flux after GM1 treatment.

In summary, GM1 did not enhance autophagy induction or flux in the HD mouse and cell models analyzed and in the experimental conditions used in this study.

3.3 EFFECTS OF GM1 ON HTT-P62 INTERACTION

Autophagic cargo recognition is impaired in HD (67). Studies in ¹¹¹Qhtt mice (that express full-length mHTT with 111 polyQ repeats, (270)), primary striatal neurons of HD94 mice (that express a chimeric mouse/human exon 1 under control of a tet-regulated system in the CNS, (271)), in 111/111 striatal cells and in lymphoblasts from HD patients showed that autophagosomes form at normal or even enhanced levels, but fail to efficiently trap cargo. This impairment has been linked to an enhanced binding of p62 to mHTT, which might block p62 ability to recognize and guide cargo to autophagic structures (67). It has been recently shown however, that binding of p62 to wtHTT is crucial for induction of selective autophagy and cargo recognition (58). As indicated earlier, GM1 triggers phosphorylation of mHTT at serine residues 13 and 16 (245). These post-translational modifications could potentially lead to conformational changes of the protein and affect protein-protein interactions, including binding to p62. To determine whether treatment with GM1 affects the interaction of HTT with p62, co-immunoprecipitation experiments for HTT and p62 after GM1 treatment were carried out in 7/7 and 111/111 cells.

Cells were grown in nutrient-rich medium, a condition in which only selective autophagy should be active. In some cases cells were treated for 5 h with the proteasomal inhibitor MG132 (10 μ M) to induce proteotoxic stress and stimulate selective autophagy of misfolded and aggregated proteins (58). These conditions were also shown to stimulate binding of p62 to wtHTT (58). In line with these observations, in our experiments treatment of cells with

MG132 increased the amount of p62 that co-immunoprecipitated with HTT, from both 7/7 and 111/111 cell lysates (Figure 3.3.1). However, more p62 co-immunoprecipitated with mHTT than with wtHTT, both in the presence or absence of MG132. These findings are in accordance with previously published results (67) and suggest that our cell models are suitable for the study of HTT-p62 interaction.

Next, formation of p62 bodies in WT or HD cells was analyzed. P62 bodies form during selective autophagy and consist mostly of polyubiquitinated proteins and p62 (272) that are eventually degraded by autophagy (273, 274). P62 bodies are recovered in a Triton X100-insoluble cell fraction, while soluble p62 remains in the supernatant. Upon proteasome inhibition with MG132, the amount of insoluble p62 increased in 7/7 cells (Figure 3.3.2), as expected for cells where misfolded proteins and aggregates accumulate following inhibition of proteasomal degradation. In 111/111 cells, insoluble p62 levels were comparable to those in 7/7 cells, both in the presence or in the absence of MG132 (Figure 3.3.2). This likely indicates that p62 body formation is not impaired in HD.

To determine, if GM1 can restore normal binding of p62 to mHTT, 7/7 and 111/111 cells were grown in nutrient-rich conditions in the absence or presence of MG132 and then treated with GM1 or vehicle for 10 min. In previous studies (245), incubation of cells with GM1 for 10 min was sufficient to trigger phosphorylation of HTT. In these experimental conditions, overall levels of p62 were slightly lower in cell lysates from 111/111 cells compared to 7/7 cells, both in the presence and in the absence of MG132 (Figure 3.3.3). As in the previous experiment, more p62 co-immunoprecipitated with mHTT than with wtHTT. Treatment with GM1 decreased the amount of p62 that co-immunoprecipitated with mHTT by 40% in normal and 18% in proteotoxic stress (MG132) conditions, while it increased p62 co-immunoprecipitation with wtHTT from cells treated with MG132 (Figure 3.3.3). In summary,

these data suggest that GM1 modulates the interaction of p62 with HTT, and decreases the abnormal interaction with mHTT.

3.4 FIGURES

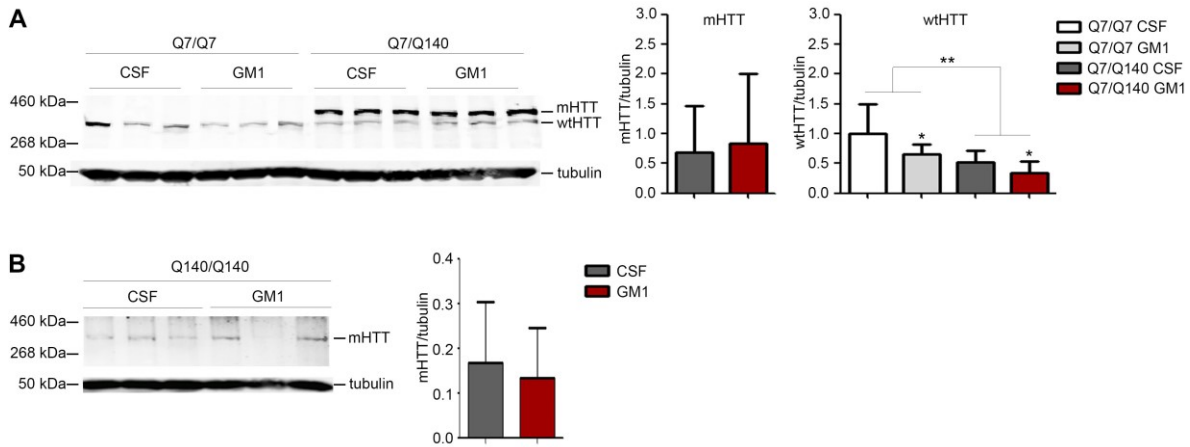


Figure 3.1.1: GM1 does not change monomeric full-length mHTT levels in the cortex of the Q140 mouse model. Q7/Q7, Q7/Q140, and Q140/Q140 mice were treated with GM1 or vehicle (CSF) by chronic intraventricular infusion. A) Representative immunoblot and densitometric analysis of wtHTT and mHTT protein levels in Q7/Q7 and Q7/Q140 mice. Mutant HTT levels were not significantly affected by GM1 treatment (n=9, T-test, $p>0.05$). On the contrary, levels of wtHTT were decreased by treatment with GM1 in both Q7/Q7 and Q7/Q140 mice. The reduction of wtHTT levels in untreated Q7/Q140, compared to untreated Q7/Q7, reflects the gene-dosage effect in the homozygous wild-type compared to heterozygous mice. Graphs show the mean \pm SD of 3 Q7/Q7 mice per group (CSF- or GM1-treated) and 9 Q7/Q140 per treatment group (CSF- or GM1-treated). Two way-ANOVA with Bonferroni's multiple comparisons post-test: * $p<0.05$ (effect of treatment); ** $p<0.005$ (effect of genotype). B) Representative immunoblot and densitometric analysis showing no significant different in the levels of mHTT protein in CSF- or GM1-treated Q140/Q140 mice. Graphs show the mean \pm SD of 4 mice treated with CSF and 5 mice treated with GM1. T-test: $p>0.05$.

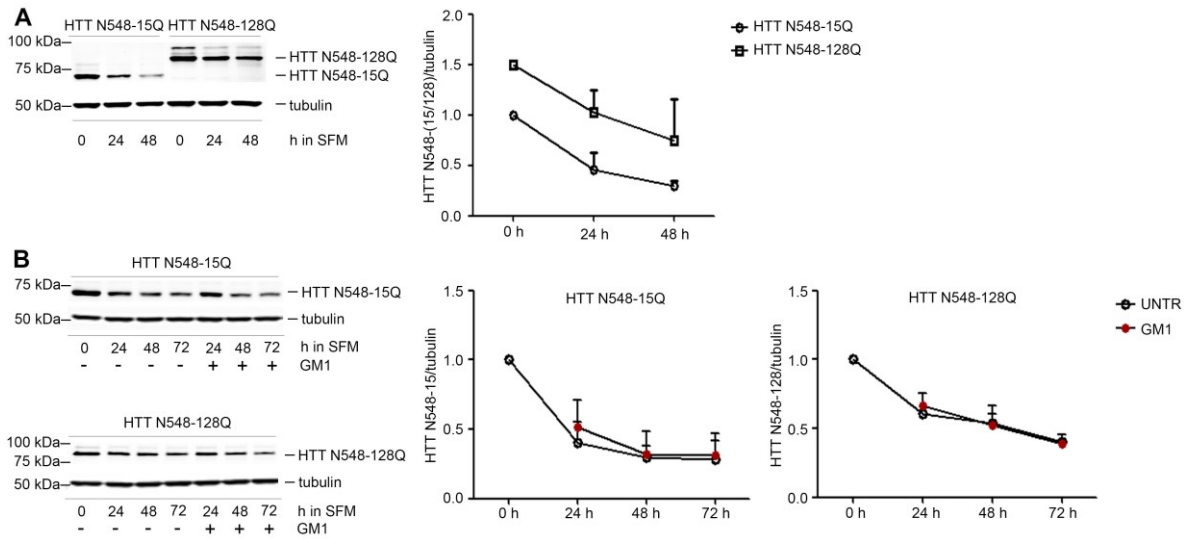


Figure 3.1.2: GM1 does not affect degradation rate of wt or mHTT N-terminal fragments in immortalized striatal cells grown in serum-free medium.

Representative immunoblot and densitometric analysis of HTT N-terminal fragments in HTT N548-15Q and HTT N548-128Q cells grown in serum free medium (SFM) (A) and treated with or without GM1 (B) for the indicated time periods. A) Both wt and mHTT fragments have similar degradation rates when cells are grown in serum-free medium. Graph shows the mean \pm SD of 2 independent experiments. B) GM1 did not change the rate of degradation of wt or mHTT fragments at any timepoint. Graph shows the mean \pm SD of 3 independent experiments. Unpaired two-tailed t-test comparing levels of wt and mHTT fragments at any individual time-point: $p > 0.05$.

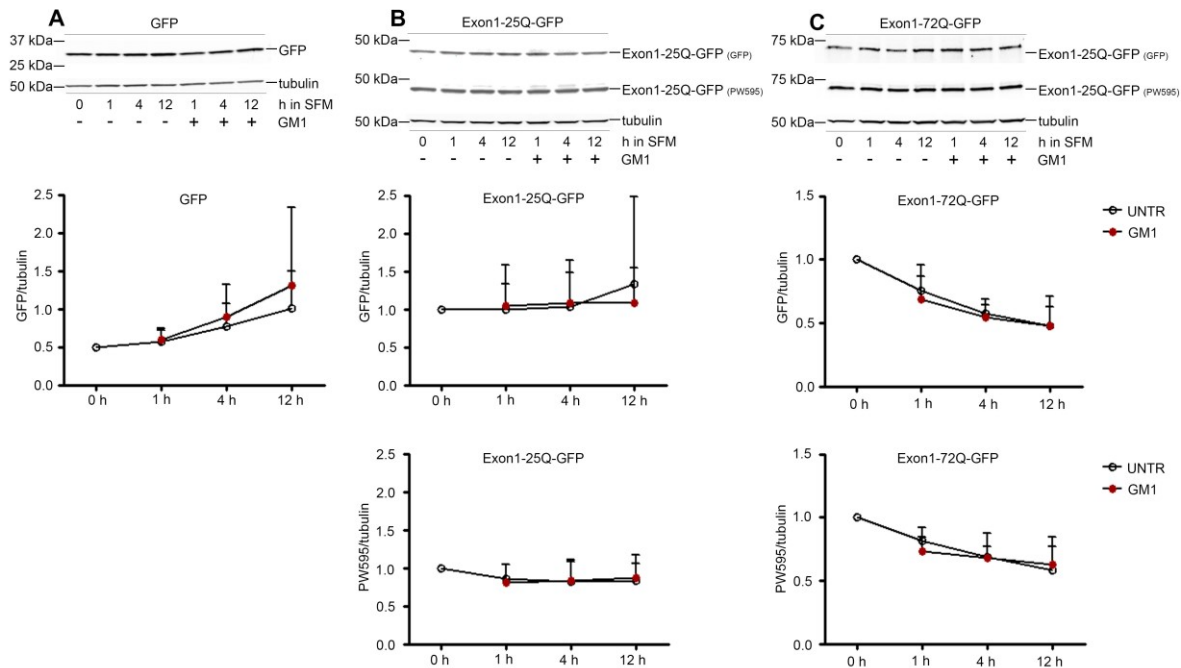


Figure 3.1.3: Treatment with GM1 does not change wt or mHTT N-terminal fragment levels in transiently transfected striatal ST14A cells. Representative immunoblot and densitometric analysis of ST14A cells that were transiently transfected with A) GFP, B) Exon 1-25Q-GFP or C) Exon 1-72Q-GFP and treated with GM1 or vehicle in serum-free medium (SFM) for the indicated time. HTT fragments were detected with either anti-GFP or anti-HTT (PW595) antibodies. T-test analysis showed that GM1 treatment did not change levels of wt (B) or mHTT N-terminal fragments (C) at any of the indicated timepoints. GFP levels were also unaffected by GM1 treatment (A). Graph shows the mean \pm SD of 3 (GFP, Exon 1-72Q-GFP) or 4 (Exon 1-25Q-GFP) independent experiments.

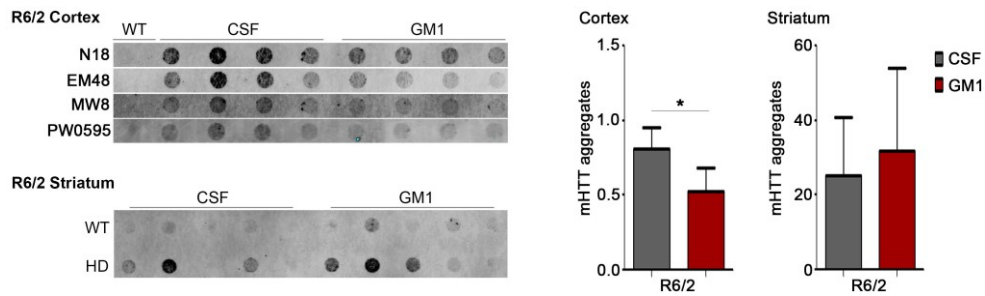


Figure 3.1.4: GM1 decreases mHTT aggregates in the cortex of R6/2 mice. R6/2 mice were treated with GM1 or vehicle (CSF) by chronic intraventricular infusion. Cortical and striatal tissues were collected and lysed and mHTT aggregates were analyzed by filter trap assay. Representative filter trap assays and densitometric analyses for R6/2 cortex and striatum are shown. In R6/2 cortex, aggregates were detected using 4 different anti-HTT antibodies (indicated on the left side of the immunoblot). Results were similar with all antibodies used. In R6/2 striatum, aggregates were detected using anti-HTT N18 antibody. Only quantification using anti-HTT N18 antibody are shown. T-test analysis shows significantly decreased mHTT aggregates in R6/2 cortex ($*p < 0.05$) after GM1 treatment. The amount of aggregates detected in the striatum of R6/2 mice was highly variable, and not significantly affected by GM1. Graphs show the mean \pm SD of 5 (R6/2 CSF/GM1 cortex) or 6 (R6/2 CSF/GM1 striatum) individual mice.

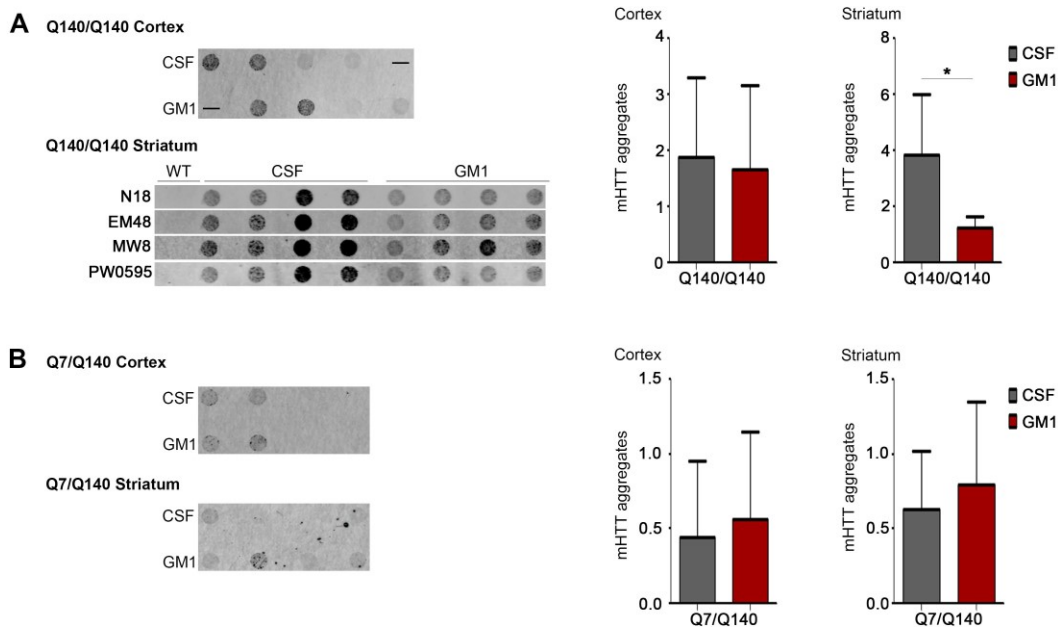


Figure 3.1.5: GM1 decreases mHTT aggregates in the striatum of Q140/Q140 mice. Q7/Q140 and Q140/Q140 mice were treated with GM1 or vehicle (CSF) by chronic intraventricular infusion. Cortical and striatal tissues were collected and lysed and mHTT aggregates were analyzed by filter trap assay. Representative filter trap assays and densitometric analyses for A) Q140/Q140 and B) Q7/Q140 cortex and striatum. In Q140/Q140 striatum, aggregates were detected using 4 different anti-HTT antibodies (indicated on the left side of the immunoblot). Results were similar with all antibodies used. In all other shown filter trap assays aggregates were detected and quantified using only anti-HTT N18 antibody. Black lines in (A) Q140/Q140 cortex indicate empty wells. A) T-test analysis shows significantly decreased mHTT aggregates in Q140/Q140 striatum ($*p < 0.05$) after GM1 treatment. Mutant HTT aggregates in Q140/Q140 cortex were unchanged. Graphs show the mean \pm SD of 4 (Q140/Q140 CSF cortex), 5 (Q140/Q140 GM1 cortex), 6 (Q140/Q140 CSF striatum), or 9 (Q140/Q140 GM1 striatum) mice. B) MHTT aggregates in

Q7/Q140 cortex and striatum were unchanged by GM1 treatment. Graphs show the mean \pm SD of 4 (Q7/Q140 CSF striatum), 5 (Q7/Q140 CSF cortex/ GM1 striatum), or 6 (Q7/Q140 GM1 cortex) mice.

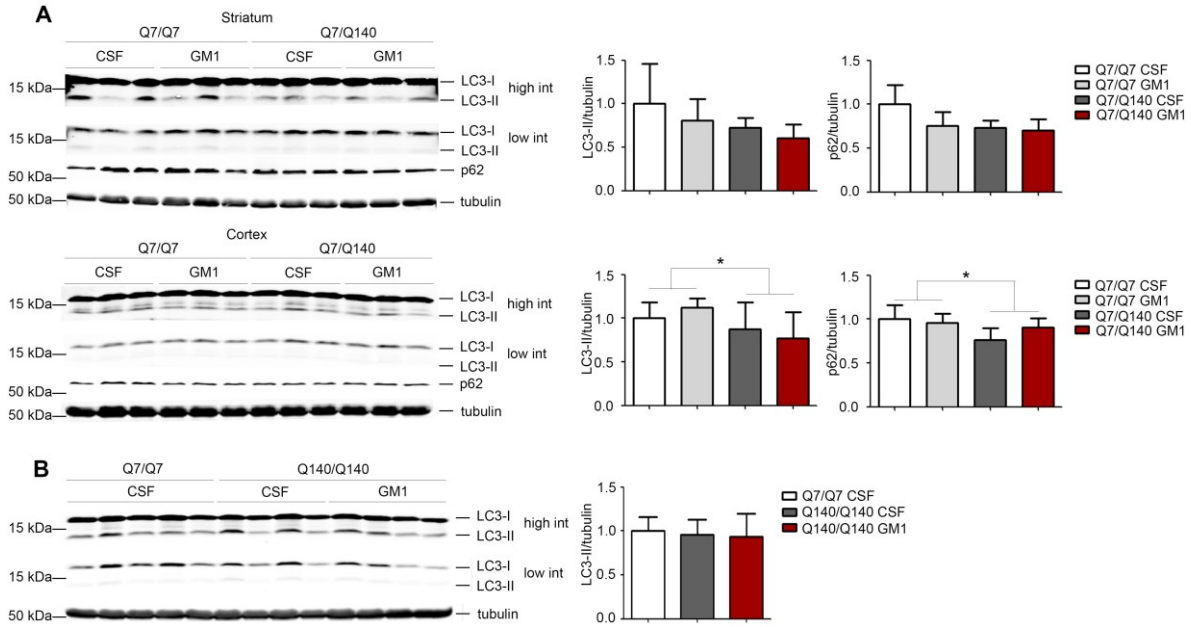


Figure 3.2.1: Levels of LC3-II and p62 in the striatum and cortex of Q140 mice are not modulated by GM1 treatment. Q7/Q7, Q7/Q140, and Q140/Q140 mice were treated with GM1 or vehicle (CSF) for 42 days by chronic intraventricular infusion. A) Representative immunoblots and densitometric analyses of LC3-II and p62 levels in Q7/Q140 striatum and cortex. No significant changes in LC3-II or p62 levels were observed in cortical and striatal tissue after GM1 treatment. However, a significant effect of genotype was detected, with decreased LC3-II and p62 levels in the cortex of Q7/Q140 mice. Graph for striatum shows the mean \pm SD of 3 mice per genotype and treatment group. Graph for cortex shows the mean \pm SD of 3 (Q7/Q7 GM1), 7 (Q7/Q7 CSF), and 8 (Q7/Q140 CSF/GM1) mice. Two-way ANOVA with Bonferroni multiple comparisons post-test: $*p < 0.05$. B) Representative immunoblot and densitometric analysis of LC3-II levels in Q140/Q140 cortex. LC3-II levels were not significantly changed by GM1 treatment. Graph shows the mean \pm SD of 7 (Q140/Q140 CSF/GM1) or 10 (Q7/Q7 CSF) mice. One-way ANOVA analysis with Bonferroni post-test.

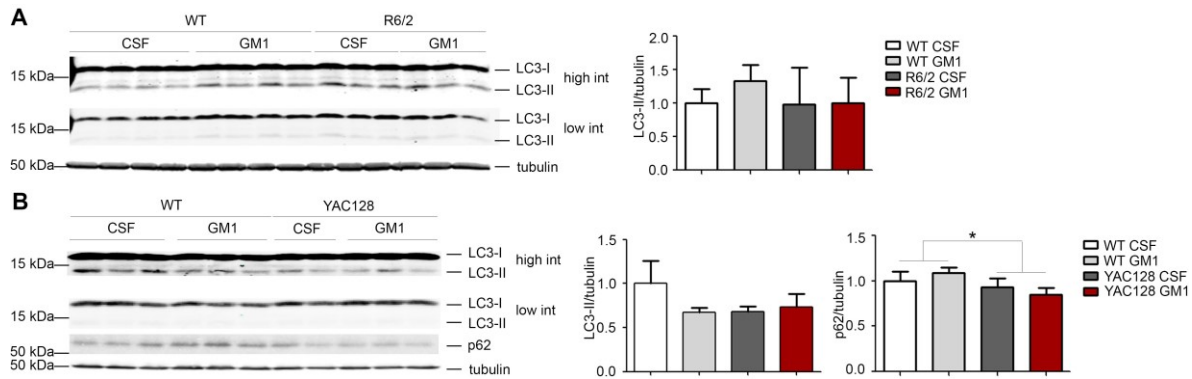


Figure 3.2.2: Levels of LC3-II and p62 are not significantly affected by treatment with GM1 in the cortex of R6/2 or YAC128 mice. R6/2 and YAC128 mice and WT littermates were treated with GM1 or vehicle (CSF) for 28 days by chronic intraventricular infusion. LC3-II and p62 levels in cortical tissue were analysed by immunoblotting. A) Representative immunoblots and densitometric analysis of LC3-II levels in R6/2 mice. Two-way ANOVA with Bonferroni multiple comparisons post-test revealed no significant changes of LC3-II levels after GM1 treatment. The graph shows the mean \pm SD of 6 (R6/2 CSF), 7 (WT GM1, R6/2 GM1) and 8 (WT CSF) mice. B) Representative immunoblots and densitometric analyses of LC3-II and p62 levels in YAC128 mice. Two-way ANOVA with Bonferroni multiple comparisons post-test revealed no significant changes of LC3-II or p62 levels after GM1 treatment. However, there was a statistically significant effect of genotype with p62 levels being decreased in YAC128 mice compared to WT littermates ($*p < 0.05$). Graphs show the mean \pm SD of 3 (WT CSF, WT GM1, and YAC128 GM1) and 2 (YAC128 CSF) mice.

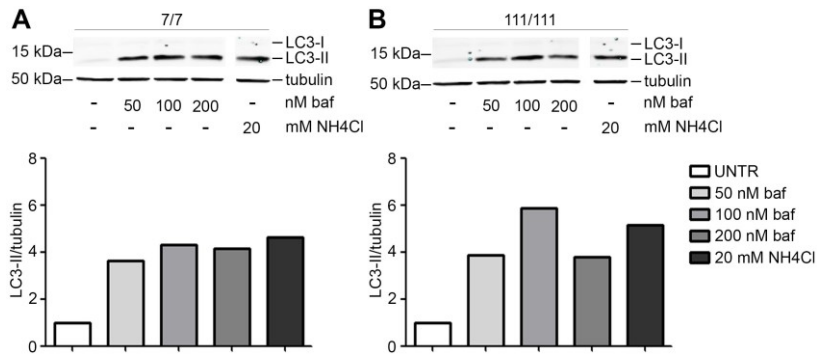


Figure 3.2.3: 100 nM bafilomycin efficiently blocks autophagic degradation in striatal 7/7 and 111/111 cells. Immunoblots and relative densitometric analyses of A) 7/7 and B) 111/111 cells that were grown in serum-free medium and treated with the indicated concentrations of bafilomycin (baf) or ammonium chloride (NH₄Cl). Bafilomycin at a concentration of 100 nM efficiently blocked autophagic degradation. Lanes for NH₄Cl were in the same gel, but intervening irrelevant bands were cut.

LC3-II levels at 12 h in the presence of bafilomycin, increasing it in 7/7 cells compared to untreated cells and decreasing LC3-II in 111/111 cells.

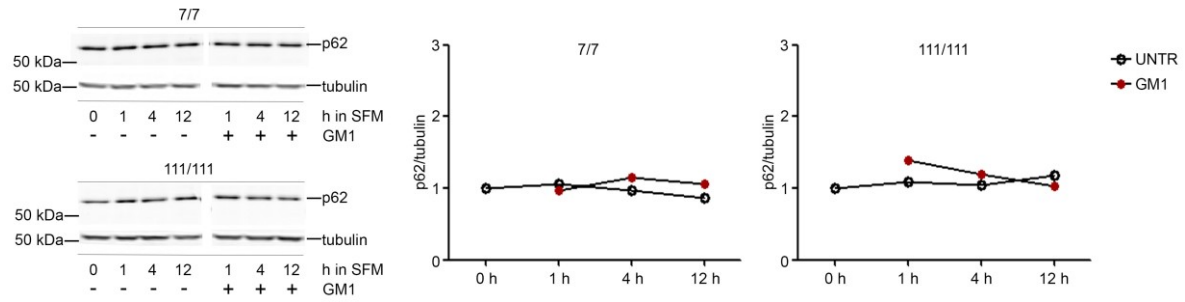


Figure 3.2.5: GM1 does not change p62 levels in striatal 7/7 or 111/111 cells.

Immunoblots and densitometric analyses of p62 levels in 7/7 and 111/111 cells grown in SFM and incubated with GM1 for the indicated times. GM1 treatment did not significantly change levels of p62 at any time-point.

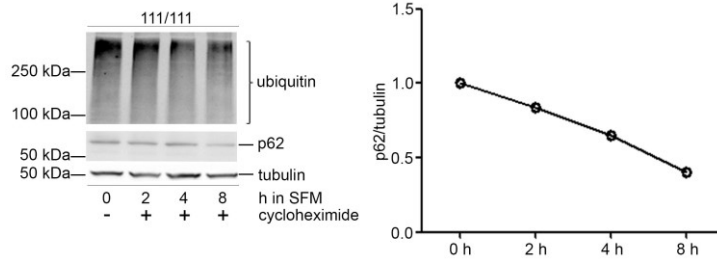


Figure 3.2.6: P62 levels decrease in serum-free conditions when protein synthesis is inhibited. Immunoblot and densitometric analysis of levels of p62 and ubiquitinated proteins in 111/111 cells grown in SFM and treated with cycloheximide for the indicated time. The graph shows the densitometric analysis of the immunoblot for p62 on the left.

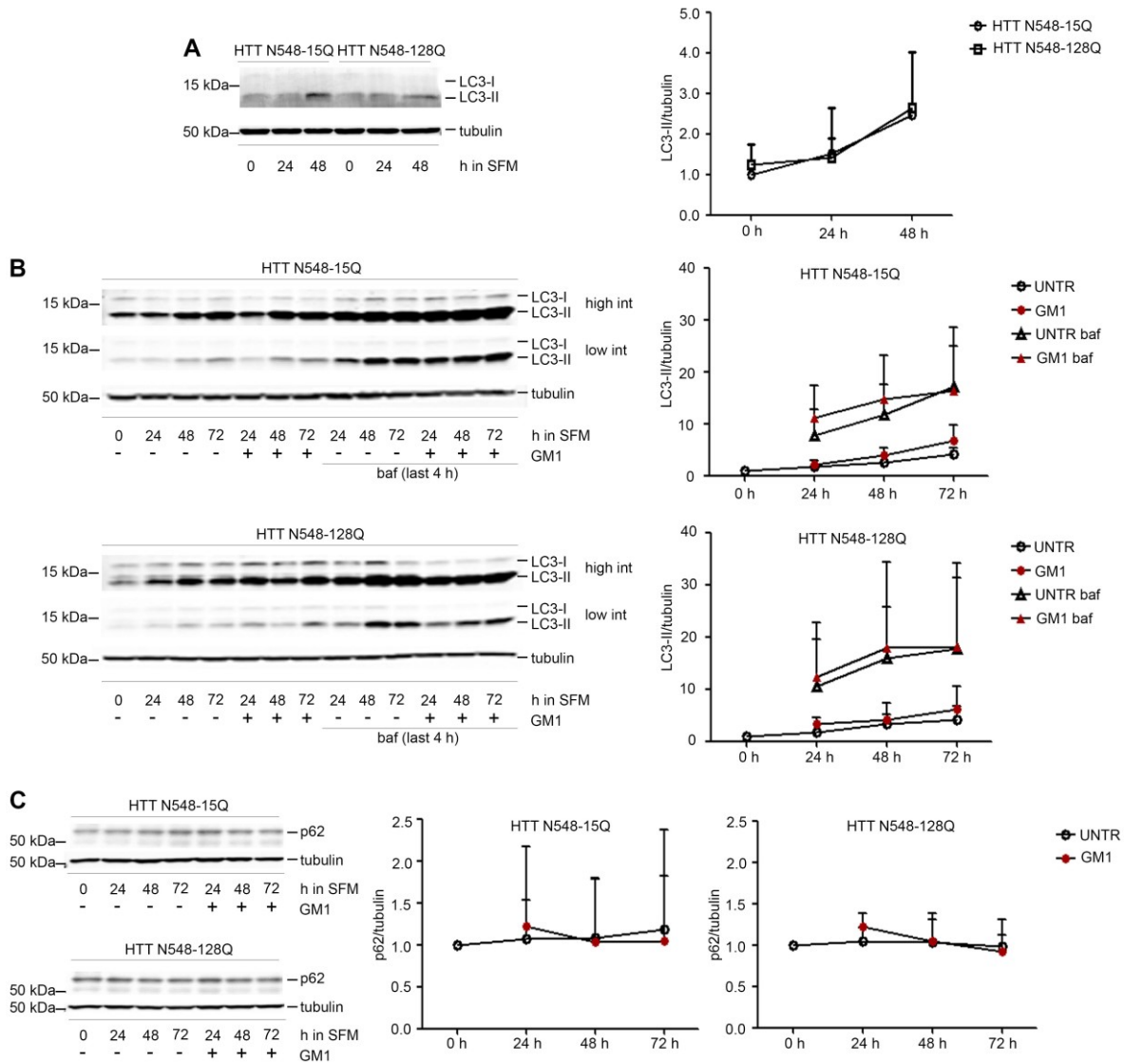


Figure 3.2.7: GM1 does not change levels of autophagy markers in striatal HTT N548-15Q or HTT N548-128Q cells. A) Representative immunoblot and densitometric analysis of LC3-II levels in HTT N548-15Q or HTT N548-128Q cells grown in SFM for the indicated time. No changes in LC3-II levels between HTT N548-15Q and HTT N548-128Q cells could be observed. Graphs show the mean \pm SD of 2 independent experiments. Representative immunoblots and densitometric analyses of LC3-II (B) and p62 (C) levels in HTT N548-15Q and HTT N548-128Q cells incubated with GM1 or vehicle in SFM for the indicated time and in the presence

of bafilomycin (baf) for the last 4 h of treatment. T-test analysis revealed no statistically significant difference in LC3-II and p62 levels after GM1 treatment at any timepoint in either genotype. Graphs show the mean \pm SD of 3 independent experiments, with the exception of bafilomycin treatments for which only two experiments were performed.

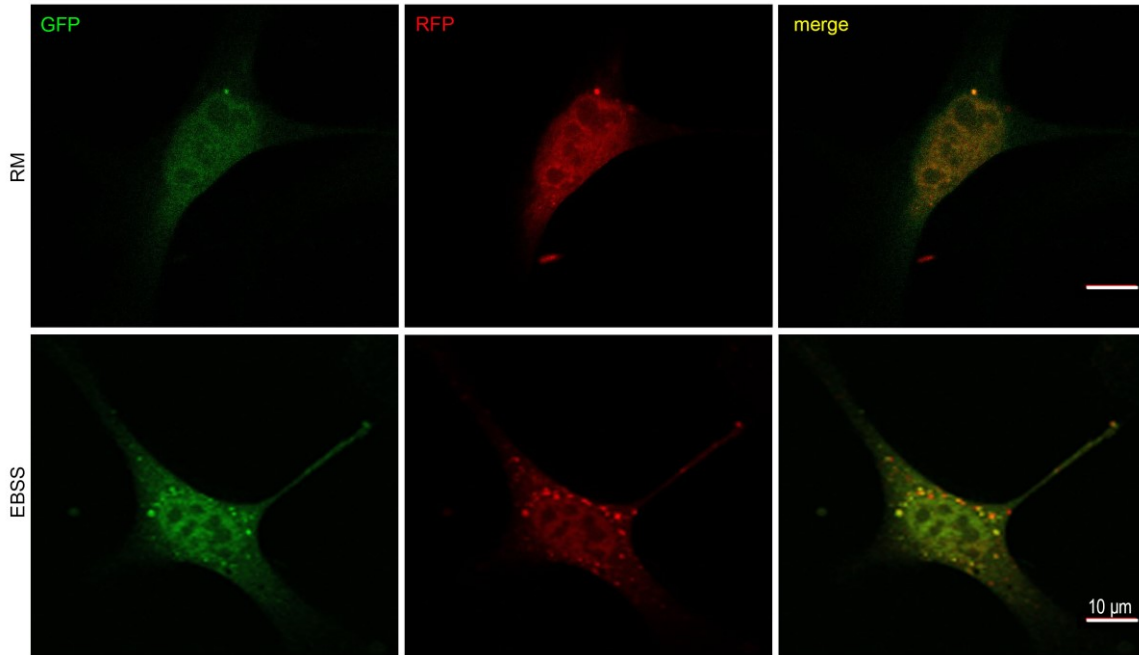


Figure 3.2.8: RFP-EGFP-LC3 intracellular distribution and localization in nutrient-rich and nutrient-deficient conditions. Confocal images of 111/111 cells transiently transfected with RFP-EGFP-LC3 and grown in either nutrient-rich (RM – regular medium) or nutrient-deficient (Earl’s balanced salt solution, EBSS) conditions for 3 h. In RM, nutrient-dependent autophagy is not active and RFP-EGFP-LC3 is diffuse in the cytosol. Only few yellow and red puncta can be detected and those most likely reflect basal levels of selective autophagy. When cells were grown in the nutrient-deficient growth medium EBSS, autophagy and autophagic flux was activated as detected by an increase in yellow (autophagosomes) and red (autolysosomes) puncta. The white line corresponds to 10 μm.

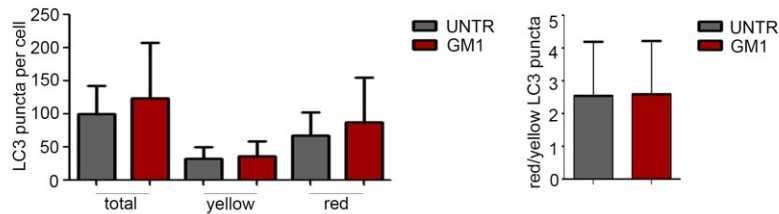
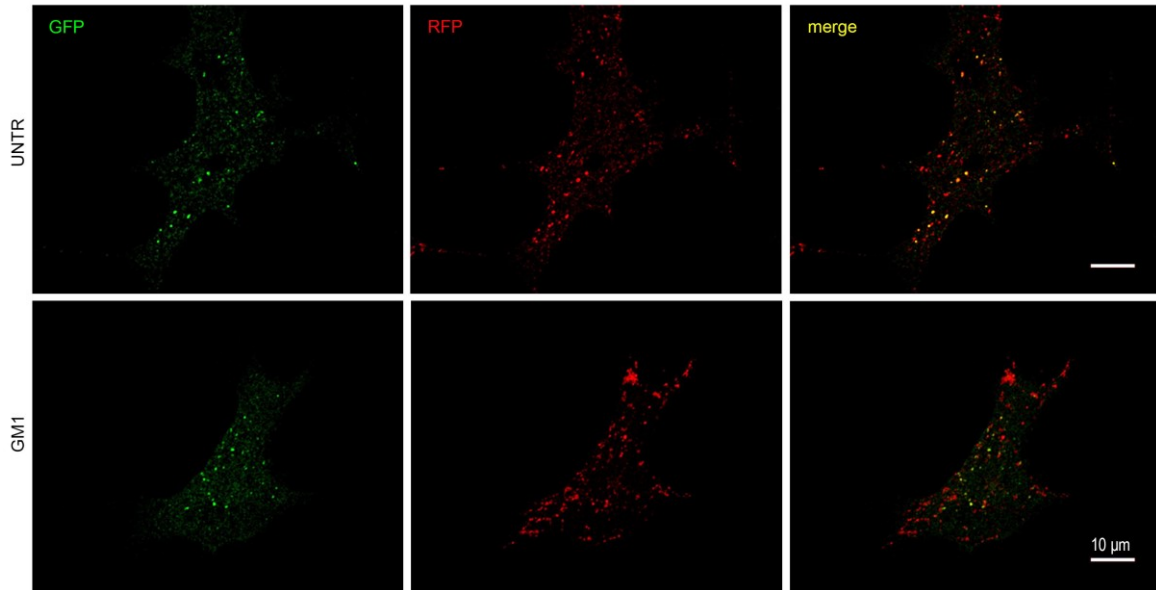


Figure 3.2.9: GM1 does not affect autophagic flux in striatal 111/111 cells transiently transfected with RFP-EGFP-LC3. Representative confocal images of 111/111 cells transiently transfected with RFP-EGFP-LC3 and treated with GM1 or vehicle in SFM for 3 h. Autophagic flux was assessed by counting total, yellow and red LC3 punctae per cell and determining the ratio red/yellow. T-test analysis did not reveal statistically significant differences after GM1 treatment. Graphs show the mean \pm SD of 23 untreated (UNTR) and 31 GM1-treated (GM1) transfected cells from two independent experiments. The white line corresponds to 10 μ m.

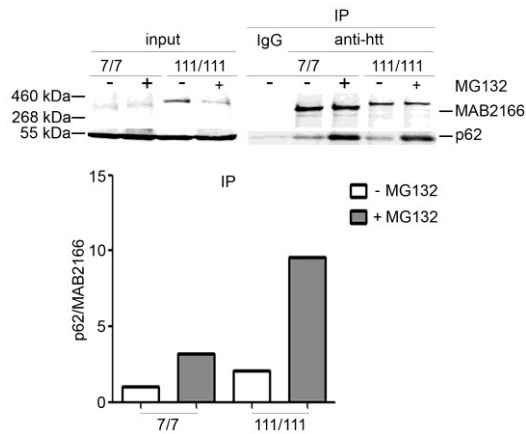


Figure 3.3.1: P62 binding to HTT in striatal cells is enhanced when the polyQ stretch is expanded. 7/7 and 111/111 cells were grown in nutrient-rich medium and incubated with 10 μ M MG132 (or vehicle) for 5 h to induce proteasome inhibition and trigger selective autophagy. HTT was immunoprecipitated from cell lysates using anti-HTT antibodies MAB2166 and MAB2168. The graph shows the densitometric analysis of the ratio of p62 over HTT (detected with MAB2166 antibody). P62 co-immunoprecipitated with HTT to a greater extent in samples treated with MG132 and more p62 co-immunoprecipitated with mHTT than with wtHTT, both in the presence and absence of MG132.

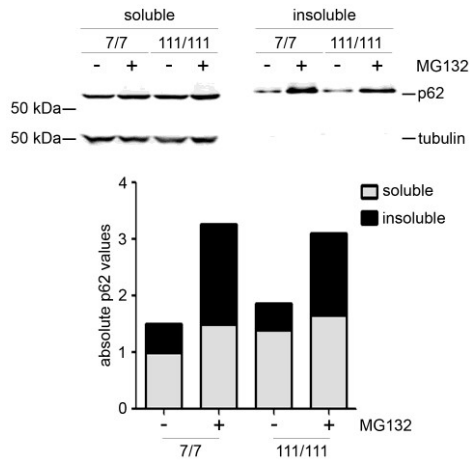


Figure 3.3.2: Normal p62-body formation in striatal 111/111 cells. 7/7 and 111/111 cells were grown in nutrient-rich medium and treated with 10 μ M MG132 or vehicle for 5 hours to block proteasomal degradation and induce selective autophagy. Immunoblot and densitometric analysis of soluble and insoluble p62 (p62-bodies or sequestosomes) levels are shown. The graph shows total p62 (soluble (light grey bars) and insoluble (black bars)) levels. With MG132 treatment p62-body formation increases as autophagy is induced, however, there is no obvious difference in p62 (soluble and insoluble) levels between 7/7 and 111/111 cells.

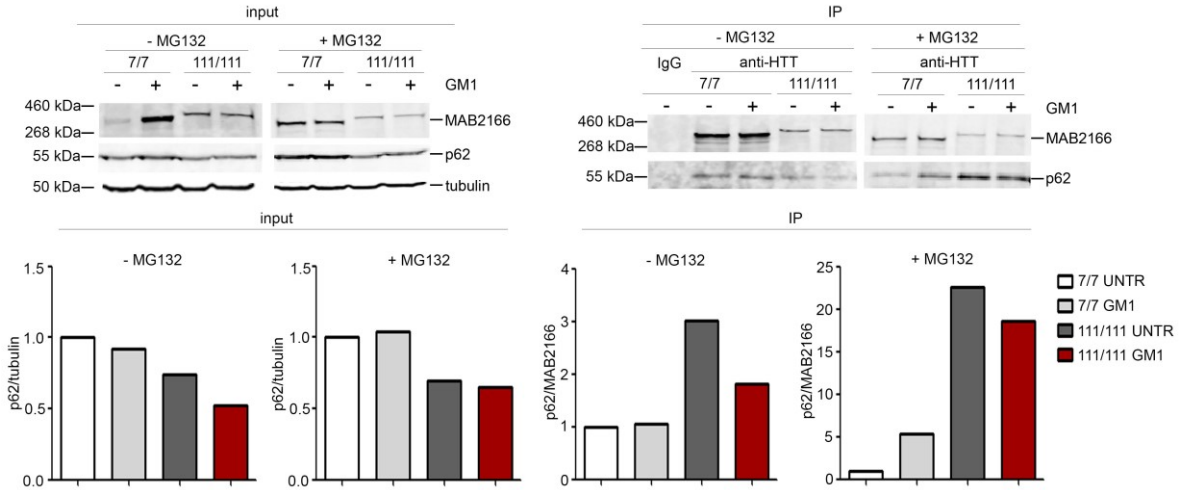


Figure 3.3.3: GM1 modulates binding of p62 to mHTT. 7/7 and 111/111 cells were grown in nutrient-rich medium in the presence or absence of 10 μ M MG132 for 5 h. After preincubation with MG132, GM1 was added for 10 minutes where indicated. Cell lysates were used to immunoprecipitate (IP) HTT. Immunoblots and relative densitometric analyses are shown. Both in the presence or absence of MG132, p62 binding to mHTT, as detected by co-immunoprecipitation, was enhanced compared to binding to wtHTT. GM1 treatment decreased the amount of p62 that co-immunoprecipitated with mHTT, but enhanced p62 co-immunoprecipitation with wtHTT in cells treated with MG132.

4 DISCUSSION

4.1 GM1 DOES NOT CHANGE MONOMERIC MHTT LEVELS, BUT DECREASES

MHTT AGGREGATES

Huntington's disease is caused by mHTT, which triggers a myriad of different toxic molecular processes in the cell, such as mitochondrial dysfunction, excitotoxicity, transcriptional dysregulation, impaired intracellular transport, aberrant lipid metabolism, and impaired selective autophagy (4, 67). Many researchers invest great effort towards finding a cure for the disease by targeting specific and individual pathogenic mechanisms downstream of mHTT expression. Although some of those interventions might be beneficial, a much better approach would be to target more directly the disease-causing gene/protein. As mentioned in the introduction of this thesis, approaches to lower mHTT protein content by gene silencing or by enhancing its degradation are under investigation. Both strategies have been shown to be neuroprotective in various HD cell and animal models (275, 276). Although gene silencing approaches are very promising, the HTT silencing agents that are currently in clinical trials do not exclusively target the *mHTT* allele, but also the allele for *wtHTT*. This might lead to potential complications or side effects, given the many functions that normal HTT carries out in the cell.

The ganglioside GM1 was shown by our group to protect HD cells from cell death (66) and to restore motor functions in an HD mouse model (245). Data from our laboratory suggests that the effects of GM1 extend beyond treatment of motor symptoms. In fact, both motor and non-motor manifestations of the disease, including impaired cognition, anxiety and depression, are corrected by treatment with GM1 in two different mouse models of the disease (246). Moreover, GM1 slows down the neurodegenerative process in R6/2 mice (247). These profound and widespread therapeutic effects can perhaps be explained, at

least in part, by the fact that GM1 is able to affect mHTT itself, by stimulating a post-translational modification of the protein (phosphorylation at serine 13 and serine 16) (245) that reduces mHTT toxicity (249). The role of this post-translational modification in HD pathology is still not completely understood. However, *in vivo* studies showed reduced mHTT aggregate formation in HD mice expressing phosphomimetic mHTT. This finding was confirmed by *in vitro* studies showing decreased amyloid fibril formation of a phosphomimetic mHTT peptide (249). In addition, the phosphorylation of HTT at serines 13 and 16 can lead to increased HTT degradation (153).

Here, I investigated, if the neuroprotective functions of GM1 in HD models were in part mediated through lowering mHTT protein levels, potentially by increasing its autophagic clearance. In support of this hypothesis, a ganglioside mix containing GM1 (amongst other gangliosides) was previously shown to enhance autophagy in cells (195). In addition, a ganglioside mix containing GM1 (amongst other gangliosides) reversed lysosomal pathology and suppression of autophagy induced by inhibition of ganglioside synthesis in a cellular model of PD (199, 200).

In my studies, I did not detect a change in the steady-state levels of N-terminal mHTT fragments in cells overexpressing Exon 1-72Q-GFP after GM1 treatment, compared to untreated controls (Figure 3.1.2). One potential caveat in these experiments was the timecourse of autophagic induction (up to 12 h), which might have been too short to induce autophagic degradation of mHTT N-terminal fragments. In previous work, a longer incubation in the presence of gangliosides, up to 24 h, was used to induce autophagy in astrocytes (195). However, in experiments using stable cell lines expressing HTT N548-128Q (Figure 3.1.3) there was no reduction in steady-state levels of mHTT N-terminal fragments even after 24, 48, or 72 h of exposure to GM1. Another factor to take into account is that cells were treated in SFM as done in previous experiments that investigated GM1's

ability to rescue cells from death in apoptotic conditions (66). SFM is devoid of growth factors that usually activate the AKT pathway and subsequently mTORC1, thereby repressing nutrient-dependent or “bulk” autophagy (156). Vice versa, when growth factors are absent mTORC1 is inhibited and nutrient-dependent autophagy is upregulated. Indeed, Figures 3.1.2 and 3.2.7 show that in our experimental conditions, autophagy was activated leading to autophagic degradation of HTT N-terminal fragments in HTT N548-15Q or HTT N548-128Q cells. This raises the question of whether upregulation of bulk autophagy in our experimental conditions might have masked stimulatory effects on autophagy by GM1.

Analysis of soluble mHTT levels in the brain of HD mouse models also showed no changes induced by GM1 treatment *in vivo*. In these experiments that used whole striatal and cortical tissue, the relative contribution of neuronal and non-neuronal cell types to the phenotype analyzed (overall levels of soluble mHTT) could not be assessed. Therefore, any potential neuronal-specific effect of GM1, if any, could have been masked by the predominance of non-neuronal cells in the tissue. Another important point to consider is that steady-state levels of mHTT might not be an accurate and sensitive readout of protein turn-over, which would be more properly assessed with metabolic labeling experiments.

Another challenge in the detection of mHTT levels is that this protein is present in cells in many different forms, such as soluble full-length, N-terminal and C-terminal fragments (75), oligomers, fibrils, or aggregates (4). These various protein species cannot all be detected by the same method or antibodies, and an accurate measurement of total mHTT levels, which includes all protein forms, is extremely difficult, if not impossible, to achieve.

Thus, although the data presented in this thesis overall point at the inability of GM1 treatment to change soluble mHTT levels, the caveats highlighted above must be kept under consideration when drawing conclusions on the effects of GM1.

Interestingly, I detected a decrease of wtHTT levels in the brain of Q7/Q7 and Q7/Q140 mice treated with GM1 compared to untreated littermates (Figure 3.1.1). Although I did not measure wtHTT mRNA expression, it is unlikely that GM1 would modulate transcription of the wt but not the mutant allele (levels of mHTT did not change). Therefore, decreased wtHTT levels in Q7/Q140 might be due to increased protein degradation. The significance of these findings will be discussed in section 4.1.

Despite the lack of effect on soluble mHTT levels, chronic infusion of GM1 resulted in a significant reduction of mHTT insoluble aggregates in R6/2 cortex and Q140/Q140 striatum, as detected by filter trap assay (Figure 3.1.4). Mutant HTT aggregates have been shown to be neurotoxic or neuroprotective depending on the context (73). In this case, the term 'neuroprotective' refers to the aggregates' role in capturing the more toxic N-terminal fragments of mHTT, which in turn decreases toxicity. Despite this beneficial effect, aggregates are still harmful for a cell as they can physically impair axonal transport and trap transcription factors (73). Therefore, overall reduction of aggregate burden, when more toxic soluble mHTT does not increase, is highly desirable in HD.

One puzzling observation in my studies was that GM1 decreased aggregates in R6/2 cortex and in Q140/Q140 striatum, but not in the R6/2 striatum or Q140/Q140 cortex. If the same mechanism was at play in both mouse models, one would have expected to see similar changes in the same brain region(s) across models. Drug distribution cannot explain the differences observed. As a matter of fact, the site of cannulation and GM1 infusion - the lateral right ventricle - was the same across models, ensuring that drug distribution would occur in similar manner in all mice treated. Moreover, the striatum is anatomically located right under the site of infusion, and therefore GM1 infused into the ventricle should more easily reach the striatum than the cortex. One possible explanation for the discrepancies observed across models is that the relatively low number of mice analyzed, together with

the very high variability within each experimental group, might not have allowed for the detection of differences among treatment groups. More animals will need to be analyzed in the future to reach statistical power and draw conclusions. Regardless of where changes occurred, another question arising from my experiments is whether the observed reduction of aggregates in GM1-treated mice was due to increased autophagic degradation or decreased formation. Both scenarios are possible. GM1 has been shown to directly interact with A β and α -syn thereby modulating their aggregation (221, 222). While GM1 mediates A β fibrillation (221, 277), it was shown to inhibit fibrillation of α -syn (222). A β can interact with the glycan group of GM1 on the outer leaflet of the plasma membrane (278), and might also interact within the endosomal compartment which both proteins can traffic to (206, 279). In the case of α -syn, a direct interaction between the protein and the sugar head group of GM1 has also been detected, but only in *in vitro* studies using small unilamellar vesicles loaded with GM1 (222). How and where exactly this interaction would occur in cells is less clear. In fact, α -syn is a cytosolic protein, while the glycan moiety of GM1 faces either the extracellular space (when GM1 is located in the plasma membrane) or the lumen of intracellular compartments (Golgi, endosomal membranes and lysosomes) (206). However, recent studies suggest that α -syn might be “excreted” by cells in the extracellular environment, and then taken up by neighboring cells through a vesicle-mediated process (280). In such cases, α -syn would potentially come in contact with the sugar headgroup of GM1 present at the plasma membrane or in the endosomal compartment. Considerations similar to those raised in the case of an interaction of GM1 with α -syn also apply to a potential interaction of GM1 with soluble and aggregated forms of mHTT. The latter are mainly located in the cytosol or nucleus, but it has been recently proposed that cell-to-cell transmission of mHTT may occur with mechanisms similar to those described for α -syn (281). Thus, GM1 could directly interact with mHTT aggregates “excreted” by cells, after endocytosis of the latter and/or within the endosomal compartment or autolysosomes.

Even in the absence of a direct interaction GM1 could still modulate mHTT aggregation, by triggering protein post-translational modifications that affect protein folding. Phosphorylation of mHTT at serines 13 and 16 could play a major role. As a matter of fact, this post-translational modification that can be triggered by administration of GM1 (245) was shown to slow down the aggregation kinetics of mHTT N-terminal peptides *in vitro* (249).

Alternatively, decreased aggregate load in animals treated with GM1 could be the result of increased autophagic degradation. This could be achieved by a general upregulation of this degradative process by GM1. In the next section I will discuss the experiments I performed to test this hypothesis and the results obtained.

4.2 GM1 DOES NOT INDUCE AUTOPHAGY OR ENHANCE AUTOPHAGIC FLUX

Autophagy is one of the major degradation pathways in cells beside the proteasome. While the proteasome mainly targets short-lived nuclear and cytosolic proteins (282), autophagy substrates have generally long half-lives and include cytosolic proteins, protein aggregates, and damaged organelles (283). Autophagy is of great importance especially for post-mitotic neurons that cannot ensure dilution of misfolded proteins and damaged organelles through cell division. This is shown by the fact that inhibition of basal autophagy in mouse neurons results in neurodegeneration (273, 284). Many proteins linked to neurodegenerative disorders, such as α -syn, tau, superoxide dismutase 1, ataxin-3, and HTT itself have been shown to be targets for autophagic degradation (283). Several studies showed that upregulation of autophagy with compounds such as rapamycin (142), lithium (285), or trehalose (143) resulted in decreased levels of soluble and aggregated mHTT in various HD cell and animal models, leading to reduced toxicity and neuroprotection. Upregulation of autophagy in PD, AD, Amyotrophic Lateral Sclerosis (ALS), or Spinocerebellar ataxia type

3 (SCA3) might therefore also have beneficial effects in clearing the proteins associated with each disease.

Gangliosides might regulate autophagy through inhibition of the Akt-mTORC1 pathway (286). In contrast, our group and others have shown that the ganglioside GM1 activates Akt (66, 287, 288). Another ganglioside, GD3, has been shown to be involved in autophagosome formation and maturation (196). It is not known, whether GM1 plays a role in autophagy.

Reduced mHTT aggregates (Figures 3.1.4 and 3.1.5) and lowered wtHTT levels (Figure 3.1.1) after GM1 treatment, as detected in my studies, might suggest increased autophagy.

However, I could never detect changes in autophagic markers such as LC3-II and p62 after GM1 treatment in any of the models used in my studies (Figures 3.2.1, 3.2.2, 3.2.4, 3.2.7 and 3.2.8). LC3-II and p62 levels were unchanged in GM1-treated R6/2 mice compared to untreated controls (Figure 3.2.2), in spite of decreased mHTT aggregates. Unfortunately, I could not measure autophagy markers in the striatum of Q140/Q140 mice, where a reduction of aggregates was also observed (Figure 3.1.5) due to unavailability of tissue for these measurements. In the heterozygous Q7/Q140 mouse model, where very little mHTT aggregates were detected (Figures 3.1.4 and 3.1.5), p62 levels were significantly decreased compared to controls (Figure 3.2.1 A). This most likely indicates enhanced autophagic flux in the cortex of Q7/Q140 mice compared to Q7/Q7 littermates, since both LC3-II and p62 are degraded in the autophagic process. Decreased p62 levels were also detected in the cortex of YAC128 mice (Figure 3.2.2 B), which overexpress full-length mHTT (254). These data are in line with previous observations of increased autophagic flux in HD models (67). Once again, GM1 treatment did not significantly affect any autophagic marker in these mice.

One important limitation of the *in vivo* studies described in this thesis is that only steady-state levels of autophagic markers could be measured. The latter might be influenced by a

number of factors, including rate of autophagic flux and *de novo* synthesis, which cannot be easily accounted for in *in vivo* studies and can therefore confound results.

To overcome these potential problems and to get a better insight on the potential effects of GM1 on autophagy, I performed experiments in cell models. In the conditions used in this thesis (serum deprivation) all cell lines, regardless of genotype, were able to activate and sustain autophagy in a similar manner, as measured by levels of LC3-II and p62 (Figures 3.2.4 and 3.2.7). Incubation with GM1 did not have significant or reproducible effects in the cell lines tested. However, and as previously mentioned, I cannot exclude that induction of autophagy in serum-free medium would have masked any further GM1-induced increase in autophagy or autophagic flux. As outlined earlier, a ganglioside mix was able to induce autophagy within 24 h (195) and therefore I would have expected GM1 to do the same in the timecourse tested (1-72 h incubation with GM1).

Another observation was that steady-state levels of p62, often used as a surrogate marker of autophagic flux (267) did not decrease when cells, both WT and HD, were grown in SFM and autophagy was induced (Figures 3.2.4 and 3.2.7). My data show that this is likely due to *de novo* p62 synthesis as the protein is degraded by autophagy: blocking protein translation with cycloheximide led to a time-dependent reduction of p62 levels (degradation) when autophagy was activated (Figure 3.2.6).

Because of the limitations of using the autophagic flux marker p62, I measured autophagic flux by confocal microscopy upon transfection of 111/111 cells with RFP-EGFP-LC3 and treatment with GM1 or vehicle for 3 h. The assessment of yellow and red puncta yielded no difference in the total amount of autophagic structures. In addition, the red/yellow ratio - which provides information on autophagic flux - revealed no changes in GM1-treated

compared to untreated cells (Figure 3.2.9). Whether a longer incubation with GM1 can modulate autophagic flux remains to be investigated.

Overall, the experiments herein described suggest that GM1 does not significantly affect induction of autophagy and autophagic flux in cells exposed to SFM.

A major problem concerning autophagy in HD models is that autophagosomes fail to efficiently trap cargo (67). This, of course, would lead to accumulation of mHTT protein aggregates, as well as dysfunctional organelles, including damaged mitochondria, among other problems. Could the effects of GM1 on protein aggregates (Figures 3.1.4 and 3.1.5) be the result of enhanced selective uptake of mHTT aggregates into autophagic structures? Could GM1 specifically modulate selective rather than bulk autophagy?

4.3 GM1 MODULATES THE INTERACTION OF MHTT WITH THE CARGO

RECOGNITION MOLECULE P62

Selective autophagy is impaired at the level of cargo recognition in HD cell and animal models. Autophagosomes form at normal or even enhanced levels but fail to efficiently trap cytosolic cargo (67). This impairment might be due to aberrant interaction of mHTT with p62. While interaction between wtHTT and p62 was shown to be necessary to induce selective autophagy (58) in co-immunoprecipitation experiments it was also shown that mHTT displays increased binding to p62 compared to the wt protein (67). It was proposed that this aberrant interaction impairs the ability of p62 to recognize cargo (67).

In my experiments, I was able to confirm, in our HD cell model, the existence of an aberrant interaction between mHTT and p62, as measured by the higher amount of p62 co-immunoprecipitated with mHTT than wtHTT (Figure 3.3.1). As expected from the role of HTT in selective autophagy, conditions that induce proteotoxic stress (proteasome inhibition by

MG132) and stimulate selective autophagy resulted in a higher amount of p62 co-immunoprecipitated with wtHTT and even higher with mHTT (Figure 3.3.1).

Proteotoxic stress also leads to increased formation of Triton X100-insoluble p62 bodies (also called sequestosomes), which consist of ubiquitin-labeled protein aggregates and are found in the cytosol of many different cell types, including neural cells (289). These membrane-free bodies are degraded by autophagy (289) and their formation is enhanced upon proteotoxic stress (58). WtHTT was shown to be necessary for p62 body formation, as its knockdown results in decreased levels of sequestosomes (58). Whether expansion of the polyQ stretch in the mHTT protein results in loss of function and decreased p62 body formation, as observed when wtHTT is knocked down (58) is not known. My experiments show similar levels of p62 bodies in WT and HD cells in basal or proteotoxic stress conditions (Figure 3.3.2). This suggests that mHTT does not impair p62 body formation. As an alternative explanation, similar steady-state levels of p62 bodies would be detected if mHTT impaired both their formation and degradation at the same time. Although this second possibility seems to be less likely, in order to exclude it one would have to measure the abundance of insoluble p62 in sequestosomes in conditions in which autophagic degradation is blocked.

The most intriguing observation in my study was that incubation of cells with GM1 for as short as 10 min affected the aberrant interaction between p62 and mHTT. In fact, GM1 decreased the amount of p62 co-immunoprecipitated with mHTT by 40% in basal and by 18% in proteotoxic stress (MG132) conditions (Figure 3.3.3). The short incubation time with GM1 in this experiment (10 min) suggests that the effect of the ganglioside on p62-mHTT interaction might be mediated by rapid cell signaling mechanisms and induction of protein post-translational modifications. Phosphorylation of HTT at serine residues 13 and 16 is a likely candidate. As previously mentioned, GM1 triggers phosphorylation of HTT at these

residues (245). How, in turn, this post-translational modification would result in changes in the interaction between p62 and mHTT remains to be investigated. It is likely that HTT phosphorylation would lead to conformational changes of the protein with potential far-reaching effects (249, 290, 291). Future studies will determine whether the interaction of mHTT with p62 is indeed modulated by the phosphorylation events mentioned above.

It is still unknown whether decreased interaction between p62 and mHTT would result in improved cargo recognition and selective autophagy in HD and whether this, in turn, would translate into beneficial effects on disease progression.

Although our data on the reduction of mHTT aggregates after treatment with GM1 suggest improvement of cargo recognition, additional experiments will be required to determine whether this is indeed the case.

Interestingly, my studies also revealed that levels of wtHTT are decreased by GM1 in Q7/Q7 and Q7/Q140 mice (Figure 3.1.1). It is not known whether wtHTT is degraded together with p62 upon cargo recognition and autophagy (58), but such a scenario might not be unlikely. Therefore, one might speculate that decreased levels of wtHTT after treatment with GM1 could potentially be due to increased autophagic degradation of the complex HTT-p62 that is involved in cargo recognition.

In summary, although GM1 did not reduce soluble mHTT levels, it decreased mHTT aggregates in specific brain areas of select HD mouse models. This reduction was not the result of a GM1-mediated upregulation of autophagy, but could be due changes in the interaction between mHTT and p62 and to restored or improved cargo recognition.

5 CONCLUSIONS

My initial hypothesis was that the beneficial effects of GM1 in HD models are at least in part mediated by stimulation of autophagy and restoration of cargo recognition in selective autophagy, with consequent enhancement of mHTT clearance.

Contrary to the initial hypothesis, I could not detect, in the models and experimental conditions used in this thesis, any general effects of GM1 on autophagy or autophagic flux, as analysis of autophagy markers LC3 and p62 in HD mouse and cell models showed no differences after GM1 treatment. GM1 did not reduce soluble mHTT levels in HD mouse or cell models, but decreased mHTT aggregates in specific brain areas in two HD mouse models. This reduction in mHTT aggregates together with no changes in soluble mHTT levels, suggests that selective autophagy of protein aggregates might be increased by GM1. As a matter of fact, GM1 decreased an aberrant interaction of mHTT with p62 that was previously shown to impair selective (67), thereby potentially improving cargo recognition and the degradation of mHTT aggregates.

Future studies will need to specifically address this point and determine whether cargo recognition is restored after GM1 treatment.

The mechanism underlying decreased interaction between mHTT and p62 after GM1 treatment remains to be investigated. We have proposed that mHTT post-translational modifications – in particular phosphorylation at Ser13 and Ser16 – might play a crucial role, by affecting polyQ conformation and mHTT binding to p62 and other proteins. Future experiments will address this hypothesis.

Enhancing selective autophagy in HD would have more profound consequences than just reducing mHTT aggregate burden. It would improve removal of dysfunctional mitochondria

which are a hallmark of the disease (24, 61, 292), and would potentially correct downstream problems linked to impaired energy supply to cells and increased oxidative stress (89, 293).

Other interventions that decrease mHTT aggregate burden and/or correct mitochondrial metabolism have been linked to neuroprotection (294-296).

The use of GM1 for the treatment of neurological disorders is not new and clinical trials in PD (234, 240, 241), stroke (232), and spinal cord injury (235, 236) have shown that peripheral administration of GM1 is safe and in some cases leads to beneficial effects. The long-term safety of GM1 in patients (242) together with its neurotrophic properties on cells (217-219) and profound effects on motor- and non-motor symptoms in three different HD mouse models (245-247) make GM1 a potential candidate for HD therapy. One important point to consider, is GM1 bioavailability in the brain after peripheral administration due to its poor ability to cross the blood-brain-barrier. Although recent evidence shows disrupted integrity of the blood-brain-barrier in HD patients, at least to a certain extent (297), whether this is enough to ensure that peripherally administered GM1 reaches therapeutic concentrations in the brain will have to be determined.

6 REFERENCES

1. Vonsattel JP, DiFiglia M. Huntington disease. *Journal of neuropathology and experimental neurology*. 1998;57(5):369-84.
2. Huntington G. On chorea. George Huntington, M.D. *The Journal of neuropsychiatry and clinical neurosciences*. 2003;15(1):109-12.
3. A novel gene containing a trinucleotide repeat that is expanded and unstable on Huntington's disease chromosomes. The Huntington's Disease Collaborative Research Group. *Cell*. 1993;72(6):971-83.
4. Zuccato C, Valenza M, Cattaneo E. Molecular mechanisms and potential therapeutical targets in Huntington's disease. *Physiological reviews*. 2010;90(3):905-81.
5. Gil JM, Rego AC. Mechanisms of neurodegeneration in Huntington's disease. *The European journal of neuroscience*. 2008;27(11):2803-20.
6. Rosas HD, Hevelone ND, Zaleta AK, Greve DN, Salat DH, Fischl B. Regional cortical thinning in preclinical Huntington disease and its relationship to cognition. *Neurology*. 2005;65(5):745-7.
7. Rosas HD, Koroshetz WJ, Chen YI, Skeuse C, Vangel M, Cudkovicz ME, et al. Evidence for more widespread cerebral pathology in early HD: an MRI-based morphometric analysis. *Neurology*. 2003;60(10):1615-20.
8. Vonsattel JP. Huntington disease models and human neuropathology: similarities and differences. *Acta neuropathologica*. 2008;115(1):55-69.
9. Ciarmiello A, Cannella M, Lastoria S, Simonelli M, Frati L, Rubinsztein DC, et al. Brain white-matter volume loss and glucose hypometabolism precede the clinical symptoms of Huntington's disease. *Journal of nuclear medicine : official publication, Society of Nuclear Medicine*. 2006;47(2):215-22.
10. Di Paola M, Luders E, Cherubini A, Sanchez-Castaneda C, Thompson PM, Toga AW, et al. Multimodal MRI analysis of the corpus callosum reveals white matter differences in presymptomatic and early Huntington's disease. *Cerebral cortex (New York, NY : 1991)*. 2012;22(12):2858-66.
11. Rosas HD, Lee SY, Bender AC, Zaleta AK, Vangel M, Yu P, et al. Altered white matter microstructure in the corpus callosum in Huntington's disease: implications for cortical "disconnection". *NeuroImage*. 2010;49(4):2995-3004.
12. Roos RA, Pruyt JF, de Vries J, Bots GT. Neuronal distribution in the putamen in Huntington's disease. *Journal of neurology, neurosurgery, and psychiatry*. 1985;48(5):422-5.
13. Aylward EH, Codori AM, Barta PE, Pearlson GD, Harris GJ, Brandt J. Basal ganglia volume and proximity to onset in presymptomatic Huntington disease. *Archives of neurology*. 1996;53(12):1293-6.
14. Halliday GM, McRitchie DA, Macdonald V, Double KL, Trent RJ, McCusker E. Regional specificity of brain atrophy in Huntington's disease. *Experimental neurology*. 1998;154(2):663-72.
15. Sharp AH, Ross CA. Neurobiology of Huntington's disease. *Neurobiology of disease*. 1996;3(1):3-15.
16. de la Monte SM, Vonsattel JP, Richardson EP, Jr. Morphometric demonstration of atrophic changes in the cerebral cortex, white matter, and neostriatum in Huntington's disease. *Journal of neuropathology and experimental neurology*. 1988;47(5):516-25.
17. Heinsen H, Strik M, Bauer M, Luther K, Ulmar G, Gangnus D, et al. Cortical and striatal neurone number in Huntington's disease. *Acta neuropathologica*. 1994;88(4):320-33.
18. Lange H, Thorner G, Hopf A, Schroder KF. Morphometric studies of the neuropathological changes in choreatic diseases. *Journal of the neurological sciences*. 1976;28(4):401-25.

19. Tartari M, Gissi C, Lo Sardo V, Zuccato C, Picardi E, Pesole G, et al. Phylogenetic comparison of huntingtin homologues reveals the appearance of a primitive polyQ in sea urchin. *Molecular biology and evolution*. 2008;25(2):330-8.
20. Trottier Y, Devys D, Imbert G, Saudou F, An I, Lutz Y, et al. Cellular localization of the Huntington's disease protein and discrimination of the normal and mutated form. *Nature genetics*. 1995;10(1):104-10.
21. Atwal RS, Xia J, Pinchev D, Taylor J, Epanand RM, Truant R. Huntingtin has a membrane association signal that can modulate huntingtin aggregation, nuclear entry and toxicity. *Human molecular genetics*. 2007;16(21):2600-15.
22. del Toro D, Alberch J, Lazaro-Dieguez F, Martin-Ibanez R, Xifro X, Egea G, et al. Mutant huntingtin impairs post-Golgi trafficking to lysosomes by delocalizing optineurin/Rab8 complex from the Golgi apparatus. *Molecular biology of the cell*. 2009;20(5):1478-92.
23. Shirendeb U, Reddy AP, Manczak M, Calkins MJ, Mao P, Tagle DA, et al. Abnormal mitochondrial dynamics, mitochondrial loss and mutant huntingtin oligomers in Huntington's disease: implications for selective neuronal damage. *Human molecular genetics*. 2011;20(7):1438-55.
24. Panov AV, Gutekunst CA, Leavitt BR, Hayden MR, Burke JR, Strittmatter WJ, et al. Early mitochondrial calcium defects in Huntington's disease are a direct effect of polyglutamines. *Nature neuroscience*. 2002;5(8):731-6.
25. Waelter S, Scherzinger E, Hasenbank R, Nordhoff E, Lurz R, Goehler H, et al. The huntingtin interacting protein HIP1 is a clathrin and alpha-adaptin-binding protein involved in receptor-mediated endocytosis. *Human molecular genetics*. 2001;10(17):1807-17.
26. Trushina E, Singh RD, Dyer RB, Cao S, Shah VH, Parton RG, et al. Mutant huntingtin inhibits clathrin-independent endocytosis and causes accumulation of cholesterol in vitro and in vivo. *Human molecular genetics*. 2006;15(24):3578-91.
27. Yanai A, Huang K, Kang R, Singaraja RR, Arstikaitis P, Gan L, et al. Palmitoylation of huntingtin by HIP14 is essential for its trafficking and function. *Nature neuroscience*. 2006;9(6):824-31.
28. Fukata Y, Fukata M. Protein palmitoylation in neuronal development and synaptic plasticity. *Nature reviews Neuroscience*. 2010;11(3):161-75.
29. Kim KY, Perkins GA, Shim MS, Bushong E, Alcasid N, Ju S, et al. DRP1 inhibition rescues retinal ganglion cells and their axons by preserving mitochondrial integrity in a mouse model of glaucoma. *Cell death & disease*. 2015;6:e1839.
30. Hoffner G, Kahlem P, Djian P. Perinuclear localization of huntingtin as a consequence of its binding to microtubules through an interaction with beta-tubulin: relevance to Huntington's disease. *Journal of cell science*. 2002;115(Pt 5):941-8.
31. Gunawardena S, Her LS, Bruschi RG, Laymon RA, Niesman IR, Gordesky-Gold B, et al. Disruption of axonal transport by loss of huntingtin or expression of pathogenic polyQ proteins in *Drosophila*. *Neuron*. 2003;40(1):25-40.
32. Desmond CR, Atwal RS, Xia J, Truant R. Identification of a karyopherin beta1/beta2 proline-tyrosine nuclear localization signal in huntingtin protein. *The Journal of biological chemistry*. 2012;287(47):39626-33.
33. Harjes P, Wanker EE. The hunt for huntingtin function: interaction partners tell many different stories. *Trends in biochemical sciences*. 2003;28(8):425-33.
34. Zhang Y, Leavitt BR, van Raamsdonk JM, Dragatsis I, Goldowitz D, MacDonald ME, et al. Huntingtin inhibits caspase-3 activation. *The EMBO journal*. 2006;25(24):5896-906.

35. Dietrich P, Shanmugasundaram R, Shuyu E, Dragatsis I. Congenital hydrocephalus associated with abnormal subcommissural organ in mice lacking huntingtin in Wnt1 cell lineages. *Human molecular genetics*. 2009;18(1):142-50.
36. Henshall TL, Tucker B, Lumsden AL, Nornes S, Lardelli MT, Richards RI. Selective neuronal requirement for huntingtin in the developing zebrafish. *Human molecular genetics*. 2009;18(24):4830-42.
37. Nguyen GD, Molero AE, Gokhan S, Mehler MF. Functions of huntingtin in germ layer specification and organogenesis. *PloS one*. 2013;8(8):e72698.
38. Dragatsis I, Efstratiadis A, Zeitlin S. Mouse mutant embryos lacking huntingtin are rescued from lethality by wild-type extraembryonic tissues. *Development (Cambridge, England)*. 1998;125(8):1529-39.
39. Duyao MP, Auerbach AB, Ryan A, Persichetti F, Barnes GT, McNeil SM, et al. Inactivation of the mouse Huntington's disease gene homolog Hdh. *Science (New York, NY)*. 1995;269(5222):407-10.
40. Nasir J, Floresco SB, O'Kusky JR, Diewert VM, Richman JM, Zeisler J, et al. Targeted disruption of the Huntington's disease gene results in embryonic lethality and behavioral and morphological changes in heterozygotes. *Cell*. 1995;81(5):811-23.
41. Zeitlin S, Liu JP, Chapman DL, Papaioannou VE, Efstratiadis A. Increased apoptosis and early embryonic lethality in mice nullizygous for the Huntington's disease gene homologue. *Nature genetics*. 1995;11(2):155-63.
42. Auerbach W, Hurlbert MS, Hilditch-Maguire P, Wadghiri YZ, Wheeler VC, Cohen SI, et al. The HD mutation causes progressive lethal neurological disease in mice expressing reduced levels of huntingtin. *Human molecular genetics*. 2001;10(22):2515-23.
43. White JK, Auerbach W, Duyao MP, Vonsattel JP, Gusella JF, Joyner AL, et al. Huntingtin is required for neurogenesis and is not impaired by the Huntington's disease CAG expansion. *Nature genetics*. 1997;17(4):404-10.
44. Elias S, McGuire JR, Yu H, Humbert S. Huntingtin Is Required for Epithelial Polarity through RAB11A-Mediated Apical Trafficking of PAR3-aPKC. *PLoS biology*. 2015;13(5):e1002142.
45. Keryer G, Pineda JR, Liot G, Kim J, Dietrich P, Benstaali C, et al. Ciliogenesis is regulated by a huntingtin-HAP1-PCM1 pathway and is altered in Huntington disease. *The Journal of clinical investigation*. 2011;121(11):4372-82.
46. Nath S, Munsie LN, Truant R. A huntingtin-mediated fast stress response halting endosomal trafficking is defective in Huntington's disease. *Human molecular genetics*. 2015;24(2):450-62.
47. Leavitt BR, Guttman JA, Hodgson JG, Kimel GH, Singaraja R, Vogl AW, et al. Wild-type huntingtin reduces the cellular toxicity of mutant huntingtin in vivo. *American journal of human genetics*. 2001;68(2):313-24.
48. Rigamonti D, Bauer JH, De-Fraja C, Conti L, Sipione S, Sciorati C, et al. Wild-type huntingtin protects from apoptosis upstream of caspase-3. *The Journal of neuroscience : the official journal of the Society for Neuroscience*. 2000;20(10):3705-13.
49. Rigamonti D, Sipione S, Goffredo D, Zuccato C, Fossale E, Cattaneo E. Huntingtin's neuroprotective activity occurs via inhibition of procaspase-9 processing. *The Journal of biological chemistry*. 2001;276(18):14545-8.
50. Gervais FG, Singaraja R, Xanthoudakis S, Gutekunst CA, Leavitt BR, Metzler M, et al. Recruitment and activation of caspase-8 by the Huntingtin-interacting protein Hip-1 and a novel partner Hipp1. *Nature cell biology*. 2002;4(2):95-105.

51. Colin E, Zala D, Liot G, Rangone H, Borrell-Pages M, Li XJ, et al. Huntingtin phosphorylation acts as a molecular switch for anterograde/retrograde transport in neurons. *The EMBO journal*. 2008;27(15):2124-34.
52. Trushina E, Dyer RB, Badger JD, 2nd, Ure D, Eide L, Tran DD, et al. Mutant huntingtin impairs axonal trafficking in mammalian neurons in vivo and in vitro. *Molecular and cellular biology*. 2004;24(18):8195-209.
53. Gauthier LR, Charrin BC, Borrell-Pages M, Dompierre JP, Rangone H, Cordelieres FP, et al. Huntingtin controls neurotrophic support and survival of neurons by enhancing BDNF vesicular transport along microtubules. *Cell*. 2004;118(1):127-38.
54. Altar CA, Cai N, Bliven T, Juhasz M, Conner JM, Acheson AL, et al. Anterograde transport of brain-derived neurotrophic factor and its role in the brain. *Nature*. 1997;389(6653):856-60.
55. Zuccato C, Tartari M, Crotti A, Goffredo D, Valenza M, Conti L, et al. Huntingtin interacts with REST/NRSF to modulate the transcription of NRSE-controlled neuronal genes. *Nature genetics*. 2003;35(1):76-83.
56. Shimojo M. Huntingtin regulates RE1-silencing transcription factor/neuron-restrictive silencer factor (REST/NRSF) nuclear trafficking indirectly through a complex with REST/NRSF-interacting LIM domain protein (RILP) and dynactin p150 Glued. *The Journal of biological chemistry*. 2008;283(50):34880-6.
57. Ochaba J, Lukacsovich T, Csikos G, Zheng S, Margulis J, Salazar L, et al. Potential function for the Huntingtin protein as a scaffold for selective autophagy. *Proceedings of the National Academy of Sciences of the United States of America*. 2014;111(47):16889-94.
58. Rui YN, Xu Z, Patel B, Chen Z, Chen D, Tito A, et al. Huntingtin functions as a scaffold for selective macroautophagy. *Nature cell biology*. 2015;17(3):262-75.
59. Paulson HL, Bonini NM, Roth KA. Polyglutamine disease and neuronal cell death. *Proceedings of the National Academy of Sciences of the United States of America*. 2000;97(24):12957-8.
60. Yang W, Dunlap JR, Andrews RB, Wetzel R. Aggregated polyglutamine peptides delivered to nuclei are toxic to mammalian cells. *Human molecular genetics*. 2002;11(23):2905-17.
61. Orr AL, Li S, Wang CE, Li H, Wang J, Rong J, et al. N-terminal mutant huntingtin associates with mitochondria and impairs mitochondrial trafficking. *The Journal of neuroscience : the official journal of the Society for Neuroscience*. 2008;28(11):2783-92.
62. Cross AJ, Slater P, Reynolds GP. Reduced high-affinity glutamate uptake sites in the brains of patients with Huntington's disease. *Neuroscience letters*. 1986;67(2):198-202.
63. Dure LS, Young AB, Penney JB. Excitatory amino acid binding sites in the caudate nucleus and frontal cortex of Huntington's disease. *Annals of neurology*. 1991;30(6):785-93.
64. Zhai W, Jeong H, Cui L, Krainc D, Tjian R. In vitro analysis of huntingtin-mediated transcriptional repression reveals multiple transcription factor targets. *Cell*. 2005;123(7):1241-53.
65. Lee WC, Yoshihara M, Littleton JT. Cytoplasmic aggregates trap polyglutamine-containing proteins and block axonal transport in a Drosophila model of Huntington's disease. *Proceedings of the National Academy of Sciences of the United States of America*. 2004;101(9):3224-9.
66. Maglione V, Marchi P, Di Pardo A, Lingrell S, Horkey M, Tidmarsh E, et al. Impaired ganglioside metabolism in Huntington's disease and neuroprotective role of GM1. *The Journal of neuroscience : the official journal of the Society for Neuroscience*. 2010;30(11):4072-80.
67. Martinez-Vicente M, Talloczy Z, Wong E, Tang G, Koga H, Kaushik S, et al. Cargo recognition failure is responsible for inefficient autophagy in Huntington's disease. *Nature neuroscience*. 2010;13(5):567-76.

68. Sugaya K, Matsubara S, Kagamihara Y, Kawata A, Hayashi H. Polyglutamine expansion mutation yields a pathological epitope linked to nucleation of protein aggregate: determinant of Huntington's disease onset. *PloS one*. 2007;2(7):e635.
69. Lomakin A, Chung DS, Benedek GB, Kirschner DA, Teplow DB. On the nucleation and growth of amyloid beta-protein fibrils: detection of nuclei and quantitation of rate constants. *Proceedings of the National Academy of Sciences of the United States of America*. 1996;93(3):1125-9.
70. Wood SJ, Wypych J, Steavenson S, Louis JC, Citron M, Biere AL. alpha-synuclein fibrillogenesis is nucleation-dependent. Implications for the pathogenesis of Parkinson's disease. *The Journal of biological chemistry*. 1999;274(28):19509-12.
71. Nucifora FC, Jr., Sasaki M, Peters MF, Huang H, Cooper JK, Yamada M, et al. Interference by huntingtin and atrophin-1 with cbp-mediated transcription leading to cellular toxicity. *Science (New York, NY)*. 2001;291(5512):2423-8.
72. Wyttenbach A, Carmichael J, Swartz J, Furlong RA, Narain Y, Rankin J, et al. Effects of heat shock, heat shock protein 40 (HDJ-2), and proteasome inhibition on protein aggregation in cellular models of Huntington's disease. *Proceedings of the National Academy of Sciences of the United States of America*. 2000;97(6):2898-903.
73. Jones L, Hughes A. Pathogenic mechanisms in Huntington's disease. *International review of neurobiology*. 2011;98:373-418.
74. Ventruti A, Cuervo AM. Autophagy and neurodegeneration. *Current neurology and neuroscience reports*. 2007;7(5):443-51.
75. Ehrnhoefer DE, Sutton L, Hayden MR. Small changes, big impact: posttranslational modifications and function of huntingtin in Huntington disease. *The Neuroscientist : a review journal bringing neurobiology, neurology and psychiatry*. 2011;17(5):475-92.
76. Gafni J, Ellerby LM. Calpain activation in Huntington's disease. *The Journal of neuroscience : the official journal of the Society for Neuroscience*. 2002;22(12):4842-9.
77. Gafni J, Hermel E, Young JE, Wellington CL, Hayden MR, Ellerby LM. Inhibition of calpain cleavage of huntingtin reduces toxicity: accumulation of calpain/caspase fragments in the nucleus. *The Journal of biological chemistry*. 2004;279(19):20211-20.
78. Kim YJ, Sapp E, Cuiffo BG, Sobin L, Yoder J, Kegel KB, et al. Lysosomal proteases are involved in generation of N-terminal huntingtin fragments. *Neurobiology of disease*. 2006;22(2):346-56.
79. Miller JP, Holcomb J, Al-Ramahi I, de Haro M, Gafni J, Zhang N, et al. Matrix metalloproteinases are modifiers of huntingtin proteolysis and toxicity in Huntington's disease. *Neuron*. 2010;67(2):199-212.
80. Carroll JB, Southwell AL, Graham RK, Lerch JP, Ehrnhoefer DE, Cao LP, et al. Mice lacking caspase-2 are protected from behavioral changes, but not pathology, in the YAC128 model of Huntington disease. *Molecular neurodegeneration*. 2011;6:59.
81. Graham RK, Deng Y, Carroll J, Vaid K, Cowan C, Pouladi MA, et al. Cleavage at the 586 amino acid caspase-6 site in mutant huntingtin influences caspase-6 activation in vivo. *The Journal of neuroscience : the official journal of the Society for Neuroscience*. 2010;30(45):15019-29.
82. Wellington CL, Singaraja R, Ellerby L, Savill J, Roy S, Leavitt B, et al. Inhibiting caspase cleavage of huntingtin reduces toxicity and aggregate formation in neuronal and nonneuronal cells. *The Journal of biological chemistry*. 2000;275(26):19831-8.
83. Warby SC, Doty CN, Graham RK, Carroll JB, Yang YZ, Singaraja RR, et al. Activated caspase-6 and caspase-6-cleaved fragments of huntingtin specifically colocalize in the nucleus. *Human molecular genetics*. 2008;17(15):2390-404.

84. Graham RK, Deng Y, Slow EJ, Haigh B, Bissada N, Lu G, et al. Cleavage at the caspase-6 site is required for neuronal dysfunction and degeneration due to mutant huntingtin. *Cell*. 2006;125(6):1179-91.
85. Lunkes A, Lindenberg KS, Ben-Haiem L, Weber C, Devys D, Landwehrmeyer GB, et al. Proteases acting on mutant huntingtin generate cleaved products that differentially build up cytoplasmic and nuclear inclusions. *Molecular cell*. 2002;10(2):259-69.
86. Sathasivam K, Neueder A, Gipson TA, Landles C, Benjamin AC, Bondulich MK, et al. Aberrant splicing of HTT generates the pathogenic exon 1 protein in Huntington disease. *Proceedings of the National Academy of Sciences of the United States of America*. 2013;110(6):2366-70.
87. Mangiarini L, Sathasivam K, Seller M, Cozens B, Harper A, Hetherington C, et al. Exon 1 of the HD gene with an expanded CAG repeat is sufficient to cause a progressive neurological phenotype in transgenic mice. *Cell*. 1996;87(3):493-506.
88. El-Daher MT, Hangen E, Bruyere J, Poizat G, Al-Ramahi I, Pardo R, et al. Huntingtin proteolysis releases non-polyQ fragments that cause toxicity through dynamin 1 dysregulation. *The EMBO journal*. 2015.
89. Jenkins BG, Koroshetz WJ, Beal MF, Rosen BR. Evidence for impairment of energy metabolism in vivo in Huntington's disease using localized ¹H NMR spectroscopy. *Neurology*. 1993;43(12):2689-95.
90. Moffett JR, Ross B, Arun P, Madhavarao CN, Namboodiri AM. N-Acetylaspartate in the CNS: from neurodiagnostics to neurobiology. *Progress in neurobiology*. 2007;81(2):89-131.
91. Koroshetz WJ, Jenkins BG, Rosen BR, Beal MF. Energy metabolism defects in Huntington's disease and effects of coenzyme Q10. *Annals of neurology*. 1997;41(2):160-5.
92. Arenas J, Campos Y, Ribacoba R, Martin MA, Rubio JC, Ablanado P, et al. Complex I defect in muscle from patients with Huntington's disease. *Annals of neurology*. 1998;43(3):397-400.
93. Gizatullina ZZ, Lindenberg KS, Harjes P, Chen Y, Kosinski CM, Landwehrmeyer BG, et al. Low stability of Huntington muscle mitochondria against Ca²⁺ in R6/2 mice. *Annals of neurology*. 2006;59(2):407-11.
94. Gu M, Gash MT, Mann VM, Javoy-Agid F, Cooper JM, Schapira AH. Mitochondrial defect in Huntington's disease caudate nucleus. *Annals of neurology*. 1996;39(3):385-9.
95. Tabrizi SJ, Cleeter MW, Xuereb J, Taanman JW, Cooper JM, Schapira AH. Biochemical abnormalities and excitotoxicity in Huntington's disease brain. *Annals of neurology*. 1999;45(1):25-32.
96. Panov AV, Burke JR, Strittmatter WJ, Greenamyre JT. In vitro effects of polyglutamine tracts on Ca²⁺-dependent depolarization of rat and human mitochondria: relevance to Huntington's disease. *Archives of biochemistry and biophysics*. 2003;410(1):1-6.
97. Yano H, Baranov SV, Baranova OV, Kim J, Pan Y, Yablonska S, et al. Inhibition of mitochondrial protein import by mutant huntingtin. *Nature neuroscience*. 2014;17(6):822-31.
98. Cui L, Jeong H, Borovecki F, Parkhurst CN, Tanese N, Krainc D. Transcriptional repression of PGC-1alpha by mutant huntingtin leads to mitochondrial dysfunction and neurodegeneration. *Cell*. 2006;127(1):59-69.
99. Beal MF, Kowall NW, Ellison DW, Mazurek MF, Swartz KJ, Martin JB. Replication of the neurochemical characteristics of Huntington's disease by quinolinic acid. *Nature*. 1986;321(6066):168-71.
100. Lee ST, Chu K, Park JE, Kang L, Ko SY, Jung KH, et al. Memantine reduces striatal cell death with decreasing calpain level in 3-nitropropionic model of Huntington's disease. *Brain research*. 2006;1118(1):199-207.

101. Faideau M, Kim J, Cormier K, Gilmore R, Welch M, Auregan G, et al. In vivo expression of polyglutamine-expanded huntingtin by mouse striatal astrocytes impairs glutamate transport: a correlation with Huntington's disease subjects. *Human molecular genetics*. 2010;19(15):3053-67.
102. Raymond LA, Andre VM, Cepeda C, Gladding CM, Milnerwood AJ, Levine MS. Pathophysiology of Huntington's disease: time-dependent alterations in synaptic and receptor function. *Neuroscience*. 2011;198:252-73.
103. Hardingham GE, Fukunaga Y, Bading H. Extrasynaptic NMDARs oppose synaptic NMDARs by triggering CREB shut-off and cell death pathways. *Nature neuroscience*. 2002;5(5):405-14.
104. Milnerwood AJ, Gladding CM, Pouladi MA, Kaufman AM, Hines RM, Boyd JD, et al. Early increase in extrasynaptic NMDA receptor signaling and expression contributes to phenotype onset in Huntington's disease mice. *Neuron*. 2010;65(2):178-90.
105. Okamoto S, Pouladi MA, Talantova M, Yao D, Xia P, Ehrnhoefer DE, et al. Balance between synaptic versus extrasynaptic NMDA receptor activity influences inclusions and neurotoxicity of mutant huntingtin. *Nature medicine*. 2009;15(12):1407-13.
106. Milnerwood AJ, Kaufman AM, Sepers MD, Gladding CM, Zhang L, Wang L, et al. Mitigation of augmented extrasynaptic NMDAR signaling and apoptosis in cortico-striatal co-cultures from Huntington's disease mice. *Neurobiology of disease*. 2012;48(1):40-51.
107. Boutell JM, Thomas P, Neal JW, Weston VJ, Duce J, Harper PS, et al. Aberrant interactions of transcriptional repressor proteins with the Huntington's disease gene product, huntingtin. *Human molecular genetics*. 1999;8(9):1647-55.
108. Steffan JS, Kazantsev A, Spasic-Boskovic O, Greenwald M, Zhu YZ, Gohler H, et al. The Huntington's disease protein interacts with p53 and CREB-binding protein and represses transcription. *Proceedings of the National Academy of Sciences of the United States of America*. 2000;97(12):6763-8.
109. Ferrante RJ, Kubilus JK, Lee J, Ryu H, Beesen A, Zucker B, et al. Histone deacetylase inhibition by sodium butyrate chemotherapy ameliorates the neurodegenerative phenotype in Huntington's disease mice. *The Journal of neuroscience : the official journal of the Society for Neuroscience*. 2003;23(28):9418-27.
110. Yeh HH, Young D, Gelovani JG, Robinson A, Davidson Y, Herholz K, et al. Histone deacetylase class II and acetylated core histone immunohistochemistry in human brains with Huntington's disease. *Brain research*. 2013;1504:16-24.
111. Ferrante RJ, Ryu H, Kubilus JK, D'Mello S, Sugars KL, Lee J, et al. Chemotherapy for the brain: the antitumor antibiotic mithramycin prolongs survival in a mouse model of Huntington's disease. *The Journal of neuroscience : the official journal of the Society for Neuroscience*. 2004;24(46):10335-42.
112. Vashishtha M, Ng CW, Yildirim F, Gipson TA, Kratter IH, Bodai L, et al. Targeting H3K4 trimethylation in Huntington disease. *Proceedings of the National Academy of Sciences of the United States of America*. 2013;110(32):E3027-36.
113. Kim MO, Chawla P, Overland RP, Xia E, Sadri-Vakili G, Cha JH. Altered histone monoubiquitylation mediated by mutant huntingtin induces transcriptional dysregulation. *The Journal of neuroscience : the official journal of the Society for Neuroscience*. 2008;28(15):3947-57.
114. Roze E, Betuing S, Deyts C, Marcon E, Brami-Cherrier K, Pages C, et al. Mitogen- and stress-activated protein kinase-1 deficiency is involved in expanded-huntingtin-induced transcriptional dysregulation and striatal death. *FASEB journal : official publication of the Federation of American Societies for Experimental Biology*. 2008;22(4):1083-93.
115. Seredenina T, Luthi-Carter R. What have we learned from gene expression profiles in Huntington's disease? *Neurobiology of disease*. 2012;45(1):83-98.

116. Steffan JS, Bodai L, Pallos J, Poelman M, McCampbell A, Apostol BL, et al. Histone deacetylase inhibitors arrest polyglutamine-dependent neurodegeneration in *Drosophila*. *Nature*. 2001;413(6857):739-43.
117. Ryu H, Lee J, Hagerty SW, Soh BY, McAlpin SE, Cormier KA, et al. ESET/SETDB1 gene expression and histone H3 (K9) trimethylation in Huntington's disease. *Proceedings of the National Academy of Sciences of the United States of America*. 2006;103(50):19176-81.
118. Parkel S, Lopez-Atalaya JP, Barco A. Histone H3 lysine methylation in cognition and intellectual disability disorders. *Learning & memory (Cold Spring Harbor, NY)*. 2013;20(10):570-9.
119. Johnson R, Zuccato C, Belyaev ND, Guest DJ, Cattaneo E, Buckley NJ. A microRNA-based gene dysregulation pathway in Huntington's disease. *Neurobiology of disease*. 2008;29(3):438-45.
120. Lee ST, Chu K, Im WS, Yoon HJ, Im JY, Park JE, et al. Altered microRNA regulation in Huntington's disease models. *Experimental neurology*. 2011;227(1):172-9.
121. Packer AN, Xing Y, Harper SQ, Jones L, Davidson BL. The bifunctional microRNA miR-9/miR-9* regulates REST and CoREST and is downregulated in Huntington's disease. *The Journal of neuroscience : the official journal of the Society for Neuroscience*. 2008;28(53):14341-6.
122. Savas JN, Makusky A, Ottosen S, Baillat D, Then F, Krainc D, et al. Huntington's disease protein contributes to RNA-mediated gene silencing through association with Argonaute and P bodies. *Proceedings of the National Academy of Sciences of the United States of America*. 2008;105(31):10820-5.
123. A randomized, placebo-controlled trial of coenzyme Q10 and remacemide in Huntington's disease. *Neurology*. 2001;57(3):397-404.
124. Hersch SM, Gevorkian S, Marder K, Moskowitz C, Feigin A, Cox M, et al. Creatine in Huntington disease is safe, tolerable, bioavailable in brain and reduces serum 8OH2'dG. *Neurology*. 2006;66(2):250-2.
125. Tabrizi SJ, Blamire AM, Manners DN, Rajagopalan B, Styles P, Schapira AH, et al. High-dose creatine therapy for Huntington disease: a 2-year clinical and MRS study. *Neurology*. 2005;64(9):1655-6.
126. Andreassen OA, Dedeoglu A, Ferrante RJ, Jenkins BG, Ferrante KL, Thomas M, et al. Creatine increase survival and delays motor symptoms in a transgenic animal model of Huntington's disease. *Neurobiology of disease*. 2001;8(3):479-91.
127. Ferrante RJ, Andreassen OA, Dedeoglu A, Ferrante KL, Jenkins BG, Hersch SM, et al. Therapeutic effects of coenzyme Q10 and remacemide in transgenic mouse models of Huntington's disease. *The Journal of neuroscience : the official journal of the Society for Neuroscience*. 2002;22(5):1592-9.
128. Cankurtaran ES, Ozalp E, Soygur H, Cakir A. Clinical experience with risperidone and memantine in the treatment of Huntington's disease. *Journal of the National Medical Association*. 2006;98(8):1353-5.
129. Seppi K, Mueller J, Bodner T, Brandauer E, Benke T, Weirich-Schwaiger H, et al. Riluzole in Huntington's disease (HD): an open label study with one year follow up. *Journal of neurology*. 2001;248(10):866-9.
130. Xie Y, Hayden MR, Xu B. BDNF overexpression in the forebrain rescues Huntington's disease phenotypes in YAC128 mice. *The Journal of neuroscience : the official journal of the Society for Neuroscience*. 2010;30(44):14708-18.
131. Giralt A, Friedman HC, Caneda-Ferron B, Urban N, Moreno E, Rubio N, et al. BDNF regulation under GFAP promoter provides engineered astrocytes as a new approach for long-term protection in Huntington's disease. *Gene therapy*. 2010;17(10):1294-308.

132. Ryu JK, Kim J, Cho SJ, Hatori K, Nagai A, Choi HB, et al. Proactive transplantation of human neural stem cells prevents degeneration of striatal neurons in a rat model of Huntington disease. *Neurobiology of disease*. 2004;16(1):68-77.
133. Hockly E, Richon VM, Woodman B, Smith DL, Zhou X, Rosa E, et al. Suberoylanilide hydroxamic acid, a histone deacetylase inhibitor, ameliorates motor deficits in a mouse model of Huntington's disease. *Proceedings of the National Academy of Sciences of the United States of America*. 2003;100(4):2041-6.
134. Mielcarek M, Landles C, Weiss A, Bradaia A, Seredenina T, Inuabasi L, et al. HDAC4 reduction: a novel therapeutic strategy to target cytoplasmic huntingtin and ameliorate neurodegeneration. *PLoS biology*. 2013;11(11):e1001717.
135. Bonelli RM, Heuberger C, Reisecker F. Minocycline for Huntington's disease: an open label study. *Neurology*. 2003;60(5):883-4.
136. Bonelli RM, Hodl AK, Hofmann P, Kapfhammer HP. Neuroprotection in Huntington's disease: a 2-year study on minocycline. *International clinical psychopharmacology*. 2004;19(6):337-42.
137. Hersch S, Fink K, Vonsattel JP, Friedlander RM. Minocycline is protective in a mouse model of Huntington's disease. *Annals of neurology*. 2003;54(6):841; author reply 2-3.
138. Carroll JB, Warby SC, Southwell AL, Doty CN, Greenlee S, Skotte N, et al. Potent and selective antisense oligonucleotides targeting single-nucleotide polymorphisms in the Huntington disease gene / allele-specific silencing of mutant huntingtin. *Molecular therapy : the journal of the American Society of Gene Therapy*. 2011;19(12):2178-85.
139. Harper SQ, Staber PD, He X, Eliason SL, Martins IH, Mao Q, et al. RNA interference improves motor and neuropathological abnormalities in a Huntington's disease mouse model. *Proceedings of the National Academy of Sciences of the United States of America*. 2005;102(16):5820-5.
140. Kordasiewicz HB, Stanek LM, Wancewicz EV, Mazur C, McAlonis MM, Pytel KA, et al. Sustained therapeutic reversal of Huntington's disease by transient repression of huntingtin synthesis. *Neuron*. 2012;74(6):1031-44.
141. Lombardi MS, Jaspers L, Spronkmans C, Gellera C, Taroni F, Di Maria E, et al. A majority of Huntington's disease patients may be treatable by individualized allele-specific RNA interference. *Experimental neurology*. 2009;217(2):312-9.
142. Ravikumar B, Vacher C, Berger Z, Davies JE, Luo S, Oroz LG, et al. Inhibition of mTOR induces autophagy and reduces toxicity of polyglutamine expansions in fly and mouse models of Huntington disease. *Nature genetics*. 2004;36(6):585-95.
143. Sarkar S, Davies JE, Huang Z, Tunnacliffe A, Rubinsztein DC. Trehalose, a novel mTOR-independent autophagy enhancer, accelerates the clearance of mutant huntingtin and alpha-synuclein. *The Journal of biological chemistry*. 2007;282(8):5641-52.
144. Bhat KP, Yan S, Wang CE, Li S, Li XJ. Differential ubiquitination and degradation of huntingtin fragments modulated by ubiquitin-protein ligase E3A. *Proceedings of the National Academy of Sciences of the United States of America*. 2014;111(15):5706-11.
145. Cuervo AM, Dice JF. Age-related decline in chaperone-mediated autophagy. *The Journal of biological chemistry*. 2000;275(40):31505-13.
146. Cuervo AM. Autophagy and aging: keeping that old broom working. *Trends in genetics : TIG*. 2008;24(12):604-12.
147. Schipper-Krom S, Juenemann K, Reits EA. The Ubiquitin-Proteasome System in Huntington's Disease: Are Proteasomes Impaired, Initiators of Disease, or Coming to the Rescue? *Biochem Res Int*. 2012;2012:837015.

148. Bett JS, Goellner GM, Woodman B, Pratt G, Rechsteiner M, Bates GP. Proteasome impairment does not contribute to pathogenesis in R6/2 Huntington's disease mice: exclusion of proteasome activator REGgamma as a therapeutic target. *Human molecular genetics*. 2006;15(1):33-44.
149. Bennett EJ, Bence NF, Jayakumar R, Kopito RR. Global impairment of the ubiquitin-proteasome system by nuclear or cytoplasmic protein aggregates precedes inclusion body formation. *Molecular cell*. 2005;17(3):351-65.
150. Holmberg CI, Staniszewski KE, Mensah KN, Matouschek A, Morimoto RI. Inefficient degradation of truncated polyglutamine proteins by the proteasome. *The EMBO journal*. 2004;23(21):4307-18.
151. Ortega Z, Lucas JJ. Ubiquitin-proteasome system involvement in Huntington's disease. *Frontiers in molecular neuroscience*. 2014;7:77.
152. Majeski AE, Dice JF. Mechanisms of chaperone-mediated autophagy. *The international journal of biochemistry & cell biology*. 2004;36(12):2435-44.
153. Thompson LM, Aiken CT, Kaltenbach LS, Agrawal N, Illes K, Khoshnan A, et al. IKK phosphorylates Huntingtin and targets it for degradation by the proteasome and lysosome. *The Journal of cell biology*. 2009;187(7):1083-99.
154. Qi L, Zhang XD, Wu JC, Lin F, Wang J, DiFiglia M, et al. The role of chaperone-mediated autophagy in huntingtin degradation. *PloS one*. 2012;7(10):e46834.
155. Koga H, Martinez-Vicente M, Arias E, Kaushik S, Sulzer D, Cuervo AM. Constitutive upregulation of chaperone-mediated autophagy in Huntington's disease. *The Journal of neuroscience : the official journal of the Society for Neuroscience*. 2011;31(50):18492-505.
156. Glick D, Barth S, Macleod KF. Autophagy: cellular and molecular mechanisms. *J Pathol*. 2010;221(1):3-12.
157. Green DR, Levine B. To be or not to be? How selective autophagy and cell death govern cell fate. *Cell*. 2014;157(1):65-75.
158. Ding WX, Yin XM. Mitophagy: mechanisms, pathophysiological roles, and analysis. *Biological chemistry*. 2012;393(7):547-64.
159. Axe EL, Walker SA, Manifava M, Chandra P, Roderick HL, Habermann A, et al. Autophagosome formation from membrane compartments enriched in phosphatidylinositol 3-phosphate and dynamically connected to the endoplasmic reticulum. *The Journal of cell biology*. 2008;182(4):685-701.
160. Hayashi-Nishino M, Fujita N, Noda T, Yamaguchi A, Yoshimori T, Yamamoto A. A subdomain of the endoplasmic reticulum forms a cradle for autophagosome formation. *Nature cell biology*. 2009;11(12):1433-7.
161. Rubinsztein DC, Shpilka T, Elazar Z. Mechanisms of autophagosome biogenesis. *Current biology : CB*. 2012;22(1):R29-34.
162. Hanna RA, Quinsay MN, Orogo AM, Giang K, Rikka S, Gustafsson AB. Microtubule-associated protein 1 light chain 3 (LC3) interacts with Bnip3 protein to selectively remove endoplasmic reticulum and mitochondria via autophagy. *The Journal of biological chemistry*. 2012;287(23):19094-104.
163. Kirkin V, Lamark T, Sou YS, Bjorkoy G, Nunn JL, Bruun JA, et al. A role for NBR1 in autophagosomal degradation of ubiquitinated substrates. *Molecular cell*. 2009;33(4):505-16.
164. Razi M, Chan EY, Tooze SA. Early endosomes and endosomal coatome are required for autophagy. *The Journal of cell biology*. 2009;185(2):305-21.
165. Maday S, Wallace KE, Holzbaur EL. Autophagosomes initiate distally and mature during transport toward the cell soma in primary neurons. *The Journal of cell biology*. 2012;196(4):407-17.

166. Wong YC, Holzbaur EL. The regulation of autophagosome dynamics by huntingtin and HAP1 is disrupted by expression of mutant huntingtin, leading to defective cargo degradation. *The Journal of neuroscience : the official journal of the Society for Neuroscience*. 2014;34(4):1293-305.
167. Webb JL, Ravikumar B, Rubinsztein DC. Microtubule disruption inhibits autophagosome-lysosome fusion: implications for studying the roles of aggresomes in polyglutamine diseases. *The international journal of biochemistry & cell biology*. 2004;36(12):2541-50.
168. Pankiv S, Johansen T. FYCO1: linking autophagosomes to microtubule plus end-directing molecular motors. *Autophagy*. 2010;6(4):550-2.
169. Feng Y, Press B, Wandinger-Ness A. Rab 7: an important regulator of late endocytic membrane traffic. *The Journal of cell biology*. 1995;131(6 Pt 1):1435-52.
170. Bucci C, Thomsen P, Nicoziani P, McCarthy J, van Deurs B. Rab7: a key to lysosome biogenesis. *Molecular biology of the cell*. 2000;11(2):467-80.
171. Jager S, Bucci C, Tanida I, Ueno T, Kominami E, Saftig P, et al. Role for Rab7 in maturation of late autophagic vacuoles. *Journal of cell science*. 2004;117(Pt 20):4837-48.
172. Mizushima N, Komatsu M. Autophagy: renovation of cells and tissues. *Cell*. 2011;147(4):728-41.
173. Kim J, Kundu M, Viollet B, Guan KL. AMPK and mTOR regulate autophagy through direct phosphorylation of Ulk1. *Nature cell biology*. 2011;13(2):132-41.
174. Russell RC, Tian Y, Yuan H, Park HW, Chang YY, Kim J, et al. ULK1 induces autophagy by phosphorylating Beclin-1 and activating VPS34 lipid kinase. *Nature cell biology*. 2013;15(7):741-50.
175. Jung CH, Jun CB, Ro SH, Kim YM, Otto NM, Cao J, et al. ULK-Atg13-FIP200 complexes mediate mTOR signaling to the autophagy machinery. *Molecular biology of the cell*. 2009;20(7):1992-2003.
176. Hosokawa N, Hara T, Kaizuka T, Kishi C, Takamura A, Miura Y, et al. Nutrient-dependent mTORC1 association with the ULK1-Atg13-FIP200 complex required for autophagy. *Molecular biology of the cell*. 2009;20(7):1981-91.
177. Steffan JS. Does Huntingtin play a role in selective macroautophagy? *Cell cycle (Georgetown, Tex)*. 2010;9(17):3401-13.
178. Martin DD, Heit RJ, Yap MC, Davidson MW, Hayden MR, Berthiaume LG. Identification of a post-translationally myristoylated autophagy-inducing domain released by caspase cleavage of huntingtin. *Human molecular genetics*. 2014;23(12):3166-79.
179. Fan W, Nassiri A, Zhong Q. Autophagosome targeting and membrane curvature sensing by Barkor/Atg14(L). *Proceedings of the National Academy of Sciences of the United States of America*. 2011;108(19):7769-74.
180. Hatzakis NS, Bhatia VK, Larsen J, Madsen KL, Bolinger PY, Kunding AH, et al. How curved membranes recruit amphipathic helices and protein anchoring motifs. *Nature chemical biology*. 2009;5(11):835-41.
181. Tellez-Nagel I, Johnson AB, Terry RD. Studies on brain biopsies of patients with Huntington's chorea. *Journal of neuropathology and experimental neurology*. 1974;33(2):308-32.
182. Cortes CJ, La Spada AR. The many faces of autophagy dysfunction in Huntington's disease: from mechanism to therapy. *Drug discovery today*. 2014;19(7):963-71.
183. Erie C, Sacino M, Houle L, Lu ML, Wei J. Altered lysosomal positioning affects lysosomal functions in a cellular model of Huntington's disease. *The European journal of neuroscience*. 2015.
184. Tettamanti G. Ganglioside/glycosphingolipid turnover: new concepts. *Glycoconjugate journal*. 2004;20(5):301-17.
185. Basu S, Kaufman B, Roseman S. Enzymatic synthesis of glucocerebroside by a glucosyltransferase from embryonic chicken brain. *The Journal of biological chemistry*. 1973;248(4):1388-94.

186. Posse de Chaves E, Sipione S. Sphingolipids and gangliosides of the nervous system in membrane function and dysfunction. *FEBS letters*. 2010;584(9):1748-59.
187. Maccioni HJ, Daniotti JL, Martina JA. Organization of ganglioside synthesis in the Golgi apparatus. *Biochimica et biophysica acta*. 1999;1437(2):101-18.
188. Schengrund CL. Gangliosides: glycosphingolipids essential for normal neural development and function. *Trends in biochemical sciences*. 2015;40(7):397-406.
189. Susuki K, Baba H, Tohyama K, Kanai K, Kuwabara S, Hirata K, et al. Gangliosides contribute to stability of paranodal junctions and ion channel clusters in myelinated nerve fibers. *Glia*. 2007;55(7):746-57.
190. Ledeen RW, Wu G, Lu ZH, Kozireski-Chuback D, Fang Y. The role of GM1 and other gangliosides in neuronal differentiation. Overview and new finding. *Annals of the New York Academy of Sciences*. 1998;845:161-75.
191. Labasque M, Faivre-Sarrailh C. GPI-anchored proteins at the node of Ranvier. *FEBS letters*. 2010;584(9):1787-92.
192. Pan B, Fromholt SE, Hess EJ, Crawford TO, Griffin JW, Sheikh KA, et al. Myelin-associated glycoprotein and complementary axonal ligands, gangliosides, mediate axon stability in the CNS and PNS: neuropathology and behavioral deficits in single- and double-null mice. *Experimental neurology*. 2005;195(1):208-17.
193. Cheng ZJ, Singh RD, Sharma DK, Holicky EL, Hanada K, Marks DL, et al. Distinct mechanisms of clathrin-independent endocytosis have unique sphingolipid requirements. *Molecular biology of the cell*. 2006;17(7):3197-210.
194. Garcia-Ruiz C, Colell A, Paris R, Fernandez-Checa JC. Direct interaction of GD3 ganglioside with mitochondria generates reactive oxygen species followed by mitochondrial permeability transition, cytochrome c release, and caspase activation. *FASEB journal : official publication of the Federation of American Societies for Experimental Biology*. 2000;14(7):847-58.
195. Hwang J, Lee S, Lee JT, Kwon TK, Kim DR, Kim H, et al. Gangliosides induce autophagic cell death in astrocytes. *Br J Pharmacol*. 2010;159(3):586-603.
196. Matarrese P, Garofalo T, Manganelli V, Gambardella L, Marconi M, Grasso M, et al. Evidence for the involvement of GD3 ganglioside in autophagosome formation and maturation. *Autophagy*. 2014;10(5):750-65.
197. Brunetti-Pierrri N, Scaglia F. GM1 gangliosidosis: review of clinical, molecular, and therapeutic aspects. *Molecular genetics and metabolism*. 2008;94(4):391-6.
198. Takamura A, Higaki K, Kajimaki K, Otsuka S, Ninomiya H, Matsuda J, et al. Enhanced autophagy and mitochondrial aberrations in murine G(M1)-gangliosidosis. *Biochemical and biophysical research communications*. 2008;367(3):616-22.
199. Wei J, Fujita M, Nakai M, Waragai M, Sekigawa A, Sugama S, et al. Protective role of endogenous gangliosides for lysosomal pathology in a cellular model of synucleinopathies. *Am J Pathol*. 2009;174(5):1891-909.
200. Wei J, Fujita M, Sekigawa A, Sekiyama K, Waragai M, Hashimoto M. Gangliosides' protection against lysosomal pathology of synucleinopathies. *Autophagy*. 2009;5(6):860-1.
201. Simpson MA, Cross H, Proukakis C, Priestman DA, Neville DC, Reinkensmeier G, et al. Infantile-onset symptomatic epilepsy syndrome caused by a homozygous loss-of-function mutation of GM3 synthase. *Nature genetics*. 2004;36(11):1225-9.
202. Sha S, Zhou L, Yin J, Takamiya K, Furukawa K, Furukawa K, et al. Deficits in cognitive function and hippocampal plasticity in GM2/GD2 synthase knockout mice. *Hippocampus*. 2014;24(4):369-82.
203. Chiavegatto S, Sun J, Nelson RJ, Schnaar RL. A functional role for complex gangliosides: motor deficits in GM2/GD2 synthase knockout mice. *Experimental neurology*. 2000;166(2):227-34.

204. Chan RB, Oliveira TG, Cortes EP, Honig LS, Duff KE, Small SA, et al. Comparative lipidomic analysis of mouse and human brain with Alzheimer disease. *The Journal of biological chemistry*. 2012;287(4):2678-88.
205. Rapport MM. Implications of altered brain ganglioside profiles in amyotrophic lateral sclerosis (ALS). *Acta neurobiologiae experimentalis*. 1990;50(4-5):505-13.
206. Chinnapen DJ, Hsieh WT, te Welscher YM, Saslowsky DE, Kaoutzani L, Brandsma E, et al. Lipid sorting by ceramide structure from plasma membrane to ER for the cholera toxin receptor ganglioside GM1. *Dev Cell*. 2012;23(3):573-86.
207. Wu G, Ledeen RW. Stimulation of neurite outgrowth in neuroblastoma cells by neuraminidase: putative role of GM1 ganglioside in differentiation. *Journal of neurochemistry*. 1991;56(1):95-104.
208. Wu G, Lu ZH, Obukhov AG, Nowycky MC, Ledeen RW. Induction of calcium influx through TRPC5 channels by cross-linking of GM1 ganglioside associated with alpha5beta1 integrin initiates neurite outgrowth. *The Journal of neuroscience : the official journal of the Society for Neuroscience*. 2007;27(28):7447-58.
209. Xie X, Wu G, Lu ZH, Ledeen RW. Potentiation of a sodium-calcium exchanger in the nuclear envelope by nuclear GM1 ganglioside. *Journal of neurochemistry*. 2002;81(6):1185-95.
210. Wu G, Xie X, Lu ZH, Ledeen RW. Sodium-calcium exchanger complexed with GM1 ganglioside in nuclear membrane transfers calcium from nucleoplasm to endoplasmic reticulum. *Proceedings of the National Academy of Sciences of the United States of America*. 2009;106(26):10829-34.
211. Chierzi S, Ratto GM, Verma P, Fawcett JW. The ability of axons to regenerate their growth cones depends on axonal type and age, and is regulated by calcium, cAMP and ERK. *The European journal of neuroscience*. 2005;21(8):2051-62.
212. Kappagantula S, Andrews MR, Cheah M, Abad-Rodriguez J, Dotti CG, Fawcett JW. Neu3 sialidase-mediated ganglioside conversion is necessary for axon regeneration and is blocked in CNS axons. *The Journal of neuroscience : the official journal of the Society for Neuroscience*. 2014;34(7):2477-92.
213. Wu G, Fang Y, Lu ZH, Ledeen RW. Induction of axon-like and dendrite-like processes in neuroblastoma cells. *Journal of neurocytology*. 1998;27(1):1-14.
214. Ledeen RW, Wu G. The multi-tasked life of GM1 ganglioside, a true factotum of nature. *Trends in biochemical sciences*. 2015;40(7):407-18.
215. Wu G, Ledeen RW. Gangliosides as modulators of neuronal calcium. *Progress in brain research*. 1994;101:101-12.
216. Mobius W, Herzog V, Sandhoff K, Schwarzmann G. Intracellular distribution of a biotin-labeled ganglioside, GM1, by immunoelectron microscopy after endocytosis in fibroblasts. *The journal of histochemistry and cytochemistry : official journal of the Histochemistry Society*. 1999;47(8):1005-14.
217. Mutoh T, Tokuda A, Miyadai T, Hamaguchi M, Fujiki N. Ganglioside GM1 binds to the Trk protein and regulates receptor function. *Proceedings of the National Academy of Sciences of the United States of America*. 1995;92(11):5087-91.
218. Pitto M, Mutoh T, Kuriyama M, Ferraretto A, Palestini P, Masserini M. Influence of endogenous GM1 ganglioside on TrkB activity, in cultured neurons. *FEBS letters*. 1998;439(1-2):93-6.
219. Hadaczek P, Wu G, Sharma N, Ciesielska A, Bankiewicz K, Davidow AL, et al. GDNF signaling implemented by GM1 ganglioside; failure in Parkinson's disease and GM1-deficient murine model. *Experimental neurology*. 2015;263:177-89.

220. Mitsuda T, Furukawa K, Fukumoto S, Miyazaki H, Urano T, Furukawa K. Overexpression of ganglioside GM1 results in the dispersion of platelet-derived growth factor receptor from glycolipid-enriched microdomains and in the suppression of cell growth signals. *The Journal of biological chemistry*. 2002;277(13):11239-46.
221. Calamai M, Pavone FS. Partitioning and confinement of GM1 ganglioside induced by amyloid aggregates. *FEBS letters*. 2013;587(9):1385-91.
222. Martinez Z, Zhu M, Han S, Fink AL. GM1 specifically interacts with alpha-synuclein and inhibits fibrillation. *Biochemistry*. 2007;46(7):1868-77.
223. Augustinsson LE, Blennow K, Blomstrand C, Brane G, Ekman R, Fredman P, et al. Intracerebroventricular administration of GM1 ganglioside to presenile Alzheimer patients. *Dementia and geriatric cognitive disorders*. 1997;8(1):26-33.
224. Yanagisawa K, Odaka A, Suzuki N, Ihara Y. GM1 ganglioside-bound amyloid beta-protein (A beta): a possible form of preamyloid in Alzheimer's disease. *Nature medicine*. 1995;1(10):1062-6.
225. Hoshino T, Mahmood MI, Mori K, Matsuzaki K. Binding and aggregation mechanism of amyloid beta-peptides onto the GM1 ganglioside-containing lipid membrane. *The journal of physical chemistry B*. 2013;117(27):8085-94.
226. Wakabayashi M, Okada T, Kozutsumi Y, Matsuzaki K. GM1 ganglioside-mediated accumulation of amyloid beta-protein on cell membranes. *Biochemical and biophysical research communications*. 2005;328(4):1019-23.
227. Oikawa N, Yamaguchi H, Ogino K, Taki T, Yuyama K, Yamamoto N, et al. Gangliosides determine the amyloid pathology of Alzheimer's disease. *Neuroreport*. 2009;20(12):1043-6.
228. Spillantini MG, Schmidt ML, Lee VM, Trojanowski JQ, Jakes R, Goedert M. Alpha-synuclein in Lewy bodies. *Nature*. 1997;388(6645):839-40.
229. Phillis JW, O'Regan MH. GM1 ganglioside inhibits ischemic release of amino acid neurotransmitters from rat cortex. *Neuroreport*. 1995;6(15):2010-2.
230. Schneider JS, Pope A, Simpson K, Taggart J, Smith MG, DiStefano L. Recovery from experimental parkinsonism in primates with GM1 ganglioside treatment. *Science (New York, NY)*. 1992;256(5058):843-6.
231. Imanaka T, Hukuda S, Maeda T. The role of GM1-ganglioside in the injured spinal cord of rats: an immunohistochemical study using GM1-antisera. *Journal of neurotrauma*. 1996;13(3):163-70.
232. Ganglioside GM1 in acute ischemic stroke. *The SASS Trial. Stroke; a journal of cerebral circulation*. 1994;25(6):1141-8.
233. Argentino C, Sacchetti ML, Toni D, Savoini G, D'Arcangelo E, Erminio F, et al. GM1 ganglioside therapy in acute ischemic stroke. *Italian Acute Stroke Study--Hemodilution + Drug. Stroke; a journal of cerebral circulation*. 1989;20(9):1143-9.
234. Schneider JS, Roeltgen DP, Mancall EL, Chapas-Crilly J, Rothblat DS, Tatarian GT. Parkinson's disease: improved function with GM1 ganglioside treatment in a randomized placebo-controlled study. *Neurology*. 1998;50(6):1630-6.
235. Klose KJ, Calancie B. Has GM1 ganglioside been shown to be effective in the restoration of neurologic function in persons with chronic spinal cord injury? A critique of an article by Judith B. Walker and Michelle Harris. *Neuroscience letters*. 1994;176(2):277-80.
236. Walker JB, Harris M. GM-1 ganglioside administration combined with physical therapy restores ambulation in humans with chronic spinal cord injury. *Neuroscience letters*. 1993;161(2):174-8.
237. Wu G, Lu ZH, Wang J, Wang Y, Xie X, Meyenhofer MF, et al. Enhanced susceptibility to kainate-induced seizures, neuronal apoptosis, and death in mice lacking ganglioside GM1.

gangliosides: protection with LIGA 20, a membrane-permeant analog of GM1. *The Journal of neuroscience : the official journal of the Society for Neuroscience*. 2005;25(47):11014-22.

238. Gray MT, Woulfe JM. Striatal blood-brain barrier permeability in Parkinson's disease. *Journal of cerebral blood flow and metabolism : official journal of the International Society of Cerebral Blood Flow and Metabolism*. 2015;35(5):747-50.

239. Chen B, Friedman B, Cheng Q, Tsai P, Schim E, Kleinfeld D, et al. Severe blood-brain barrier disruption and surrounding tissue injury. *Stroke; a journal of cerebral circulation*. 2009;40(12):e666-74.

240. Schneider JS, Gollomp SM, Sendek S, Colcher A, Cambi F, Du W. A randomized, controlled, delayed start trial of GM1 ganglioside in treated Parkinson's disease patients. *Journal of the neurological sciences*. 2013;324(1-2):140-8.

241. Schneider JS, Cambi F, Gollomp SM, Kuwabara H, Brasic JR, Leiby B, et al. GM1 ganglioside in Parkinson's disease: Pilot study of effects on dopamine transporter binding. *Journal of the neurological sciences*. 2015;356(1-2):118-23.

242. Schneider JS, Sendek S, Daskalakis C, Cambi F. GM1 ganglioside in Parkinson's disease: Results of a five year open study. *Journal of the neurological sciences*. 2010;292(1-2):45-51.

243. Denny CA, Desplats PA, Thomas EA, Seyfried TN. Cerebellar lipid differences between R6/1 transgenic mice and humans with Huntington's disease. *Journal of neurochemistry*. 2010;115(3):748-58.

244. Desplats PA, Denny CA, Kass KE, Gilmartin T, Head SR, Sutcliffe JG, et al. Glycolipid and ganglioside metabolism imbalances in Huntington's disease. *Neurobiology of disease*. 2007;27(3):265-77.

245. Di Pardo A, Maglione V, Alpaugh M, Horkey M, Atwal RS, Sassone J, et al. Ganglioside GM1 induces phosphorylation of mutant huntingtin and restores normal motor behavior in Huntington disease mice. *Proceedings of the National Academy of Sciences of the United States of America*. 2012;109(9):3528-33.

246. Alpaugh M GD, Morales LC, Lackey S, Kar P, Kerr B, Todd K and Sipione S. Therapeutic and disease-modifying effects of ganglioside GM1 in mouse models of Huntington's disease. AD/PD Conference; March 18, 2015; Nice, France2015.

247. Alpaugh M ML, Galleguillos D, Horkey M, DiPardo A, Paw K, Todd K and Sipione S. Disease-modifying effects of ganglioside GM1 in HD mouse models. 8th CHDI Conference on Huntington Disease; Venice, Italy2013.

248. Humbert S, Bryson EA, Cordelieres FP, Connors NC, Datta SR, Finkbeiner S, et al. The IGF-1/Akt pathway is neuroprotective in Huntington's disease and involves Huntingtin phosphorylation by Akt. *Dev Cell*. 2002;2(6):831-7.

249. Gu X, Greiner ER, Mishra R, Kodali R, Osmand A, Finkbeiner S, et al. Serines 13 and 16 are critical determinants of full-length human mutant huntingtin induced disease pathogenesis in HD mice. *Neuron*. 2009;64(6):828-40.

250. Jeong H, Then F, Melia TJ, Jr., Mazzulli JR, Cui L, Savas JN, et al. Acetylation targets mutant huntingtin to autophagosomes for degradation. *Cell*. 2009;137(1):60-72.

251. McLin JP, Thompson LM, Steward O. Differential susceptibility to striatal neurodegeneration induced by quinolinic acid and kainate in inbred, outbred and hybrid mouse strains. *The European journal of neuroscience*. 2006;24(11):3134-40.

252. Yang L, Calingasan NY, Chen J, Ley JJ, Becker DA, Beal MF. A novel azulenyl nitron antioxidant protects against MPTP and 3-nitropropionic acid neurotoxicities. *Experimental neurology*. 2005;191(1):86-93.

253. Stack EC, Kubilus JK, Smith K, Cormier K, Del Signore SJ, Guelin E, et al. Chronology of behavioral symptoms and neuropathological sequela in R6/2 Huntington's disease transgenic mice. *The Journal of comparative neurology*. 2005;490(4):354-70.
254. Slow EJ, van Raamsdonk J, Rogers D, Coleman SH, Graham RK, Deng Y, et al. Selective striatal neuronal loss in a YAC128 mouse model of Huntington disease. *Human molecular genetics*. 2003;12(13):1555-67.
255. Van Raamsdonk JM, Pearson J, Slow EJ, Hossain SM, Leavitt BR, Hayden MR. Cognitive dysfunction precedes neuropathology and motor abnormalities in the YAC128 mouse model of Huntington's disease. *The Journal of neuroscience : the official journal of the Society for Neuroscience*. 2005;25(16):4169-80.
256. Menalled LB, Sison JD, Dragatsis I, Zeitlin S, Chesselet MF. Time course of early motor and neuropathological anomalies in a knock-in mouse model of Huntington's disease with 140 CAG repeats. *The Journal of comparative neurology*. 2003;465(1):11-26.
257. Rising AC, Xu J, Carlson A, Napoli VV, Denovan-Wright EM, Mandel RJ. Longitudinal behavioral, cross-sectional transcriptional and histopathological characterization of a knock-in mouse model of Huntington's disease with 140 CAG repeats. *Experimental neurology*. 2011;228(2):173-82.
258. Hickey MA, Kosmalska A, Enayati J, Cohen R, Zeitlin S, Levine MS, et al. Extensive early motor and non-motor behavioral deficits are followed by striatal neuronal loss in knock-in Huntington's disease mice. *Neuroscience*. 2008;157(1):280-95.
259. Trettel F, Rigamonti D, Hilditch-Maguire P, Wheeler VC, Sharp AH, Persichetti F, et al. Dominant phenotypes produced by the HD mutation in STHdh(Q111) striatal cells. *Human molecular genetics*. 2000;9(19):2799-809.
260. O'Reilly DR. p53 and transformation by SV40. *Biology of the cell / under the auspices of the European Cell Biology Organization*. 1986;57(3):187-96.
261. Gelman A, Rawet-Slobodkin M, Elazar Z. Huntingtin facilitates selective autophagy. *Nature cell biology*. 2015;17(3):214-5.
262. . Available from: <https://en.wikipedia.org/wiki/GM1>.
263. Scherzinger E, Lurz R, Turmaine M, Mangiarini L, Hollenbach B, Hasenbank R, et al. Huntingtin-encoded polyglutamine expansions form amyloid-like protein aggregates in vitro and in vivo. *Cell*. 1997;90(3):549-58.
264. Menzies FM, Moreau K, Puri C, Renna M, Rubinsztein DC. Measurement of autophagic activity in mammalian cells. *Current protocols in cell biology / editorial board, Juan S Bonifacino [et al]*. 2012;Chapter 15:Unit 15.6.
265. Klionsky DJ, Abeliovich H, Agostinis P, Agrawal DK, Aliev G, Askew DS, et al. Guidelines for the use and interpretation of assays for monitoring autophagy in higher eukaryotes. *Autophagy*. 2008;4(2):151-75.
266. Sahani MH, Itakura E, Mizushima N. Expression of the autophagy substrate SQSTM1/p62 is restored during prolonged starvation depending on transcriptional upregulation and autophagy-derived amino acids. *Autophagy*. 2014;10(3):431-41.
267. Klionsky DJ, Abeliovich H, Agostinis P, Agrawal DK, Aliev G, Askew DS, et al. Guidelines for the use and interpretation of assays for monitoring autophagy in higher eukaryotes. *Autophagy*. 2008;4(2):151-75.
268. Kovacs AL, Seglen PO. Inhibition of hepatocytic protein degradation by methylaminopurines and inhibitors of protein synthesis. *Biochimica et biophysica acta*. 1981;676(2):213-20.
269. Kimura S, Noda T, Yoshimori T. Dissection of the autophagosome maturation process by a novel reporter protein, tandem fluorescent-tagged LC3. *Autophagy*. 2007;3(5):452-60.

270. Wheeler VC, Auerbach W, White JK, Srinidhi J, Auerbach A, Ryan A, et al. Length-dependent gametic CAG repeat instability in the Huntington's disease knock-in mouse. *Human molecular genetics*. 1999;8(1):115-22.
271. Yamamoto A, Lucas JJ, Hen R. Reversal of neuropathology and motor dysfunction in a conditional model of Huntington's disease. *Cell*. 2000;101(1):57-66.
272. Komatsu M, Waguri S, Koike M, Sou YS, Ueno T, Hara T, et al. Homeostatic levels of p62 control cytoplasmic inclusion body formation in autophagy-deficient mice. *Cell*. 2007;131(6):1149-63.
273. Komatsu M, Waguri S, Chiba T, Murata S, Iwata J, Tanida I, et al. Loss of autophagy in the central nervous system causes neurodegeneration in mice. *Nature*. 2006;441(7095):880-4.
274. Calvo-Garrido J, Escalante R. Autophagy dysfunction and ubiquitin-positive protein aggregates in Dictyostelium cells lacking Vmp1. *Autophagy*. 2010;6(1):100-9.
275. Ravikumar B, Rubinsztein DC. Role of autophagy in the clearance of mutant huntingtin: a step towards therapy? *Molecular aspects of medicine*. 2006;27(5-6):520-7.
276. Wild EJ, Tabrizi SJ. Targets for future clinical trials in Huntington's disease: what's in the pipeline? *Movement disorders : official journal of the Movement Disorder Society*. 2014;29(11):1434-45.
277. Ikeda K, Yamaguchi T, Fukunaga S, Hoshino M, Matsuzaki K. Mechanism of amyloid beta-protein aggregation mediated by GM1 ganglioside clusters. *Biochemistry*. 2011;50(29):6433-40.
278. Manna M, Mukhopadhyay C. Binding, conformational transition and dimerization of amyloid-beta peptide on GM1-containing ternary membrane: insights from molecular dynamics simulation. *PloS one*. 2013;8(8):e71308.
279. Rajendran L, Knobloch M, Geiger KD, Diemel S, Nitsch R, Simons K, et al. Increased Aβ production leads to intracellular accumulation of Aβ in flotillin-1-positive endosomes. *Neurodegenerative diseases*. 2007;4(2-3):164-70.
280. Angot E, Steiner JA, Lema Tome CM, Ekstrom P, Mattsson B, Bjorklund A, et al. Alpha-synuclein cell-to-cell transfer and seeding in grafted dopaminergic neurons in vivo. *PloS one*. 2012;7(6):e39465.
281. Pecho-Vrieseling E, Rieker C, Fuchs S, Bleckmann D, Esposito MS, Botta P, et al. Transneuronal propagation of mutant huntingtin contributes to non-cell autonomous pathology in neurons. *Nature neuroscience*. 2014;17(8):1064-72.
282. Bercovich B, Stancovski I, Mayer A, Blumenfeld N, Laszlo A, Schwartz AL, et al. Ubiquitin-dependent degradation of certain protein substrates in vitro requires the molecular chaperone Hsc70. *The Journal of biological chemistry*. 1997;272(14):9002-10.
283. Sarkar S, Rubinsztein DC. Huntington's disease: degradation of mutant huntingtin by autophagy. *FEBS J*. 2008;275(17):4263-70.
284. Hara T, Nakamura K, Matsui M, Yamamoto A, Nakahara Y, Suzuki-Migishima R, et al. Suppression of basal autophagy in neural cells causes neurodegenerative disease in mice. *Nature*. 2006;441(7095):885-9.
285. Sarkar S, Floto RA, Berger Z, Imarisio S, Cordenier A, Pasco M, et al. Lithium induces autophagy by inhibiting inositol monophosphatase. *The Journal of cell biology*. 2005;170(7):1101-11.
286. Tommasino C, Marconi M, Ciarlo L, Matarrese P, Malorni W. Autophagic flux and autophagosome morphogenesis require the participation of sphingolipids. *Apoptosis : an international journal on programmed cell death*. 2015;20(5):645-57.
287. Zakharova IO, Sokolova TV, Vlasova YA, Furaev VV, Rychkova MP, Avrova NF. GM1 ganglioside activates ERK1/2 and Akt downstream of Trk tyrosine kinase and protects PC12 cells against hydrogen peroxide toxicity. *Neurochemical research*. 2014;39(11):2262-75.

288. Duchemin AM, Ren Q, Neff NH, Hadjiconstantinou M. GM1-induced activation of phosphatidylinositol 3-kinase: involvement of Trk receptors. *Journal of neurochemistry*. 2008;104(6):1466-77.
289. Bjorkoy G, Lamark T, Brech A, Outzen H, Perander M, Overvatn A, et al. p62/SQSTM1 forms protein aggregates degraded by autophagy and has a protective effect on huntingtin-induced cell death. *The Journal of cell biology*. 2005;171(4):603-14.
290. Steffan JS, Agrawal N, Pallos J, Rockabrand E, Trotman LC, Slepko N, et al. SUMO modification of Huntingtin and Huntington's disease pathology. *Science (New York, NY)*. 2004;304(5667):100-4.
291. Arndt JR, Brown RJ, Burke KA, Legleiter J, Valentine SJ. Lysine residues in the N-terminal huntingtin amphipathic alpha-helix play a key role in peptide aggregation. *Journal of mass spectrometry : JMS*. 2015;50(1):117-26.
292. Choo YS, Johnson GV, MacDonald M, Detloff PJ, Lesort M. Mutant huntingtin directly increases susceptibility of mitochondria to the calcium-induced permeability transition and cytochrome c release. *Human molecular genetics*. 2004;13(14):1407-20.
293. Butterfield DA, Howard BJ, LaFontaine MA. Brain oxidative stress in animal models of accelerated aging and the age-related neurodegenerative disorders, Alzheimer's disease and Huntington's disease. *Current medicinal chemistry*. 2001;8(7):815-28.
294. Chopra V, Fox JH, Lieberman G, Dorsey K, Matson W, Waldmeier P, et al. A small-molecule therapeutic lead for Huntington's disease: preclinical pharmacology and efficacy of C2-8 in the R6/2 transgenic mouse. *Proceedings of the National Academy of Sciences of the United States of America*. 2007;104(42):16685-9.
295. Ehrnhoefer DE, Duennwald M, Markovic P, Wacker JL, Engemann S, Roark M, et al. Green tea (-)-epigallocatechin-gallate modulates early events in huntingtin misfolding and reduces toxicity in Huntington's disease models. *Human molecular genetics*. 2006;15(18):2743-51.
296. Van Raamsdonk JM, Pearson J, Rogers DA, Lu G, Barakauskas VE, Barr AM, et al. Ethyl-EPA treatment improves motor dysfunction, but not neurodegeneration in the YAC128 mouse model of Huntington disease. *Experimental neurology*. 2005;196(2):266-72.
297. Drouin-Ouellet J, Sawiak SJ, Cisbani G, Lagace M, Kuan WL, Saint-Pierre M, et al. Cerebrovascular and blood-brain barrier impairments in Huntington's disease: Potential implications for its pathophysiology. *Annals of neurology*. 2015;78(2):160-77.